PERFORMANCE OF A VISCOUS TOPPING TURBINE

A THESIS

Presented to

The Faculty of the Division

of Graduate Studies

By

Andrew M. Coons

In Partial Fulfillment

of the Requirements for the Degree

Master of Science in Mechanical Engineering

Georgia Institute of Technology

June, 1976

PERFORMANCE OF A VISCOUS

TOPPING TURBINE

Approved:

5-76

R. J. Colwell, Chairman

T. W. Jackson, Chairman

C. W. Gorton

Date approved by Chairman: 5-5-76

ACKNOWLEDGMENTS

This thesis is dedicated to my Lord and Savior Jesus Christ.

My sincerest gratitude is also due to my advisors, Dr. G. T. Colwell and Dr. T. W. Jackson, whose encouragement and guidance have been invaluable. I am additionally indebted to Drs. Colwell, Jackson and C. W. Gorton for careful reading and suggestions.

TABLE OF CONTENTS

Page

ACKNOWLEDGMENTS. ii

LIST OF TABLES v

LIST OF ILLUSTRATIONS. vi

NOMENCLATURE ix

SUMMARY. xi

Chapter

I. INTRODUCTION. 1

1-1. The Concept of the Viscous Turbine
1-2. Literature Survey

II. THEORETICAL DEVELOPMENT 6

2-1. Turbine and Compressor Models
2-2. Fundamental Equations
2-3. Wall Stress and Convection Factors
2-4. Simultaneous Solution of Fundamental Equations
2-5. Efficiency Definitions

III. SOLUTION TECHNIQUES 20

3-1. Computer Analysis (Non-Variable Area)
3-2. Computer Analysis (Variable Area)
3-3. Friction Factor Subroutine

IV. RESULTS OF ANALYSIS 28

4-1. Comparison of Theoretical and Experimental Data
4-2. Limiting Cases and Outer Wall Losses
4-3. Turbine Optimization
4-4. Variable Area Turbine
4-5. Single Stage Unit Efficiencies
4-6. Multiple Stage Unit Efficiencies
4-7. Heat Transfer Effects
4-8. Supersonic Turbine
4-9. General Turbine Performance Data

Chapter Page

V. CONCLUSIONS AND RECOMMENDATIONS. 99

APPENDICES. 102

REFERENCES. 119

LIST OF TABLES

Table Page

1. Optimum Cases. 96

2. Turbine Entrance Conditions. 98

LIST OF ILLUSTRATIONS

Figure		Page
1-1.	Wheel Geometry.	2
1-2.	Schematic Diagram of Generating System.	3
2-1.	Control Volume.	7
2-2.	Control Volume Force Balance.	10
2-3.	Open Brayton Cycle.	19
2-4.	Open Brayton Cycle with Reheat.	19
3-1.	Geometry of a Larger Rotor.	21
3-2.	Program Flowchart	23
4-1.	Experimental and Theoretical Data Correlation in Compressor	29
4-2.	Experimental and Theoretical Data Correlation in Compressor	30
4-3.	Experimental and Theoretical Data Correlation in Compressor	31
4-4.	Compressor Performance.	33
4-5.	Turbine Performance	35
4-6.	Compressor Performance.	36
4-7.	Compressor Performance.	37
4-8.	Turbine Performance	38
4-9.	Turbine Performance	39
4-10.	Turbine Performance	40
4-11.	Turbine Performance	41
4-12.	Turbine Performance	42

Figure		Page
4-13.	Turbine Performance.	43
4-14.	Turbine Performance.	44
4-15.	Turbine Performance.	46
4-16.	Turbine Performance.	47
4-17.	Turbine Performance.	48
4-18.	Turbine Performance.	49
4-19.	Turbine Performance.	50
4-20.	Compressor Performance	51
4-21.	Compressor Performance	52
4-22.	Compressor Performance	53
4-23.	Compressor Performance	54
4-24.	Compressor Performance	55
4-25.	Compressor Performance	56
4-26.	Comparison of Variable Area and Regular Turbines	58
4-27.	Comparison of Variable Area and Regular Turbines	59
4-28.	Variable Area Turbine Performance.	60
4-29.	Variable Area Turbine Performance.	61
4-30.	Viscous Engine	62
4-31.	Brayton Cycle Efficiencies	64
4-32.	Single Stage Unit Efficiency	65
4-33.	Single Stage Unit Efficiency	66
4-34.	Single Stage Unit Efficiency	67
4-35.	Single Stage Unit Efficiency	68
4-36.	Comparison of Variable Area and Regular Turbines for Single Unit Efficiencies	70

Figure		Page
4-37.	Single Unit Efficiency with Variable Area Turbine.	71
4-38.	Axial Flow Compressor and Viscous Turbines in Series Schematic of Possible Topping Cycle . . .	72
4-39.	Supersonic Turbine Performance	76
4-40.	Supersonic Turbine Performance	77
4-41.	Supersonic Turbine Performance	78
4-42.	Supersonic Turbine Performance	79
4-43.	Supersonic Turbine Performance	80
4-44.	Supersonic Turbine Performance	81
4-45.	Turbine Performance.	82
4-46.	Turbine Performance.	83
4-47.	Turbine Performance.	84
4-48.	Turbine Performance.	85
4-49.	Turbine Performance.	86
4-50.	Turbine Performance.	87
4-51.	Case 1 Turbine Performance	88
4-52.	Case 1 Turbine Performance	89
4-53.	Case 1 Turbine Performance	90
4-54.	Case 1 Turbine Performance	91
4-55.	Case 2 Turbine Performance	92
4-56.	Case 2 Turbine Performance	93
4-57.	Case 2 Turbine Performance	94
4-58.	Case 2 Turbine Performance	95

GLOSSARY OF ABBREVIATIONS

H	slot height (inch)
W	slot width (inch)
DIA	rotor diameter (inch)
WIDTH	turbine length (ft)
dA	change in slot flow area across control volume element $(in)^2$
dP	change in pressure across control volume element (psi)
dT	change in temperature across control volume element (°R)
$d\rho$	change in density across control volume element (lb_m/in^3)
dV	change in velocity across control volume element (in/sec)
DX	length of control volume element (in)
S	wheel rim speed (in/sec)
q	heat transfer from rotor to air (Btu/lb_m)
τ_c	shear stress between air and static outer wall (psi)
τ_w	shear stress between air and rotor (psi)
V	air velocity absolute (in/sec)
P	air pressure (psia)
P_1	air inlet stagnation pressure (psia)
P_2	air exit stagnation pressure (psia)
T	air temperature (°R)

ρ	air density (lb_m/in^3)
$\dot{M}$	total mass flowrate (lb_m/sec)
MD	mass flowrate per slot (lb_m/sec)
t	time (sec)
AA	total turbine flow area (in^2)
A	flow area per slot (in^2)
g_c	Newton constant, 32.174 ft-lb_m/lb_f-sec^2
M	mass in control volume (lb_m)
F	forces on control volume (lb_f)
Q	heat addition (Btu/sec)
W_s	mechanical work (Btu/sec)
h	enthalpy (Btu/lb_m)
$\bar{n}$	control volume surface normal
h_w	convection factor (Btu/in^2-°R-sec)
C_p	specific heat at constant pressure (Btu/lb_m-°R)
T_w	wheel surface temperature (°R)
R	gas constant, 53.3 ft-lb_f/lb_m-°R
D_h	hydraulic diameter (in)
Re	Reynolds number
μ	air viscosity lb_m/ft-sec
f	friction factor
k	ratio of specific heats C_p/C_v = 1.4
eff_T	turbine efficiency
T_1	inlet stagnation temperature (°R)
T_2	exit stagnation temperature (°R)
eff_u	unit efficiency
hp	horsepower output

SUMMARY

One-dimensional mathematical models have been developed which approximate flow behavior in a viscous turbine and a viscous compressor. The models were validated by comparison with available experimental data for the viscous compressor and by comparison with limiting cases where the solutions are known. Detailed performance characteristics, including efficiency, pressure ratio, and shaft horsepower, of both turbine and compressor were generated.

Potential use of a viscous topping turbine for application in fossil fuel power plants has been studied. Unit operation with single and multiple wheel staged turbines has been evaluated for efficiency and net output in shaft horsepower. The effects of varying flow area, heat transfer, and supersonic flow have been studied.

Results of varied turbine and compressor parameters have been displayed in graphical fashion. The concept has been evaluated and the results indicate a possibility of providing a more efficient system to derive electrical energy from fossil fuel. Recommendations for further study are included.

CHAPTER I

INTRODUCTION

1-1. The Concept of the Viscous Turbine

The idea of using topping turbines in fossil fuel plants in order to increase overall efficiency of electrical power generation has been known for a long time. However, conventional gas turbines are not suitable for use in coal burning power plants due to blade erosion caused by impingement of unburned particles and ash. In addition, turbine inlet temperatures are limited.

Several years ago at the Georgia Institute of Technology, Drs. T. W. Jackson and G. T. Colwell conceived an idea for a grooved disk, as shown in Figure 1-1, operating as a viscous turbine which may have the temperature and durability characteristics needed for installation in the burner locations on existing coal boilers. The turbine, without complex surfaces for blades, would operate on viscous drag as the high temperature combustion gases passed through the grooves at high velocities.

An overall efficiency analysis of a topping turbine unit, including compressor and viscous turbines in an electrical steam plant, is illustrated in Figure 1-2. The benefit of the topping turbine is that it utilizes expansion

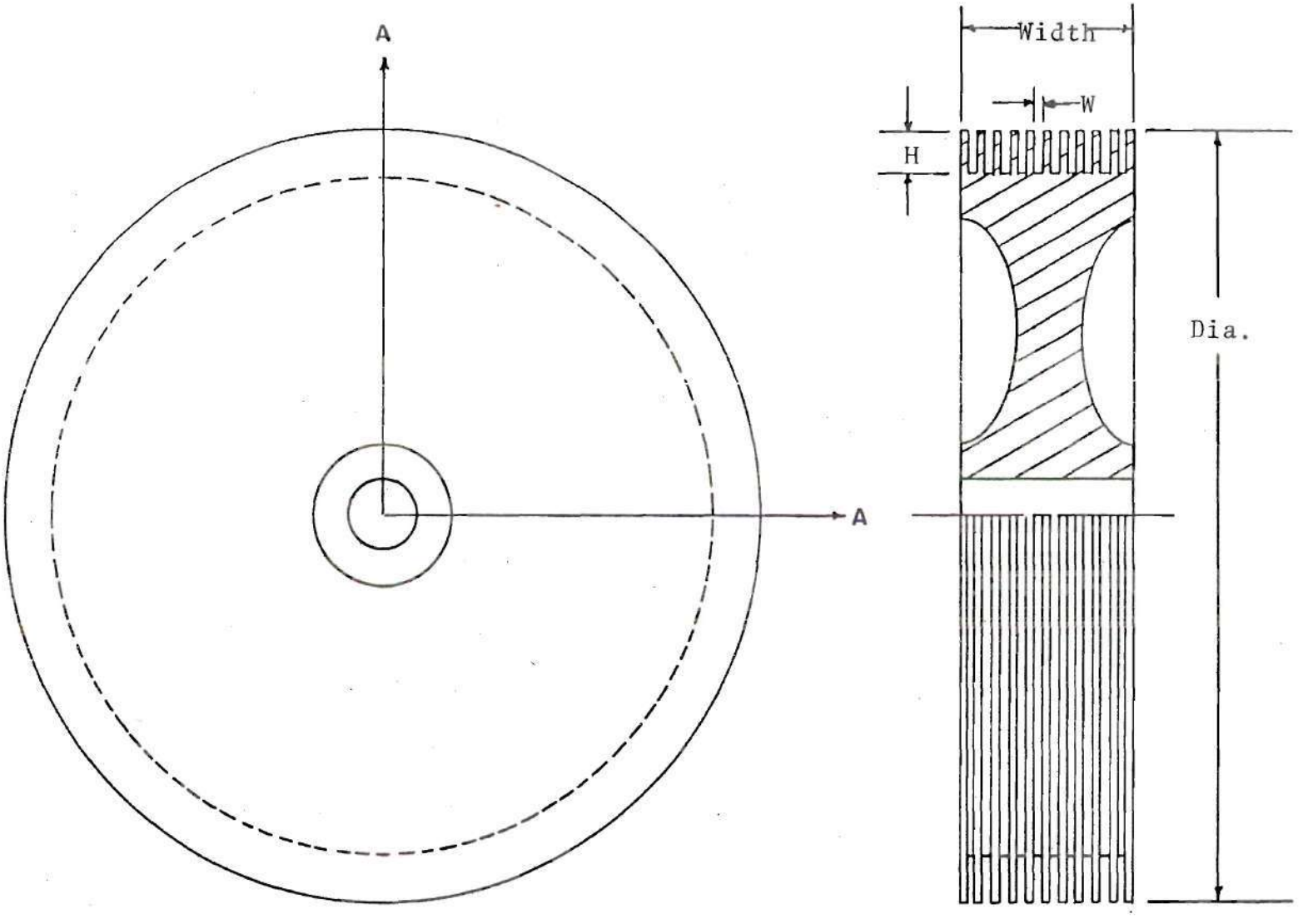

Figure 1-1. Wheel Geometry

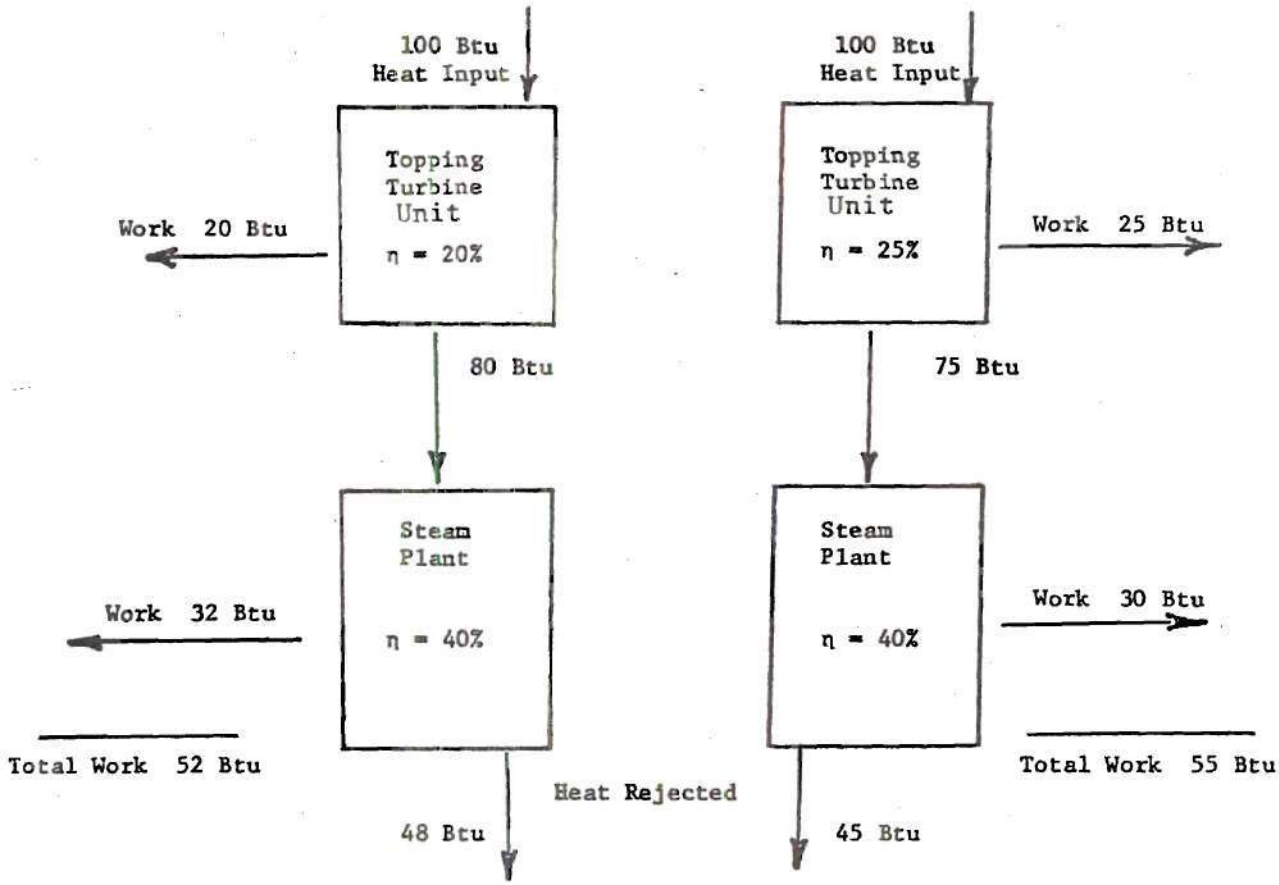

Combined Efficiency

$$\eta_T = \frac{52}{100} = 52\%$$

Improvement over ordinary plant

$$I = \frac{12}{40} = \underline{\underline{30\%}}$$

$$\eta_T = \frac{55}{100} = 55\%$$

$$I = \frac{15}{40} = 37.5\%$$

Figure 1-2. Schematic Diagrams of Generating Systems Using Coal Burning Topping Turbines and Estimates of Output Improvements for Two Topping Turbine Efficiencies of 20% and 25% Over a Standard Steam Plant Operating at 40% Efficiency

of the combustion gases to obtain output above and beyond ordinary plant operation without additional heat input. The heat energy leaving the turbine is available for use in the conventional Rankine-steam cycle. By similar analysis to Figure 1-2, a 10 percent thermal efficiency from the topping turbine unit will yield a 15 percent improvement over ordinary steam plants. An entire unit utilizing the grooved disk as turbine and compressor was considered feasible until this study revealed relatively low compressor efficiency and that only limited turbine pressure ratios are possible due to choking. Higher unit efficiencies are possible by combining a series of turbines with an axial compressor at a higher pressure ratio.

1-2. Literature Survey

The concept of the viscous turbine has been studied and refined at Georgia Tech. Under Dr. Colwell's direction, a viscous compressor was analyzed both experimentally and theoretically by Dusadeenoad in 1970 [1].* Further investigation by Caldwell [2] displayed the importance of effective sealing on efficiency. Based on this work, a patent was issued to Drs. Jackson and Colwell jointly in 1973 [3]. The compressor was further demonstrated in a three-dimensional theoretical study for laminar incompressible flow by Yalcin [4].

---

*Numbers in brackets indicate references.

Though the earliest recognition of a viscous turbine was by Nikolai Tesla [5] in 1913, no reference has been located which gives performance characteristics of a high speed viscous turbine. This thesis has employed fundamental engineering concepts to predict turbine and compressor performance. Texts by John [6], Schlichting [7], White [8] and Reynolds [9] were used to develop the models employed. Material properties were taken from Kreith [10] and Keenan and Kaye [11]. A computer manual by Cooper and Smith also served as a valuable reference [12].

CHAPTER II

THEORETICAL DEVELOPMENT

2-1. Turbine and Compressor Models

Theoretical performance characteristics of the viscous turbine and compressor are generated with one-dimensional mathematical models. The models consist of a series of finite elements which compose the turbine or compressor arc on the circumference of the wheel. Each element is represented by a stationary control volume as shown in Figure 2-1. The effects of variable area are included in the mathematical equations, however, they reduce to the non-variable form when $dA = 0$.

The fundamental equations of continuity, momentum, and energy coupled with the equation of state for air must be satisfied within each control volume element. The shear stresses on the surfaces of the elements are determined using laminar and turbulent friction factors for duct flow. Forces in the directions shown in Figure 2-1 are considered positive. Heat into the fluid and work on the fluid are also positive. The turbine will have negative values for τ_w, q, and work. These are handled in a general way in the derivations.

2-2. Fundamental Equations

Steady mass flow through the arc greatly reduces the

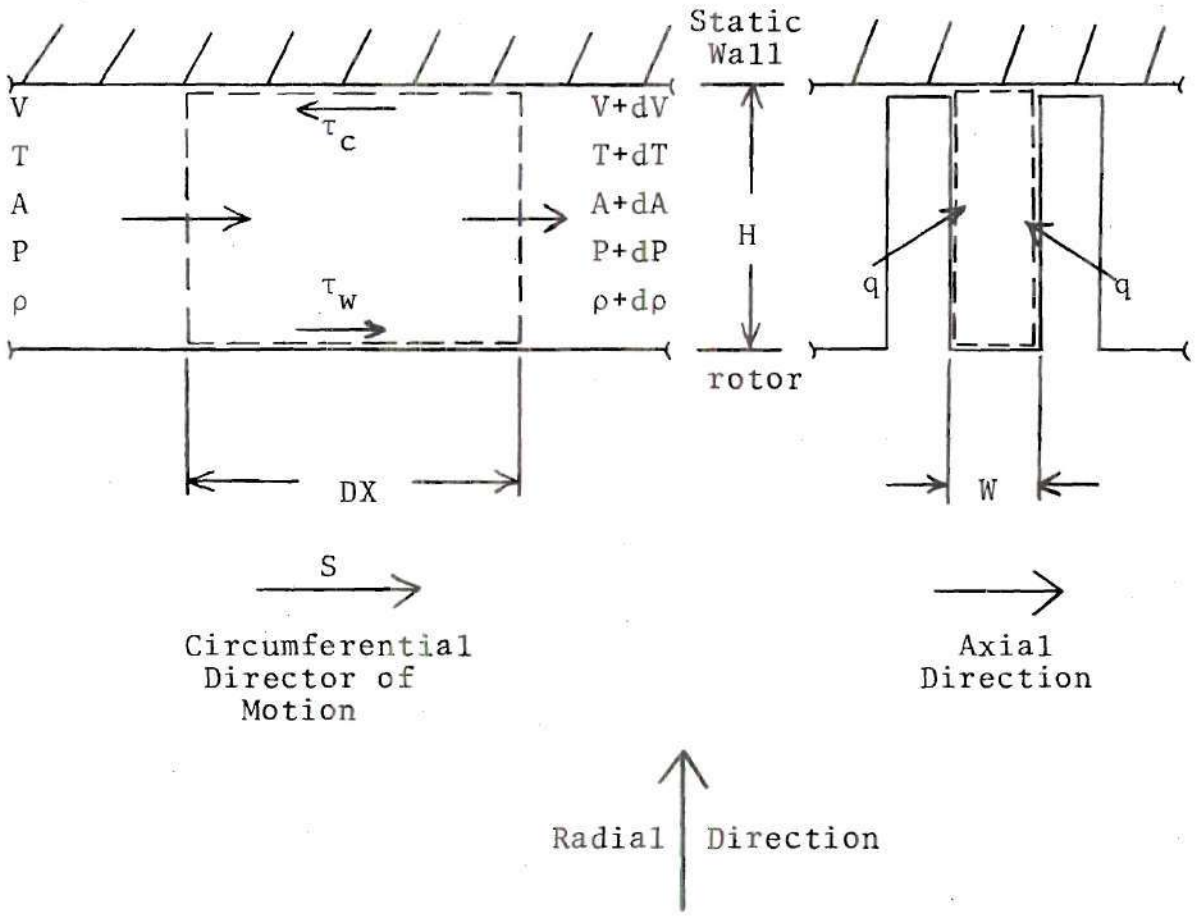

Figure 2-1. Control Volume

complexity of the fundamental equations. The equations are further simplified by choosing the intervals sufficiently small such that material properties specific heat and viscosity are constant within each element. With sufficiently small intervals, second and third order differentials may also be considered negligible. For example, $d\rho dV << d\rho V$. Thus $d\rho dV$ is assumed zero.

Continuity Equation

Conservation of mass in control volume form is:

$$\frac{dM}{dt} = \frac{\alpha}{\alpha t} \iiint_{c.v.} \rho \, dVol + \iint_{s} \rho \, \bar{V} \cdot \bar{n} \, dA$$

For steady flow,

$$0 = (\rho+d\rho)\ (V+dV)\ (A+dA) - \rho VA$$

Neglecting second and third order differentials,

$$\frac{d\rho}{\rho} + \frac{dA}{A} + \frac{dV}{V} = 0$$

$$d\rho = - \frac{\rho dV}{V} - \frac{\rho dA}{A}$$

And the mass flowrate is:

$$\dot{M} = \rho VA = \text{constant}$$

Momentum Equation

Rate of change of momentum in a control volume is:

$$\frac{d(MV)}{dt} = \frac{\alpha}{\alpha t} \iiint_{c.v.} \rho V \, dVol + \iint_{s} V\rho(\bar{V}\cdot\bar{n})dA$$

By Newton's Second Law,

$$\frac{d(MV)}{dt} = q_c \quad \Sigma\bar{F}$$

Summing forces in Figure 2-2 and neglecting second order differentials,

$$\Sigma F = -(p+dp)(A+dA) + (p+p/2)dA$$

$$+ pA + \tau_w(2H+W)DX - \tau_c W(DX)$$

Where,

$\tau_w > 0$ in the compressor

$\tau_w < 0$ in the turbine

Now,

$$\frac{d(MV)}{dt} = \rho AVdV$$

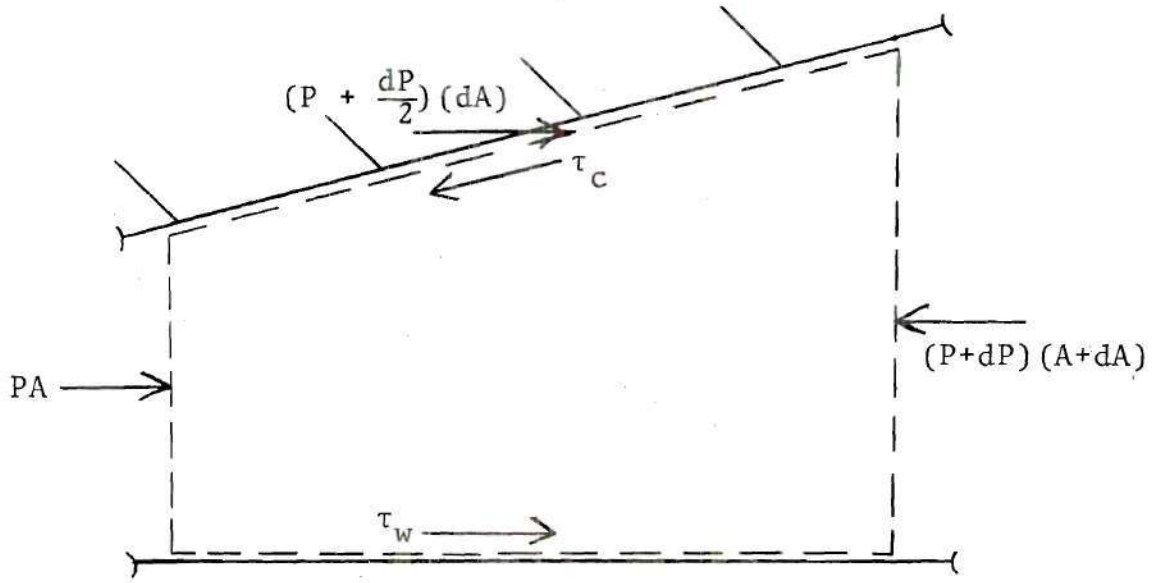

Figure 2-2. Control Volume Force Balance

$$-AdP + \tau_w (2H+W)DX - \tau_c W(DX) = \frac{\rho AVdV}{q_c}$$

Letting $A = HW$, $\rho AV = \dot{M}$

$$dP = \frac{-\dot{M}dV}{HWq_c} + \frac{\tau_w(2H+W)DX}{HW} - \frac{\tau_c DX}{H}$$

Energy Equation

Rate change of energy in a control volume is:

$$\frac{dE}{dt} = \frac{\alpha}{\alpha t} \iiint_{c.v.} e\rho dVol + \iint_{s} e\rho(\bar{V}\cdot\bar{n})dA$$

$$e = u + \frac{V^2}{2q_c}$$

$$\frac{dE}{dt} = \frac{d}{dt}\,(Q+W_s) \; - \; \frac{p}{\rho}\,\dot{M}$$

where Q represents heat addition, W_s represents mechanical work, and $-p/\rho\dot{M}$ is flow work.

Since

$$h = u + \frac{P}{\rho}$$

then,

$$\frac{d(W_s+Q)}{dt} = \iint_s (h + \frac{V^2}{2q_c})\rho(\bar{V}\cdot\bar{n})dA$$

Simplifying and neglecting second order differentials,

$$\frac{dW_s}{dt} + \frac{dQ}{dt} = \dot{M}(dh + \frac{VdV}{q_c})$$

$$\frac{dW_s}{dt} = \text{(shear force) x (wheel speed)}$$

$$\frac{dW_s}{dt} = \tau_w(2H+W)DX\ S$$

$$\frac{dQ}{dt} = \left(\begin{matrix}\text{Convection}\\ \text{Factor}\end{matrix}\right) \times (\text{Area}) \times \left(\begin{matrix}\text{Temperature}\\ \text{Difference}\end{matrix}\right)$$

$$\frac{dQ}{dt} = h_w\ (2H+W)DX(T_w-T)$$

Assuming air to be a perfect gas,

$$dh = C_p dT$$

Then,

$$\frac{\tau_w(2H+W)DX(S)}{\dot{M}} + \frac{h_w(2H+W)DX(T_w-T)}{\dot{M}} = C_p dT + \frac{VdV}{g_c}$$

$$dT = \frac{-VdV}{c_p g_c} + \frac{\tau_w(2H+W)DX(S)}{C_p\dot{M}} + \frac{h_w(2H+W)DX(T_w-T)}{C_p\dot{M}}$$

State Equation

The state equation for air as a perfect gas is:

$$Pv = RT$$

$$\rho = P/RT$$

$$d\rho = \frac{dP}{RT} - \frac{P}{RT^2}\,dT$$

Where,

$$R = 53.3 \frac{\text{ft lb}_f}{\text{lb}_m \ ^\circ R}$$

2-3. Wall Stresses and Convection Factors

Reynold's number (Re) for flow in pipes of non-circular cross section is based on hydraulic diameter.

$$D_h = \frac{2HW}{(H+W)}$$

Then for Re and τ_c relative to the stationary housing,

$$Re = \frac{\rho \ V \ D_h}{M}$$

$$\tau_c = f\rho V^2/8 \ q_c$$

And for Re and τ_w relative to the rotating wheel,

$$Re = \frac{\rho |(S-V)| D_h}{M}$$

$$\tau_w = \frac{f\rho |S-V| (S-V)}{8 \ q_c}$$

If S>V, as in the compressor, τ_w will be greater than zero.

However, if S<V the above relation will generate a negative τ_w as required by the turbine.

Empirical correlations for Re and f are

$$f = 64/Re \qquad Re < 2000$$

$$\frac{1}{\sqrt{f}} = 2.0 \log_{10} (Re\sqrt{f}) - .8 \qquad Re > 2000$$

(Reference 7, equations 5.11, 20.30), and by Reynold's analogy,

$$h_w = \frac{f\rho|S-V|C_p}{8.0}$$

2-4. Simultaneous Solution of Fundamental Equations

A summary of the fundamental equations is now given.

Continuity

$$d\rho = \frac{-\rho dV}{V} - \frac{\rho dA}{A}$$

Momentum

$$dP = \frac{-\dot{M}\, dV}{HW\, g_c} + C_1$$

where

$$C_1 = \frac{\tau_w (2H+W)DX}{HW} - \frac{\tau_c DX}{H}$$

Energy

$$dT = \frac{-VdV}{C_p g_c} + C_2$$

where,

$$C_2 = \frac{\tau_w (2H+W)DX(S)}{C_p \dot{M}} + \frac{h_w (2H+W)DX(T_w-T)}{C_p \dot{M}}$$

State

$$d\rho = \frac{dP}{RT} - \frac{P}{RT^2} dT$$

These constitute four coupled equations with four unknowns. Since $d\rho$, dP, and dT are all first order functions of dV, the fundamental equations may be solved in a straightforward manner by substituting the continuity momentum, and energy equations into the state equation. With some simplification, this yields:

$$dV = C_4/C_3$$

where,

$$C_3 = [-\rho/V + \frac{\dot{M}}{HWRTg_c} - \frac{PV}{RT^2C_pg_c}]$$

and

$$C_4 = [\frac{C_1}{RT} - \frac{C_2P}{RT^2} + \frac{\rho dA}{A}]$$

Then $d\rho$, dP and dT follow directly as functions of C_4 and C_3 ($dV = C_4/C_3$).

$$d\rho = \frac{-\rho}{V}\frac{C_4}{C_3}$$

$$dP = \frac{-\dot{M}}{HW\ g_c}\frac{C_4}{C_3} + C_1$$

$$dT = \frac{-V}{C_p\ g_c}\frac{C_4}{C_3} + C_2$$

2-5. Efficiency Definitions

Turbine efficiency is defined as the ratio of actual turbine work output to the isentropic work between the same pressures.

$$\text{eff}_T = \frac{(\text{Shear Force}) \times (\text{Wheel Speed})}{(\text{Isentropic Work } P_1 \rightarrow P_2)}$$

$$= \frac{|\tau_w|\,(2H+W)\,(DX)\,S}{C_p\ T_1\ \dot{M}\ [1-(\frac{P_2}{P_1})^{\frac{1-k}{K}}]}$$

Compressor efficiency is the reciprocal of the turbine efficiency. It is the ratio of isentropic work to actual work.

$$\text{eff}_c = \frac{(\text{isentropic work } P_1 \rightarrow P_2)}{(\text{shear force}) \times (\text{wheel speed})} = \frac{C_p T_1 \dot{M}[(\frac{P_2}{P_1})^{\frac{1-k}{k}} - 1]}{\tau_w (2H+W)DX(S)}$$

Unit Efficiency

The turbine, when combined with a compressor and heat source, forms a unit operating as an open Brayton cycle shown in Figure 2-3. An open Brayton cycle with reheat is shown in Figure 2-4.

The efficiency of either unit is defined by

$$\text{eff}_u = \frac{(\text{Total Turbine Work}) - (\text{Compressor Work})}{(\text{Total Heat Input})}$$

If an axial compressor with 80 percent efficiency is used, the work of compression is

$$\text{Compressor Work} = \frac{\dot{M} C_p \ 530°R \ [(\frac{P_2}{14.7})^{\frac{1-k}{k}} - 1]}{.8}$$

The total turbine work is shear force by wheel speed.

$$\text{Turbine Work} = \tau_w (2H+W)DX(S)$$

and the heat inputs are

$$\text{Initial Heat Input} = C_p \dot{M} (T_3 - T_2)$$

$$\text{Reheat} = C_p \dot{M} (T_{4a} - T_{3a})$$

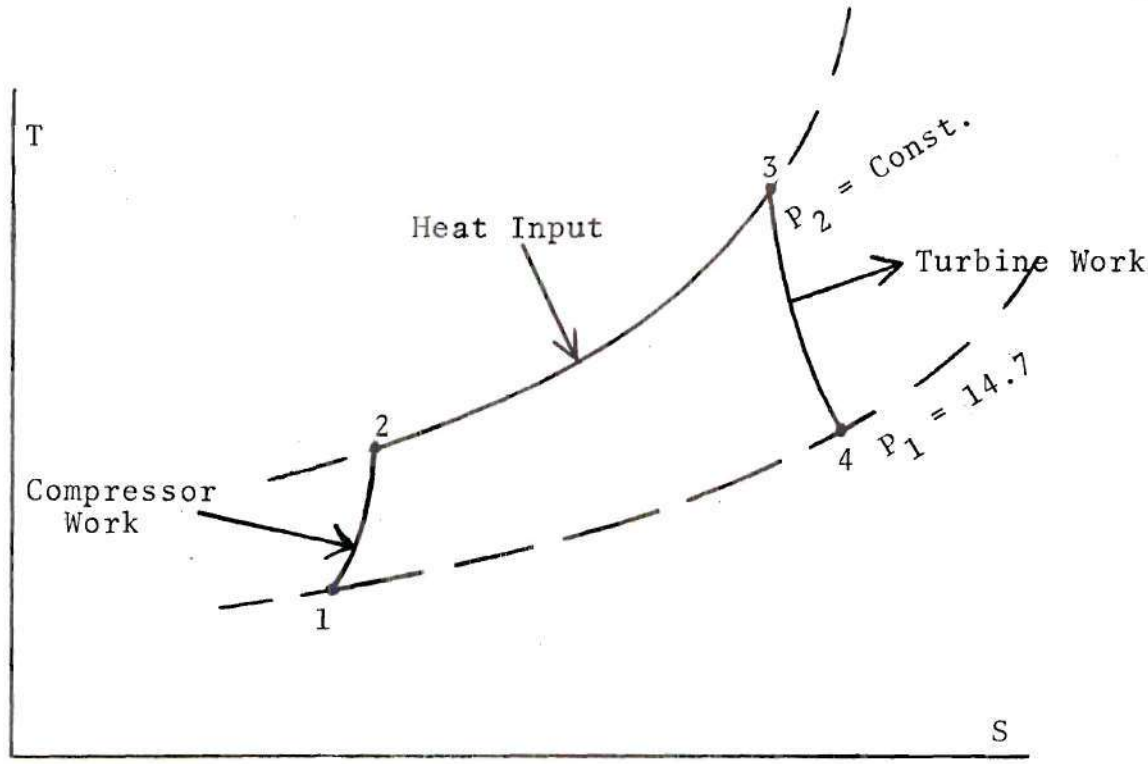

Figure 2-3. Open Brayton Cycle

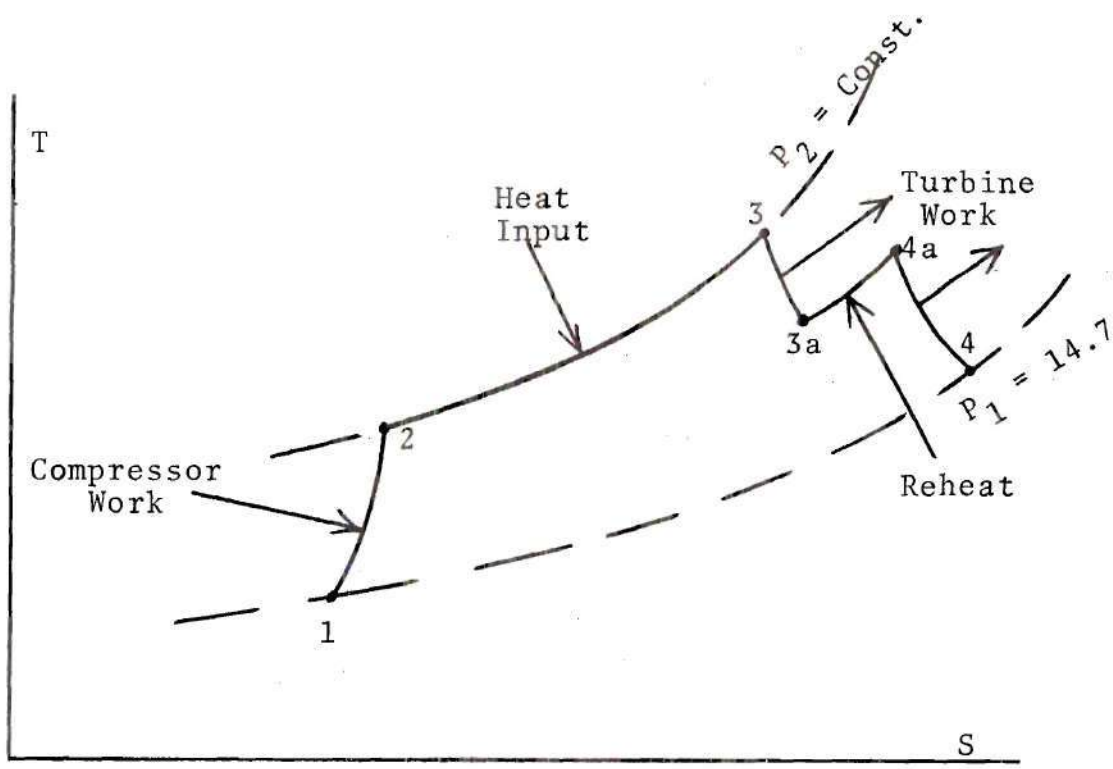

Figure 2-4. Open Brayton Cycle with Reheat

CHAPTER III

SOLUTION TECHNIQUES

3-1. Computer Analysis (Non-Variable Area)

The arc length of the turbine or compressor is divided into one hundred finite increments, each of which constitutes a control volume as shown in Figure 2-1. The length of each element is dependent on the wheel diameter and the degrees of arc desired (Figure 3-1). Iterating the control volume analysis a hundred times has the effect of marching through the turbine or compressor. Various flowrates are used to map and then optimize performance.

The same analysis was performed using a single control volume attached to the disk. This control volume was allowed to sweep through the arc at the wheel speed. Properties within the element were transient as the control volume moved through the arc. The results were identical. However, due to the complexity of the single element transient analysis, the iteration technique has been employed exclusively in this report.

A computer program has been written to perform the analysis required to determine turbine and compressor operational characteristics. All parameters related to the geometry or operation of the disk as well as entrance

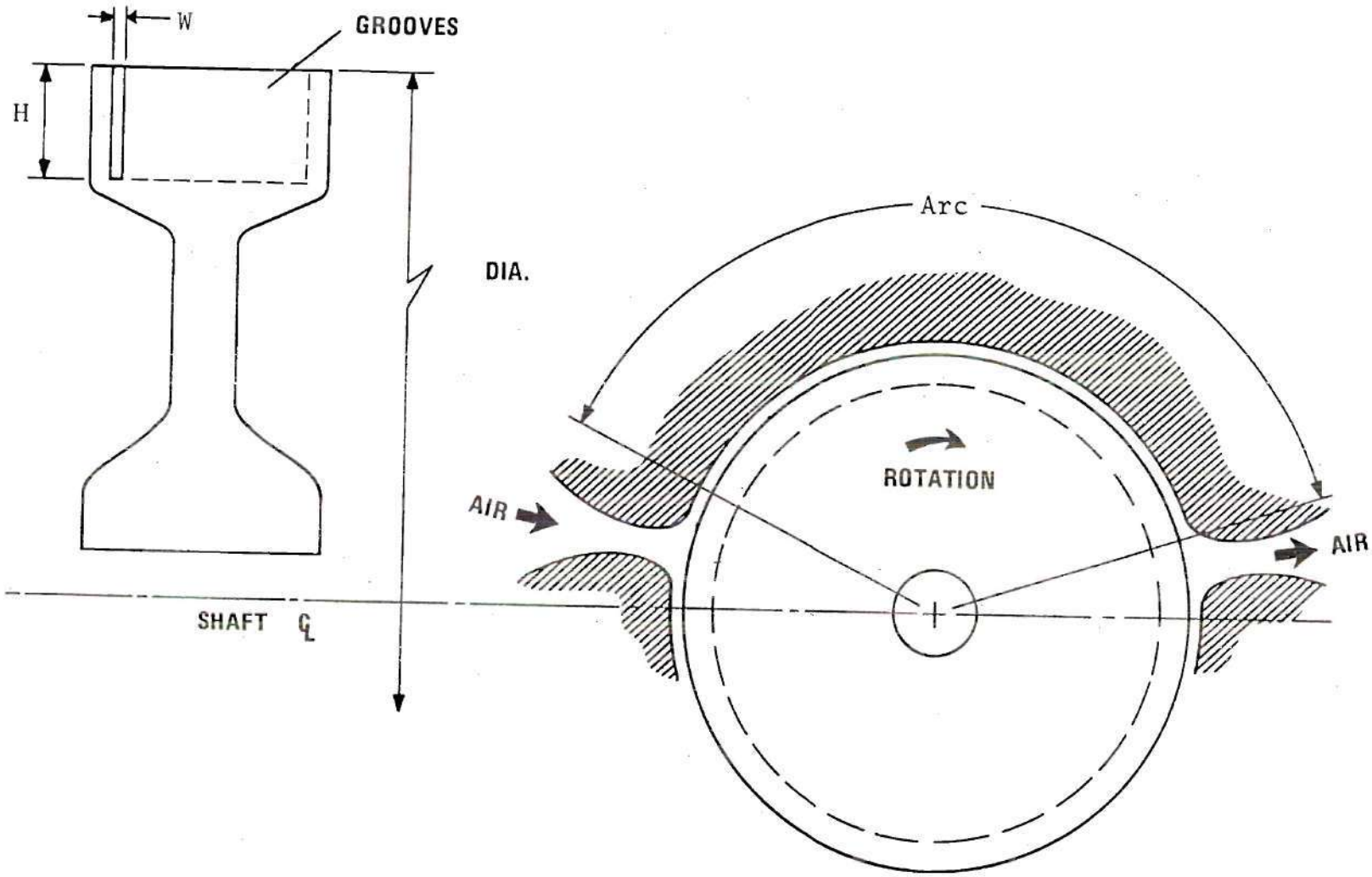

Figure 3-1. Geometry of Larger Rotor

conditions may be varied. The program, given in Appendix A, is in standard Fortran IV-G user language. Subroutines, which employ a plotter to display generated data, are called as necessary.

A simplified flowchart is shown in Figure 3-2. Geometry and speed of the turbine or compressor along with stagnation properties of the entering air are read into the computer. Mass flowrates are then selected starting at just above zero and increasing to choked flow. Static properties and velocity are calculated using standard isentropic relations. The control volume analysis as described in Chapter II is now iterated to determine exit properties at each element from the entrance properties plus the differentials calculated (eq. P(J+1) = P(J) + d(P).

Material properties, specific heat and viscosity, are primarily a function of air temperature which varies along the arc. They are described within each control volume element by the following curve fitting relationships:

Viscosity, lb_m/ ft-sec

$$\mu = 1.285 \left(\frac{T}{560°R}\right)^{1.35} \left(\frac{1000°R}{T+440°R}\right)$$

Specific heat, Btu/lb_m-°R

$$C_p = \left(\frac{T}{1000} - 1\right) .02 + .2486$$

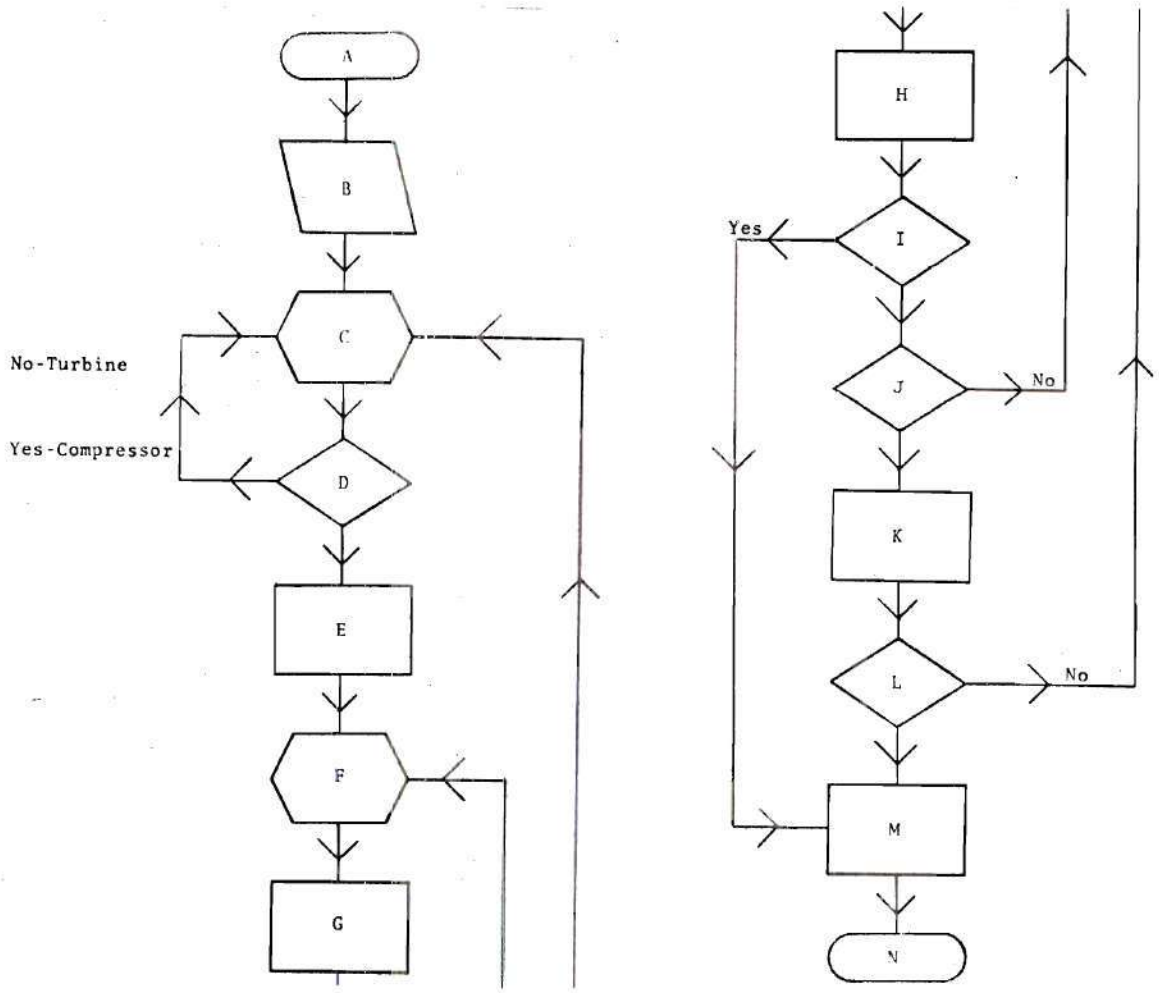

Figure 3-2. Program Flowchart

Description of Figure 3-2

A Start, dimension statements, call plot

B Input data, wheel geometry, speed, stagnation entrance properties

C Specify a flowrate

D Is gas velocity greater than wheel speed? No--turbine return to C, yes--compressor return to C.

E Isentropic converging section

F Specify increment in control volume analysis

G Perform control volume analysis by solving fundamental equations

H Calculate control volume exit properties (e.g. P(J+1) = P(J)+dP)

I Is flow choked? Yes--go to M

J Have 100 iterations been completed? No--return to F

K Isentropic diverging section. Calculate P_1-P_2, eff_T, eff_u, H_p, T_1-T_2

L Is maximum flowrate reached? No--return to C. Yes--read additional data if available

M Draw axis, plot data

N Stop. Data set, subroutine

Accumulative properties such as work and heat transfer are numerically integrated along the arc by the computer which adds the contributions of each increment. Choking will limit the mass flow through the rectangular cross section, in a manner similar to Fanno or Rayleigh flow. This is signified in the operation of the program by change of sign of the C3 term in the denominator of dV. When this occurs, attempts to run at higher flowrates are useless. Then program operation is passed to the plotter.

Following a successful march through the arc, without choking, isentropic relations are again used to determine stagnation properties of the gas leaving the disk. These, with the accumulated work term are used to calculate efficiencies, power and temperature and pressure differences. Higher flowrates are then attempted until choking occurs or in the case of the compressor, when inlet gas velocity exceeds wheel speed which results in zero pressure increase and an ineffective compressor.

3-2. Computer Analysis (Variable Area)

In the previous discussion, for constant cross sectional flow, dA was zero and took no part in turbine performance. When variable areas are incorporated into the analysis, two possibilities exist. First, dA could be specified as constant or as some function of arc position. Then the turbine performance could be determined for any particular

variable area geometry. The user would be left to randomly try geometries in an attempt to optimize performance.

A second technique, however, is a more direct method to optimize turbine performance. Since the fluid stresses vary as the square of gas velocity, the optimum velocity for turbine performance is first established. Then the area profile required to maintain that velocity is calculated. The maximum height to width ratio is arbitrarily limited to ten in order to remain within reasonable machining capabilities. Since the varying area maintains constant velocity through the turbine, exceeding height to width ratio of ten indicates flowrate too great for the turbine, and is equivalent to choking.

To maintain constant velocity through the turbine,

$$dV = 0 = \frac{C_4}{C_3}$$

Therefore,

$$C_4 = 0$$

$$\frac{C_1}{RT} - \frac{C_2 P}{RT^2} + \rho \frac{dA}{A} = 0$$

and

$$\frac{dA}{A} = \frac{1}{\rho}\left[\frac{C_2 P}{RT^2} - \frac{C_1}{RT}\right]$$

3-3. Friction Factor Subroutine

A subroutine has been written to calculate turbulent and laminar friction factors from Reynolds numbers. Using the empirical relations of Section 2-3 the subroutine (Appendix B) calculates the friction factor directly for Reynolds numbers less than 2000 from

$$f = 64/Re \tag{7}$$

Reynolds numbers greater than 2000 require use of Prandtl's Law of Friction Factors,

$$\frac{1}{\sqrt{f}} = 2.0 \log_{10} (Re\sqrt{f}) - .8 \tag{7}$$

In order to solve this equation, the subroutine is strictly a trial and error convergence routine. Beginning with $f = .05$ the program adds or subtracts $.025 (\frac{1}{2})^n$, where n equals the number of prior attempts, depending on whether the previous guess was high or low. Using this technique the computer approaches the correct f for a given Re. Ten iterations result in accuracy within four percent.

CHAPTER IV

RESULTS OF ANALYSIS

4-1. Comparison of Theoretical and Experimental Data

Measurements are not available for actual high speed viscous turbine performance. However, a viscous compressor has been tested (references 1 and 2). Figures 4-1, 4-2 and 4-3 compare empirical data from these reports and theoretical data from the computer model discussed in Chapter III for a 6.6 inch diameter compressor at various rotational speeds. The correlation is remarkably good at low speeds with increasing disparity at higher speeds. This was expected due to the increased difficulty of sealing the test apparatus at higher speeds and pressures. Whereas, the computer model has assumed perfect seals with no leakage at any speed.

Logically speaking, sealing should not be as critical in a viscous turbine as in the compressor. In the compressor, air has the tendency to leak back from the high pressure outlet opposite to the flow to the atmosphere. However, all of the turbine gases exit and there is no tendency for low pressure air to leak back into the higher pressure inlet region. Therefore, correlation between theoretical and empirical turbine data is expected to be even better than that shown for the compressor.

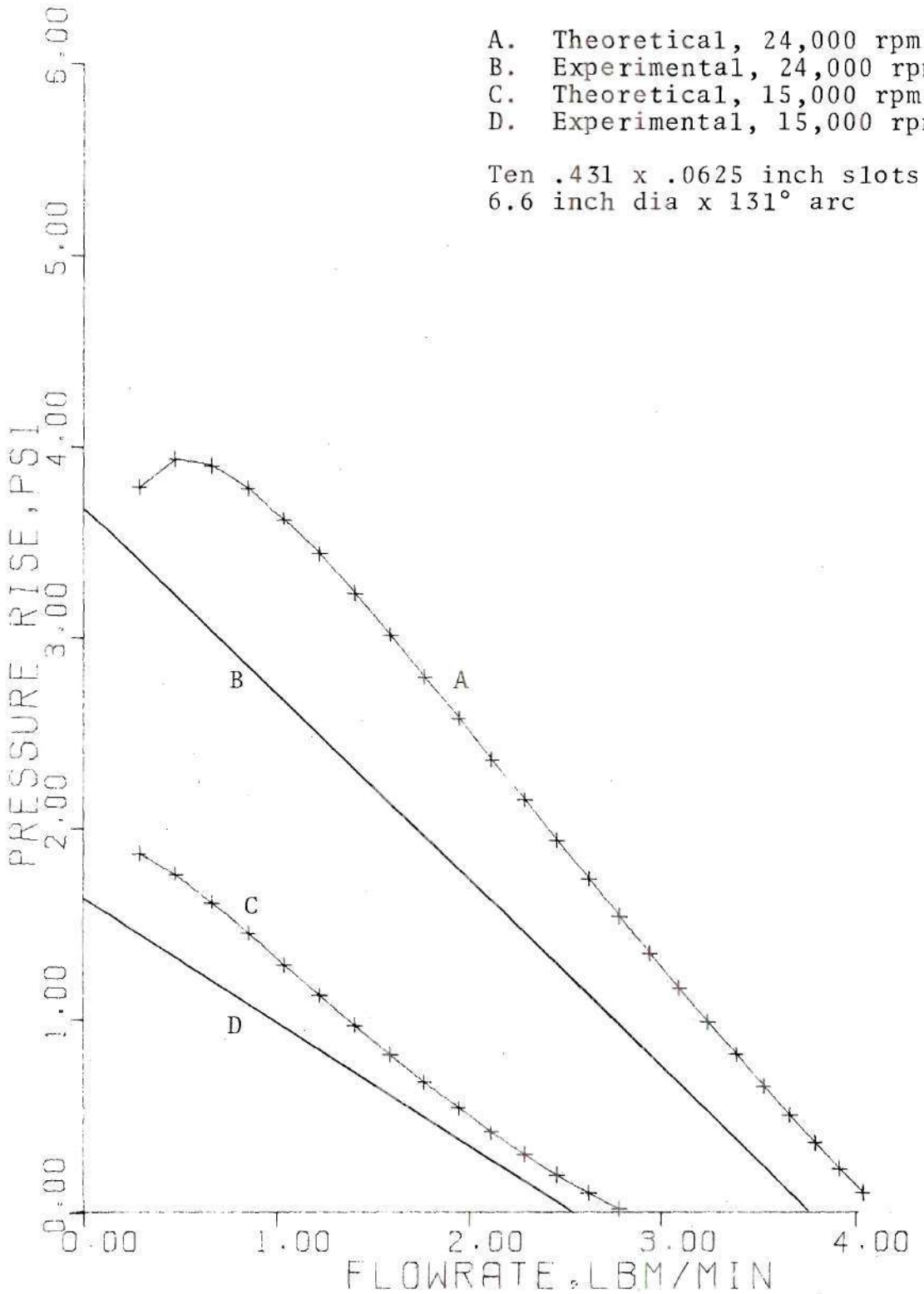

Figure 4-1. Experimental and Theoretical Data Correlation in Compressor

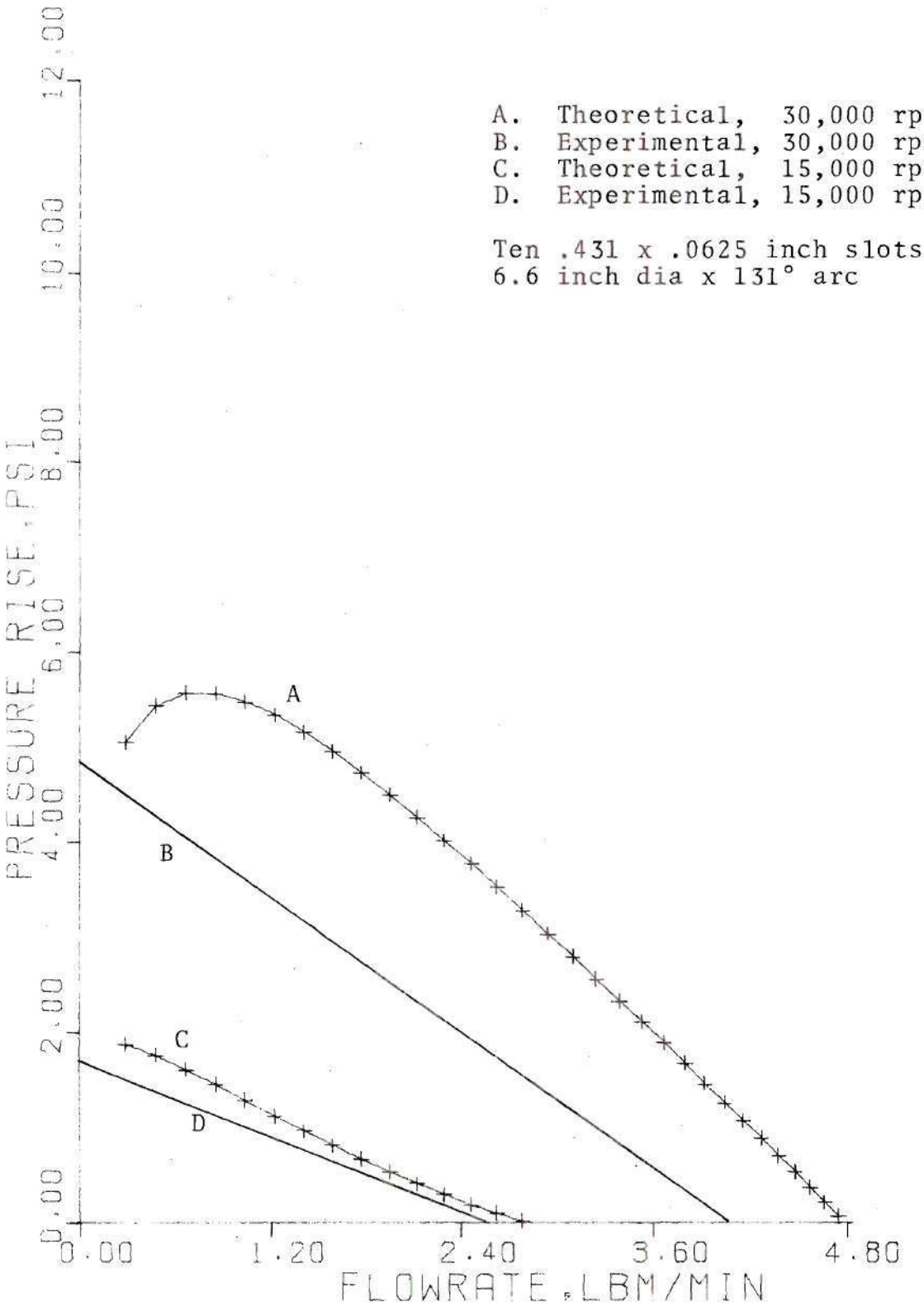

Figure 4-2. Experimental and Theoretical Data Correlation in Compressor

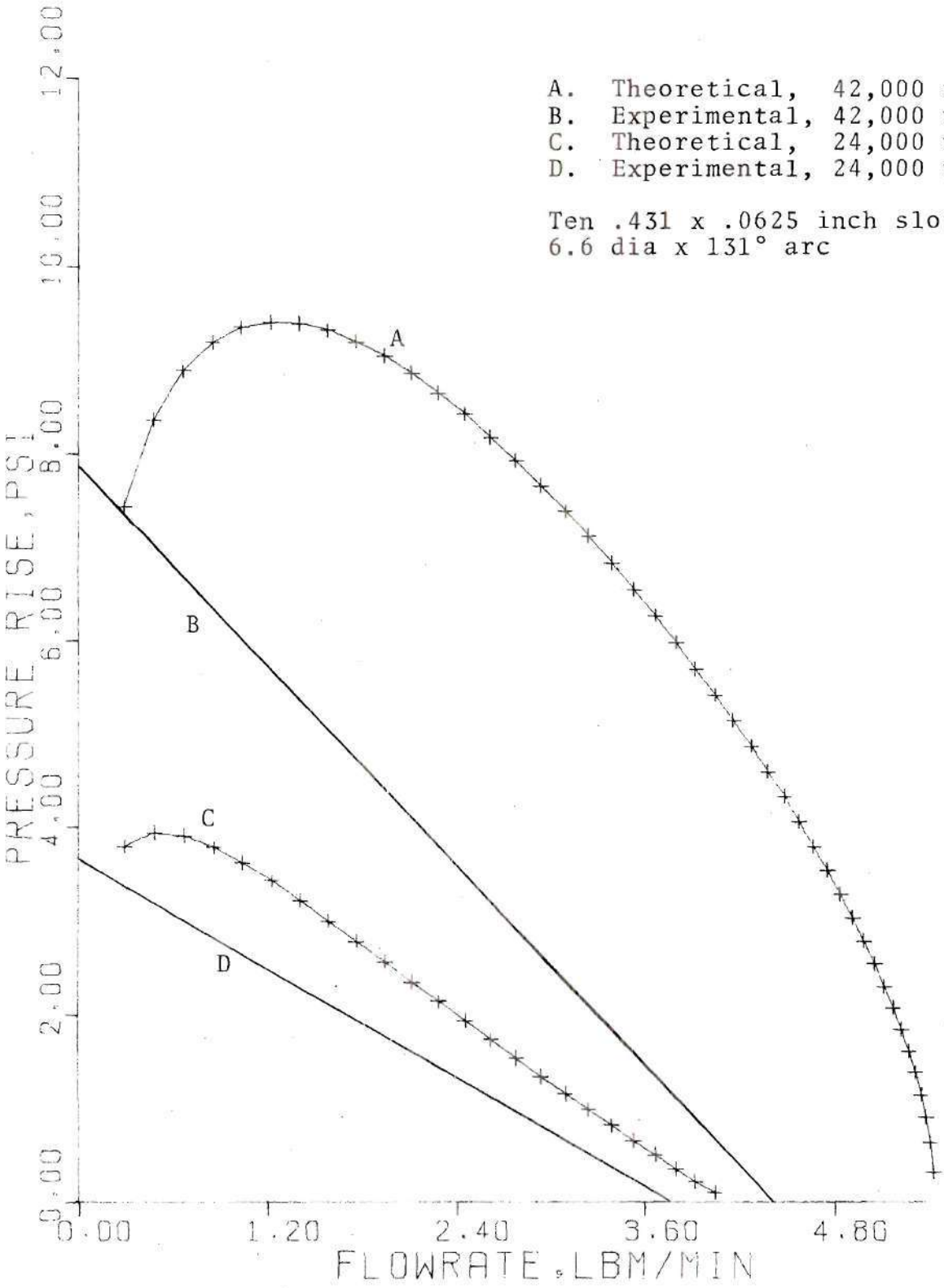

Figure 4-3. Experimental and Theoretical Data Correlation in Compressor

4-2. Limiting Cases and Outer Wall Losses

In order that the analysis be valid, it must correctly evaluate the limiting cases where solutions are known.

Zero Wheel Speed

The first such case is adiabatic flow when the wheel is static. These computer predictions are the same as well tabulated Fanno flow. For a 60 inch diameter turbine with 1.5 x .15 inch slots and a flowrate of 33.7 lb_m/min at an entrance pressure of 50 psia and temperature of 3960°R, the model predicts a total pressure drop of 28.2 psi Fanno flow for the same arc length and conditions predicts a 28.4 psia total pressure drop.

Gas Velocity Relative to Wheel Speed

Neglecting the outer wall drag, the computer model indicates net work in for wheel speed greater than gas velocity and work out for wheel speed less than gas velocity as expected. However, addition of the static wall stress causes negative pressure rise at gas velocity equal to and slightly lower than wheel speed due to the losses along the wall. In Figure 4-4 the curve without wall stress crosses the axis at the flowrate where velocity equals wheel speed. With the wall stress, zero pressure differential is found at slightly lower velocities.

Converging-Diverging Section Without Friction

Air flow without heat transfer or friction is isentropic. Under these conditions, the program was found to agree with

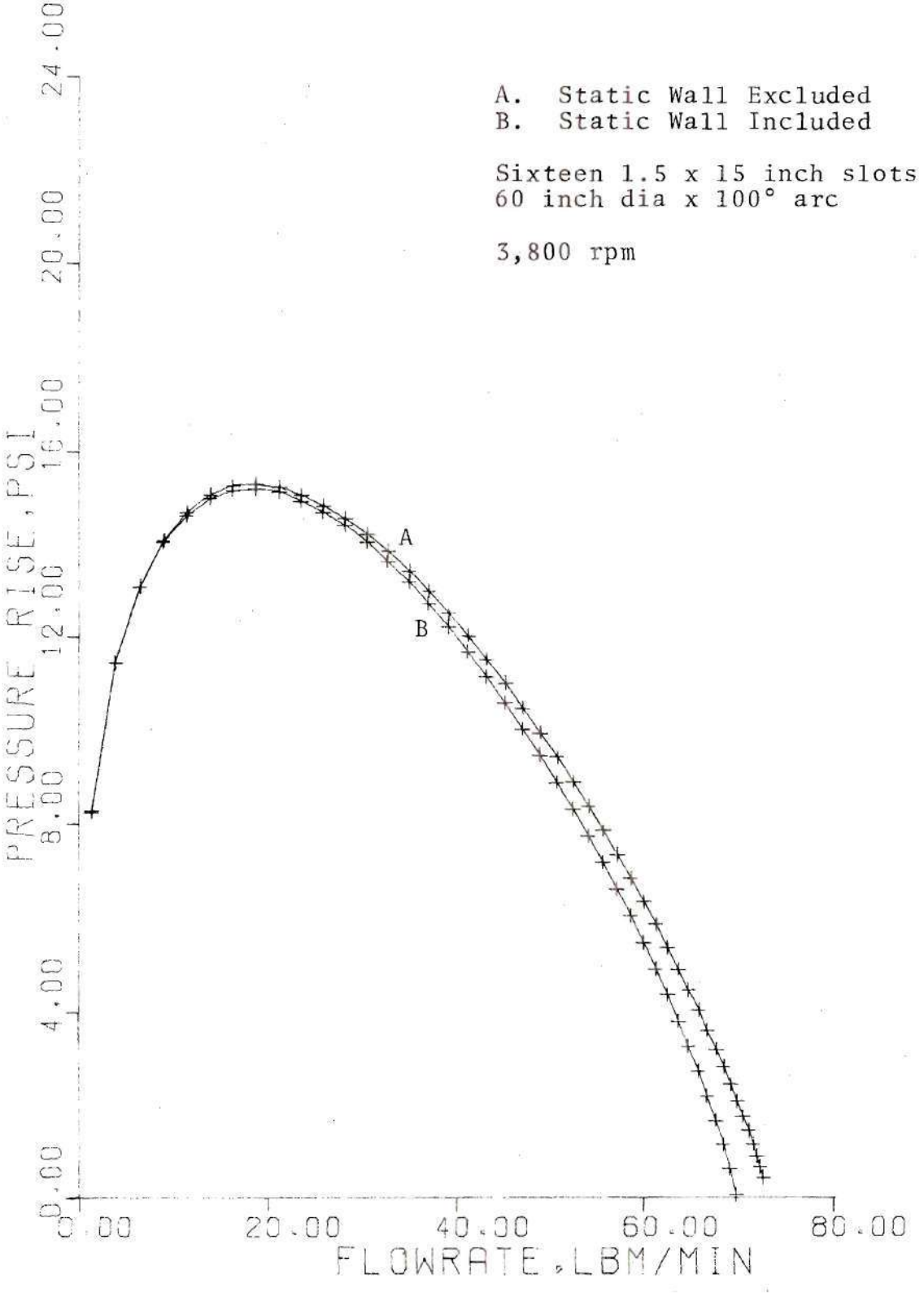

Figure 4-4. Compressor Performance

isentropic tables within 2 percent except for mach numbers between .95 and 1.05. The finite difference method breaks down in this range due to the rapid change in velocity over a small distance as choked flow is approached.

Effect of Outer Wall Drag on Efficiency

Figures 4-5 and 4-6 show the effects of the outer wall on compressor and turbine efficiency. As was expected, the static losses reduce both compressor and turbine efficiency. The effects are most pronounced as gas velocities approach wheel speed. This is because the static wall losses become relatively larger compared to the small pressure differences created by a very small relative speed between the gas and rotor. Figure 4-7 shows the disparity in efficiency increasing as the pressure differential approaches zero.

4-3. Turbine Optimization

Allowing a maximum slot height to width ratio of ten to facilitate manufacture of the disks, optimum turbine efficiency as shown in Figure 4-8 has been determined to be 44 percent. Figure 4-8 also clearly illustrates the transition between laminar and turbulent flow through the rotor slots. The effects of other parameters on turbine performance are demonstrated in Figures 4-9 through 4-14. Variable arc length produces the same effects as variable diameter at equivalent rim speed and is not included.

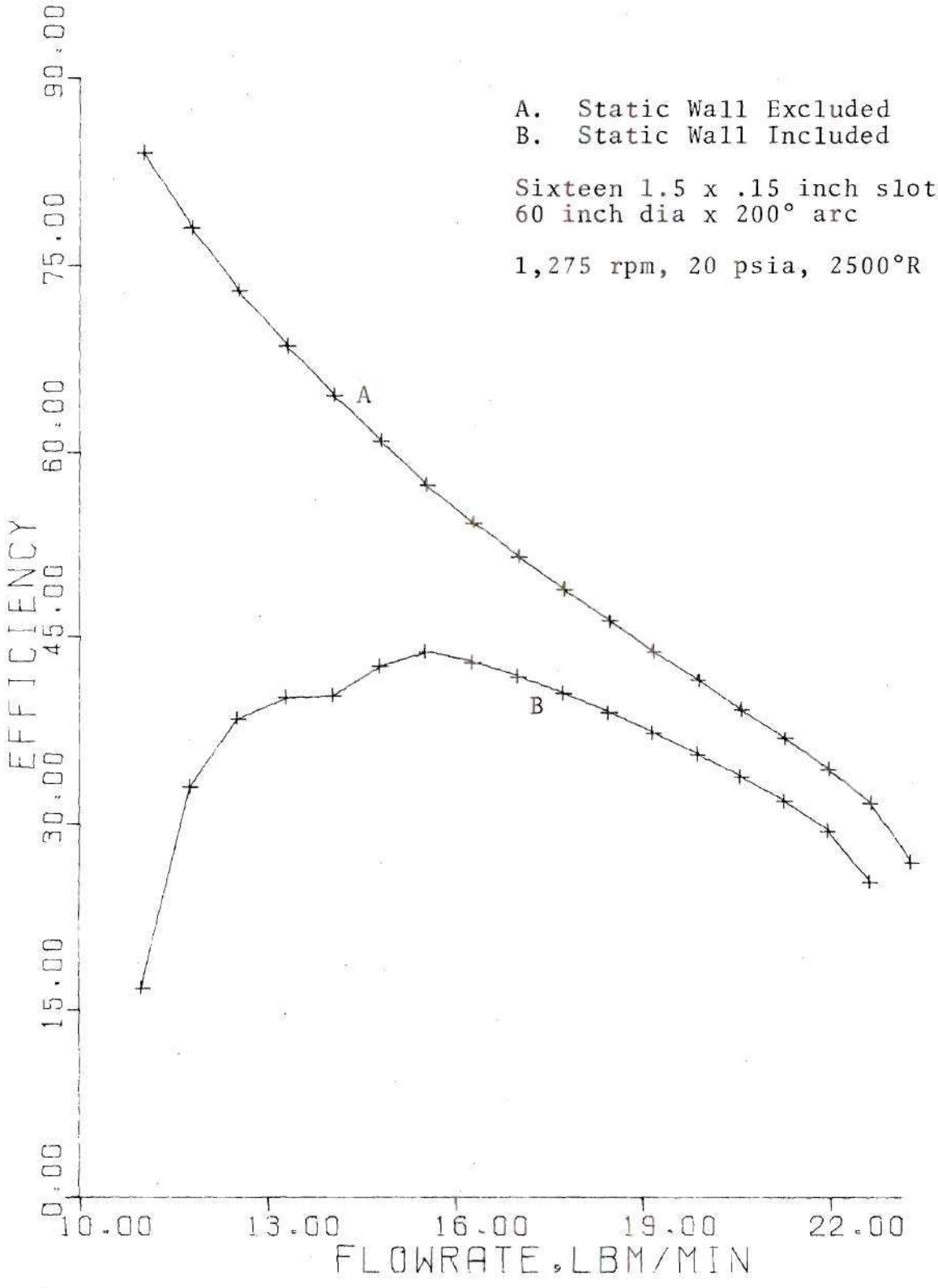

Figure 4-5. Turbine Performance

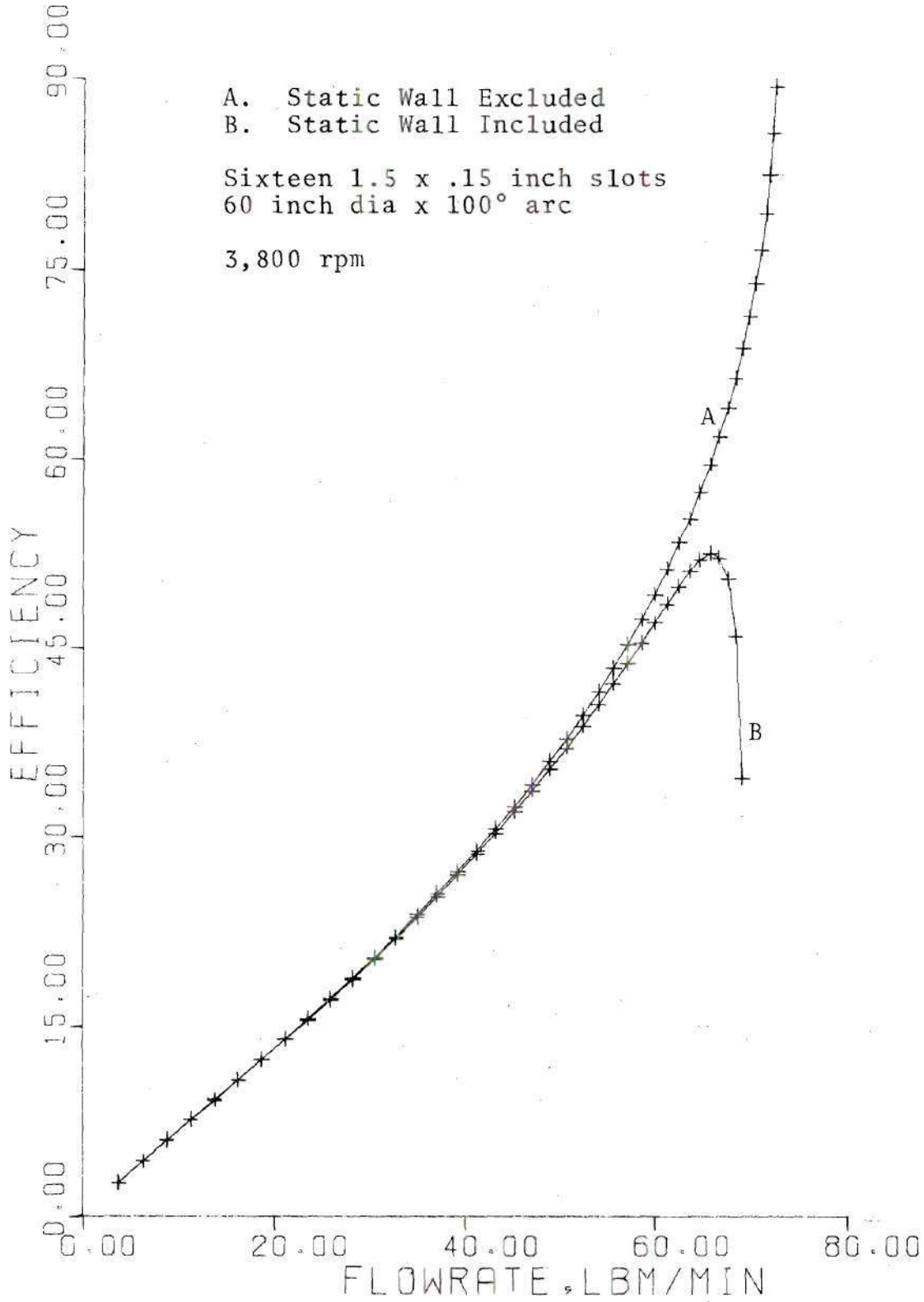

Figure 4-6. Compressor Performance

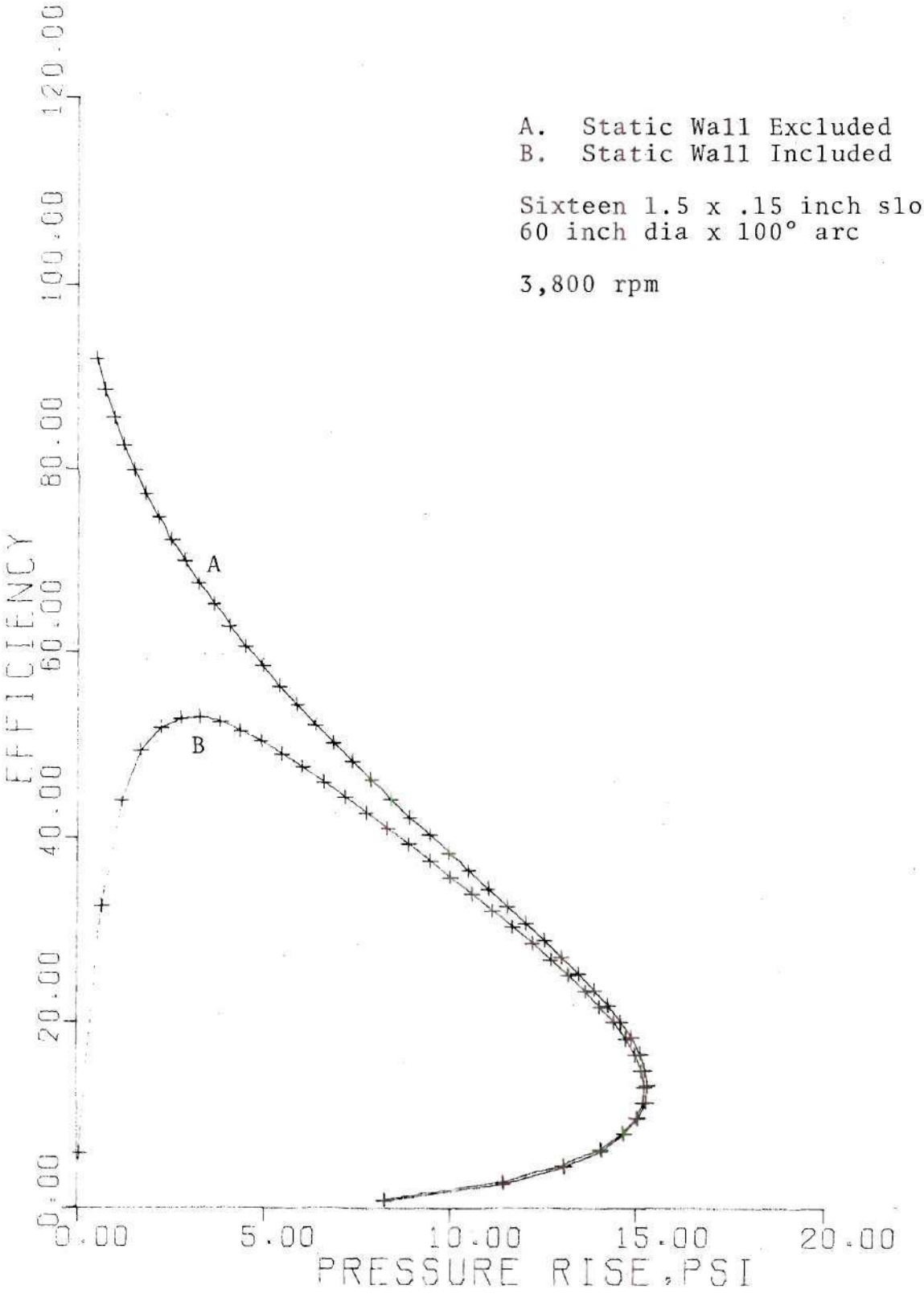

Figure 4-7. Compressor Performance

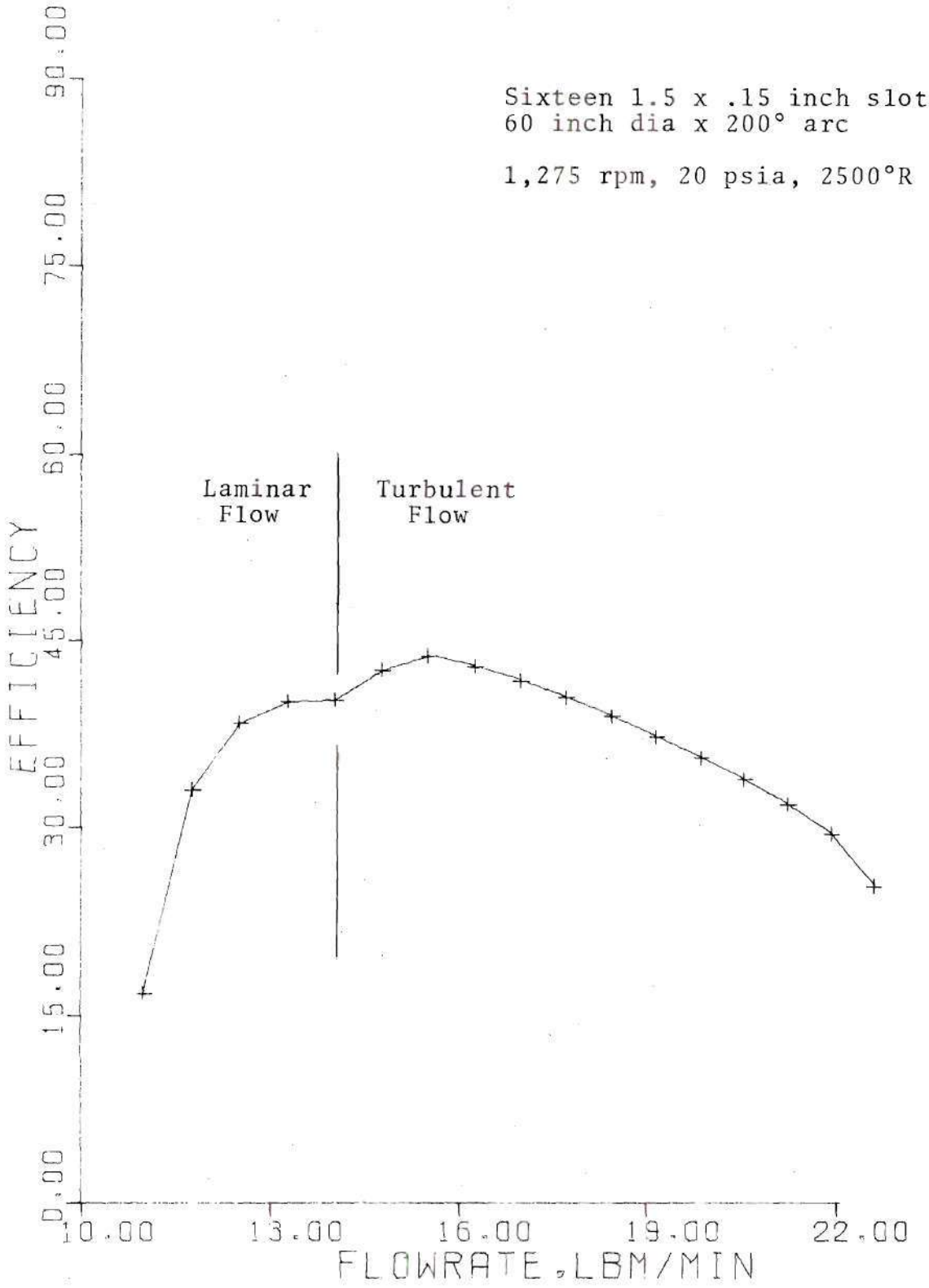

Figure 4-8. Turbine Performance

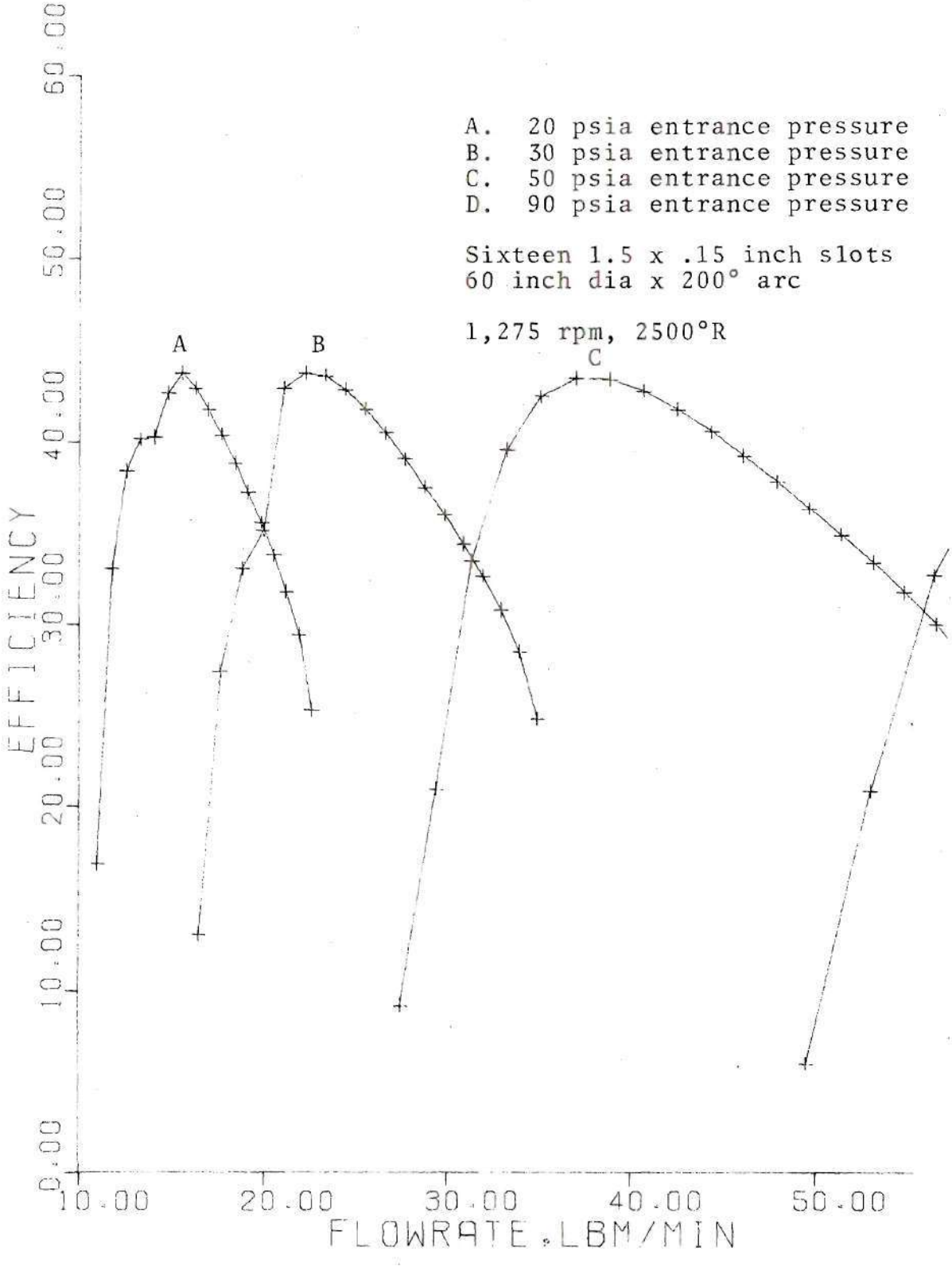

Figure 4-9. Turbine Performance

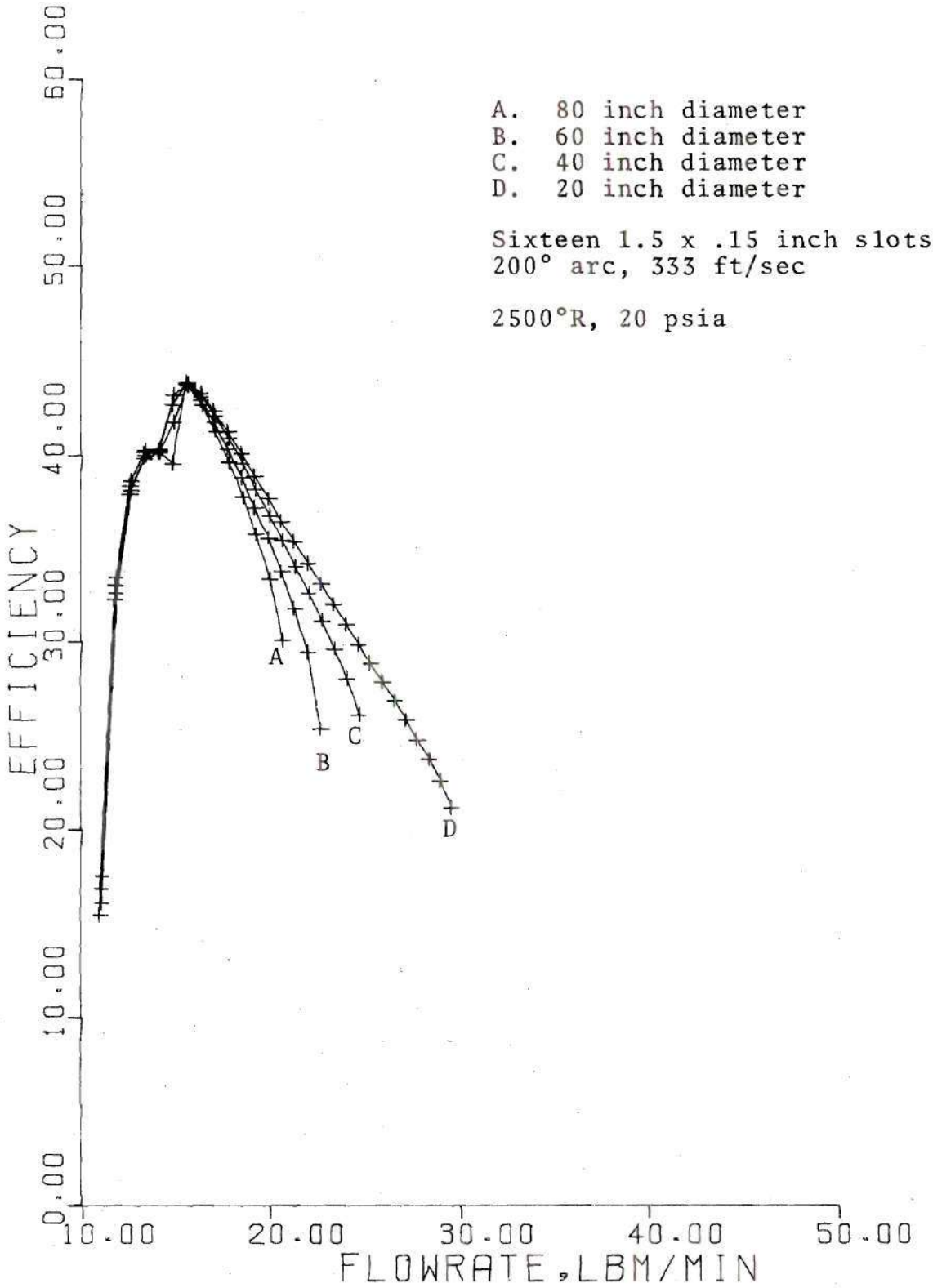

Figure 4-10. Turbine Performance

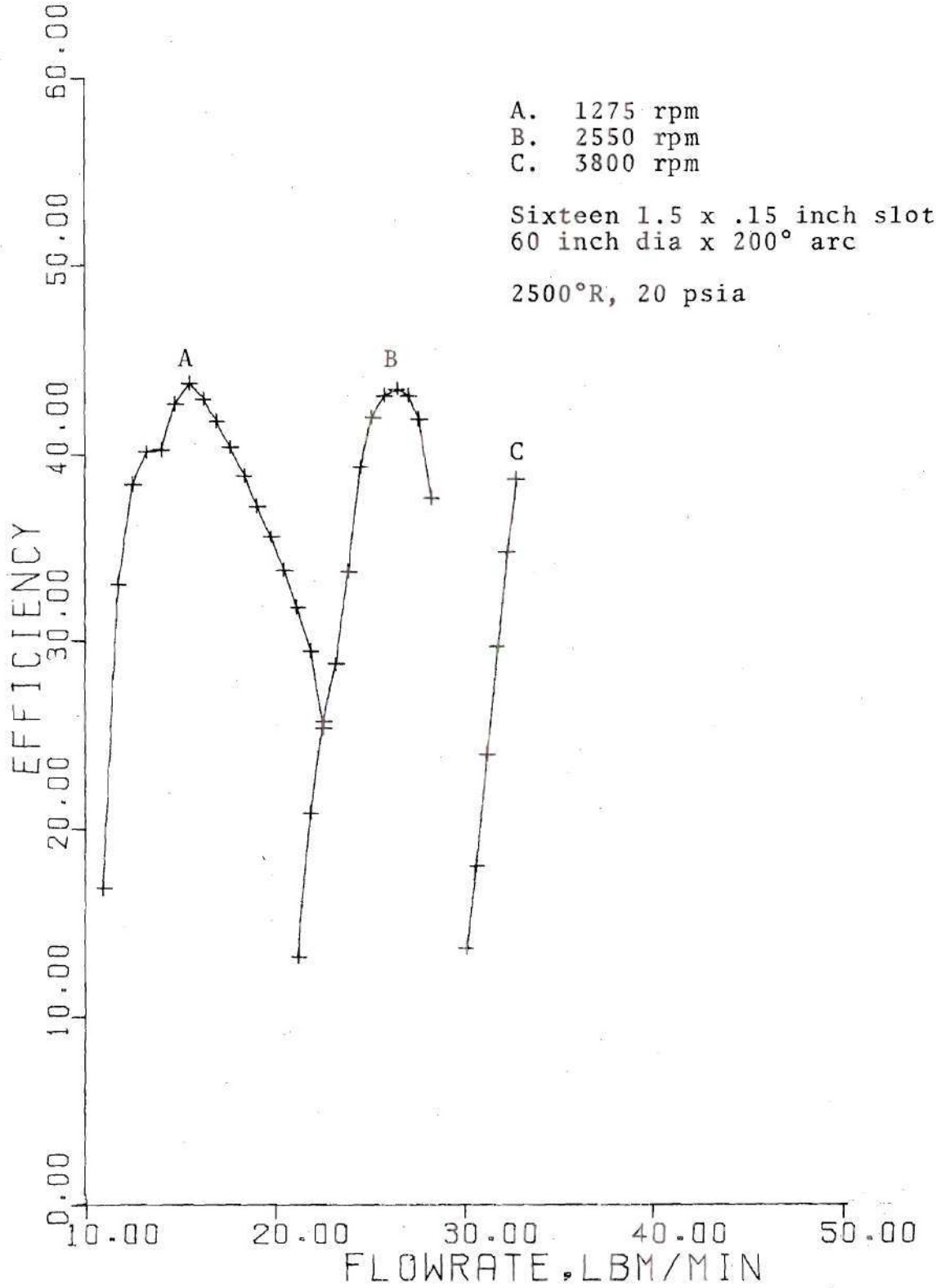

Figure 4-11. Turbine Performance

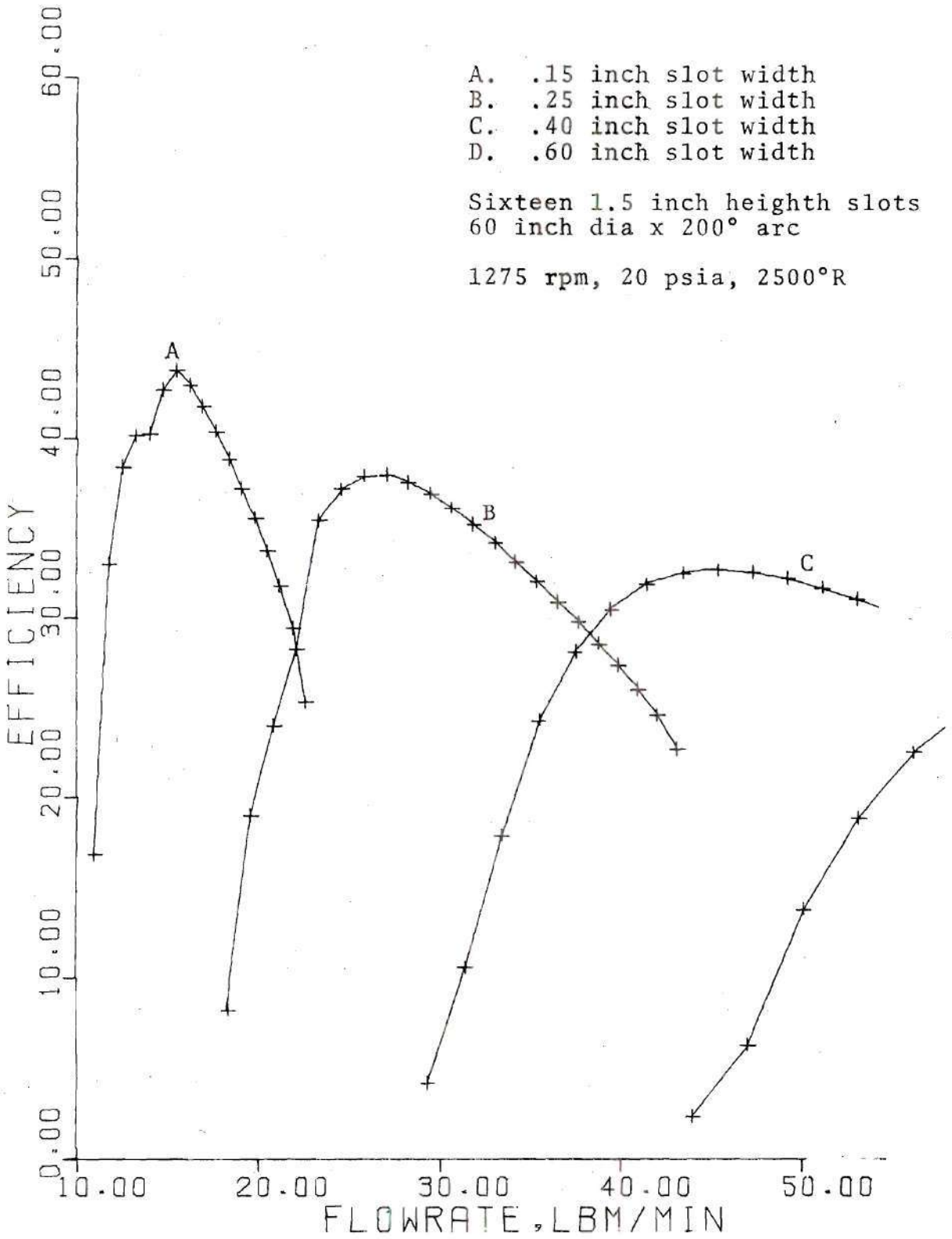

Figure 4-12. Turbine Performance

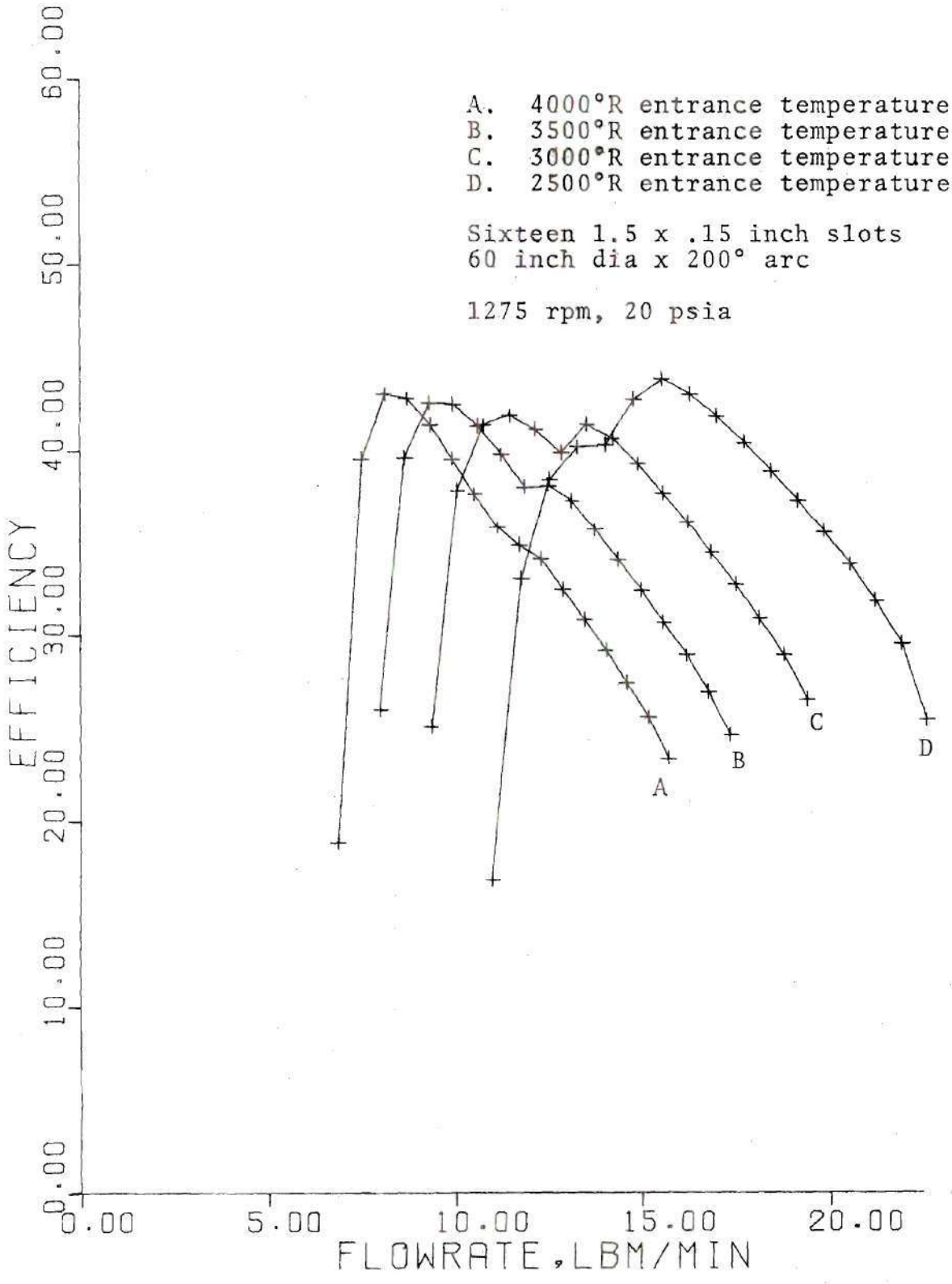

Figure 4-13. Turbine Performance

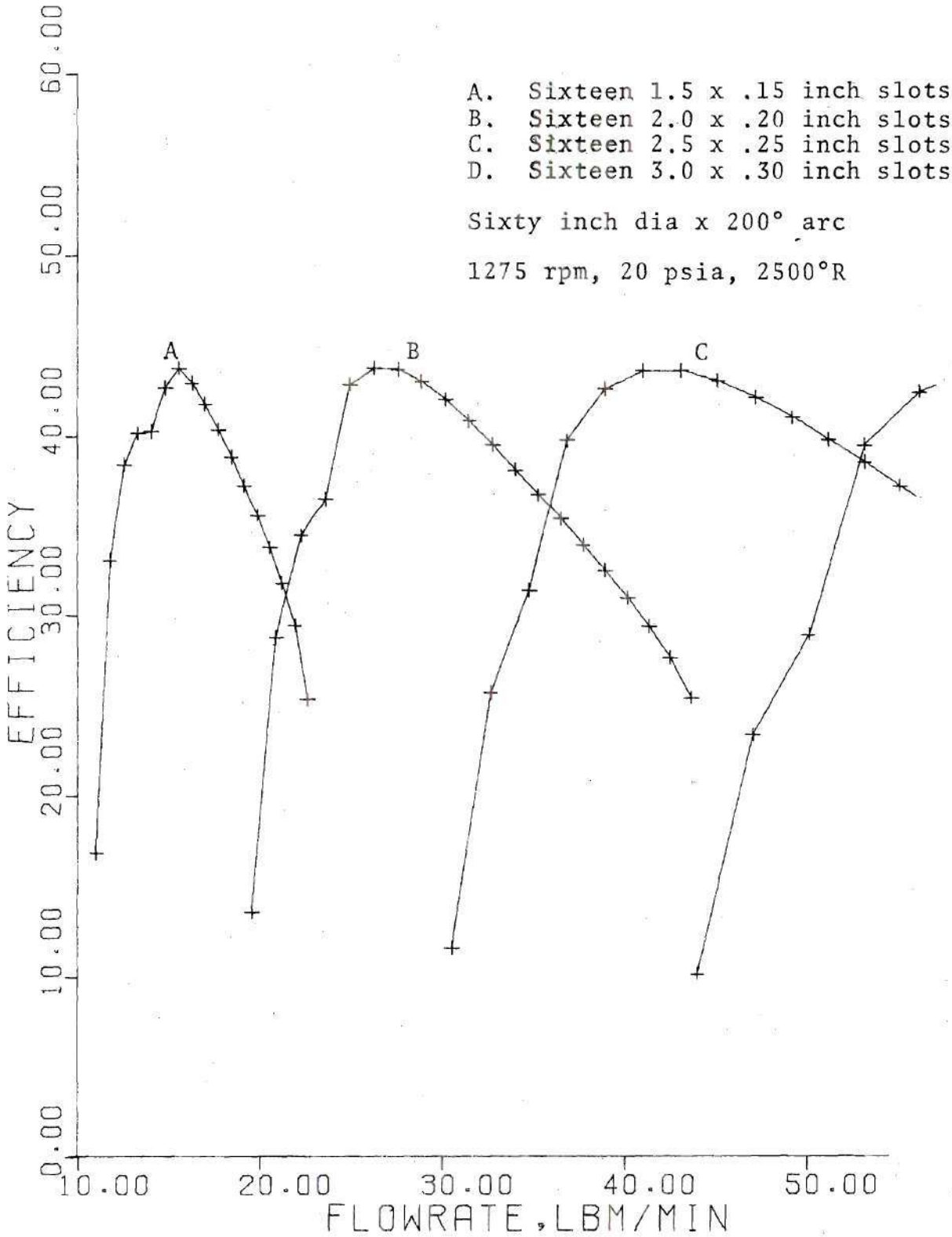

Figure 4-14. Turbine Performance

With exception of the slot width (Figure 4-12), the parameters have only minor effect on peak efficiency. Henceforth a minimum slot width of 1/10 the slot height will be considered. Geometry and rotational speed of the turbine do have significant effect on the output as reflected in the pressure drop (Figures 4-15 and 4-17). Even more meaningful are Figures 4-16, 4-18 and 4-19 which reveal a tradeoff between pressure ratio and efficiency. The inverse relationship was expected, considering that greater pressure ratios allow greater deviation from the ideal isentropic case.

Figure 4-18 shows combined efficiency and output increasing with turbine size or diameter for a given rim speed. Hence, the efficiency, output, and size (cost) of the turbine are all mutual tradeoffs. The same tradeoffs apply to a viscous rotating compressor. Figures 4-20 through 4-25 show a maximum compressor efficiency of 58 percent and a maximum pressure increase of 25 psi.

4-4. Variable Area Turbine

The pressure ratios of the viscous turbines are limited by choking. A concept of including a comb in the static housing to vary turbine flow area as a function of arc position has potential for increasing turbine pressure ratios. Increasing flow area, decreases gas velocity retarding choking and allowing greater entrance mach numbers and therefore greater relative velocity between the gas and

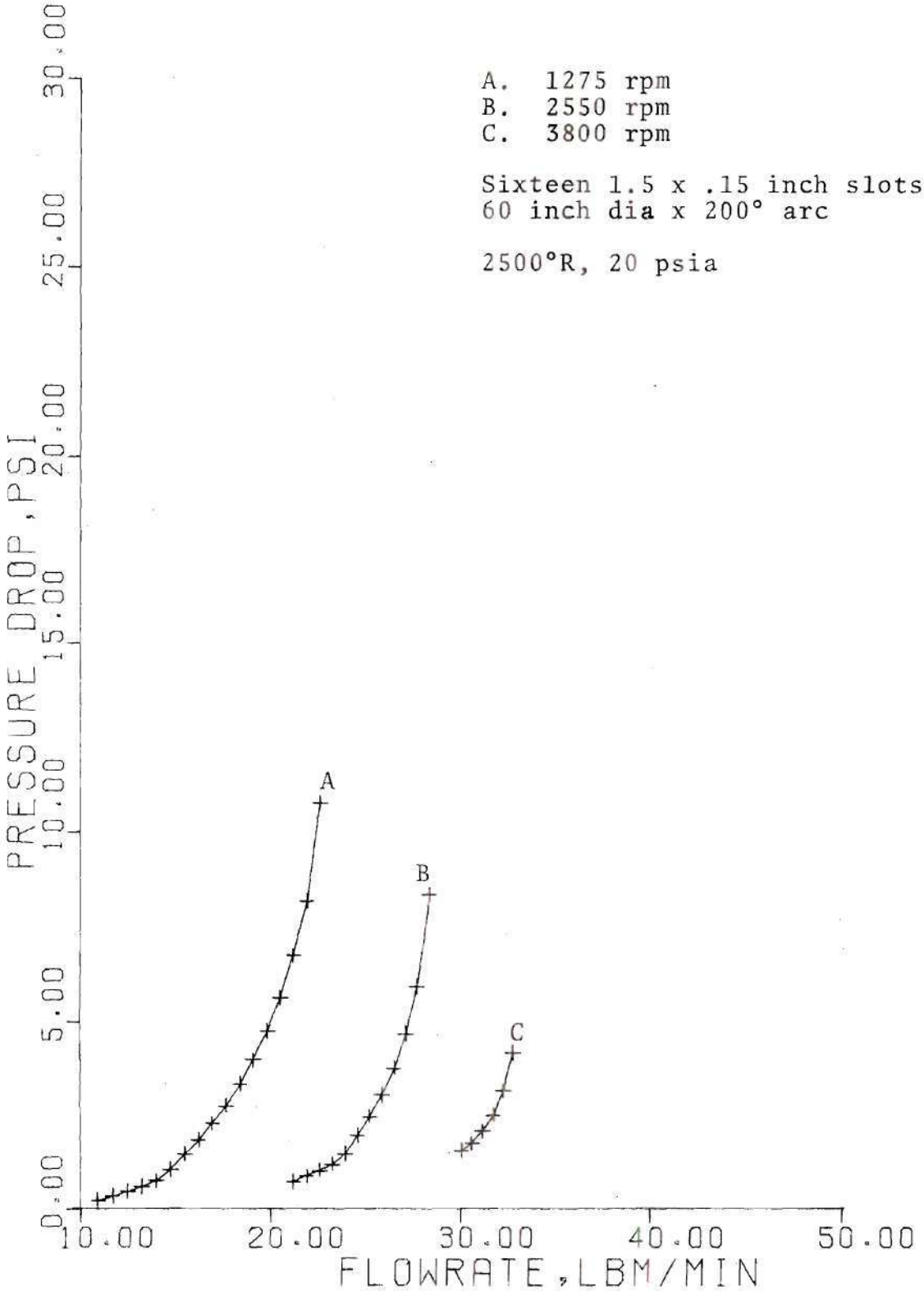

Figure 4-15. Turbine Performance

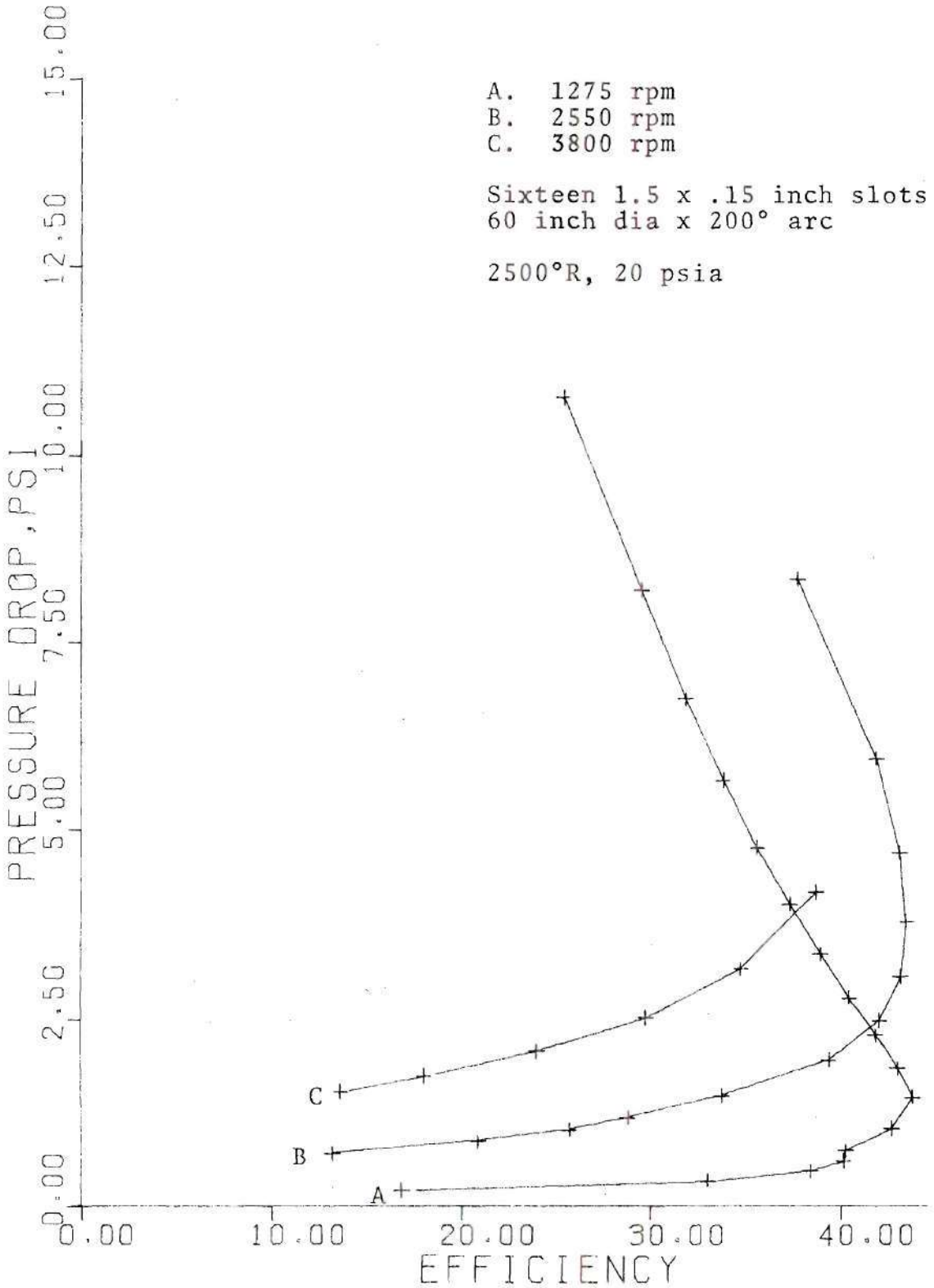

Figure 4-16. Turbine Performance

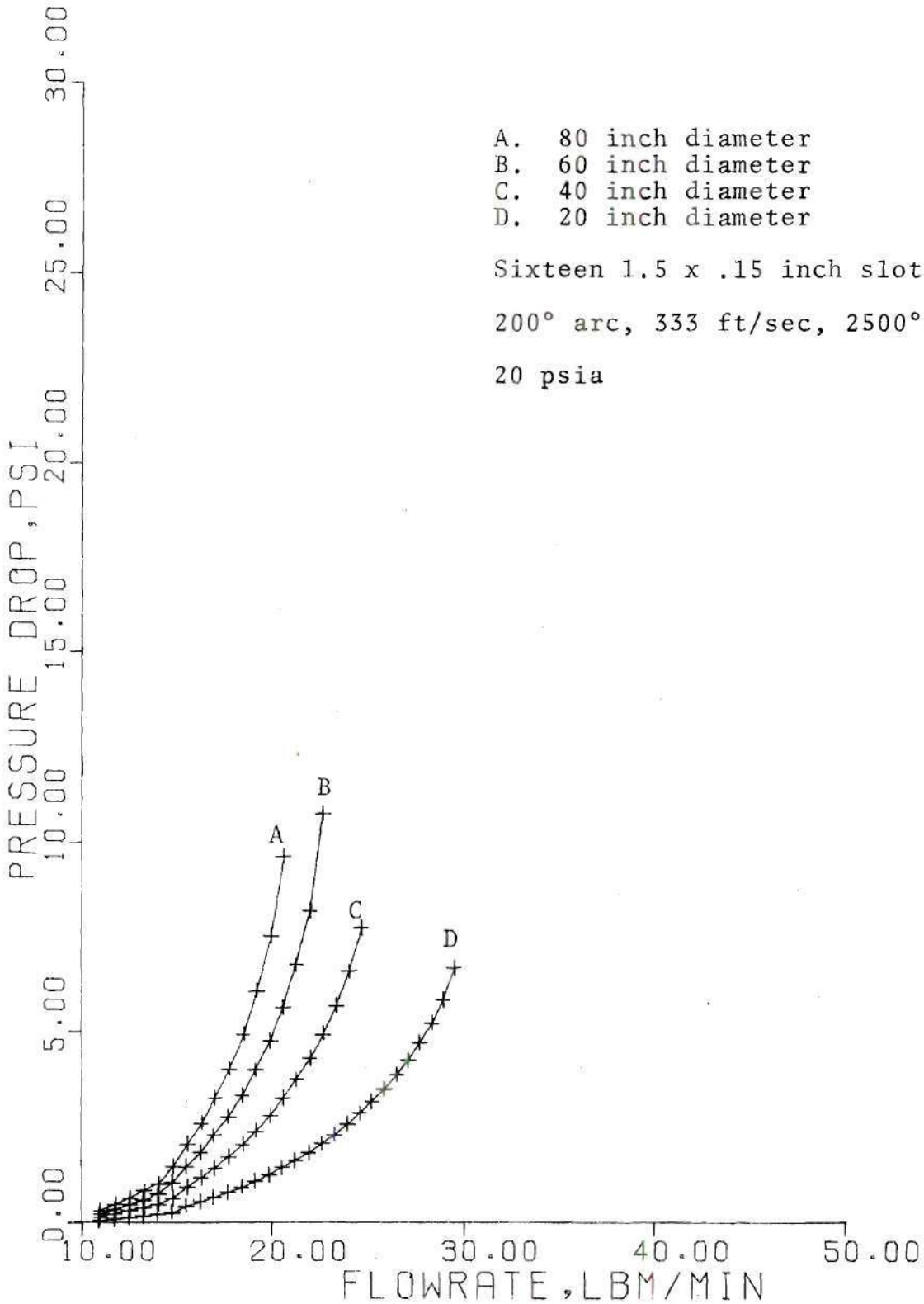

Figure 4-17. Turbine Performance

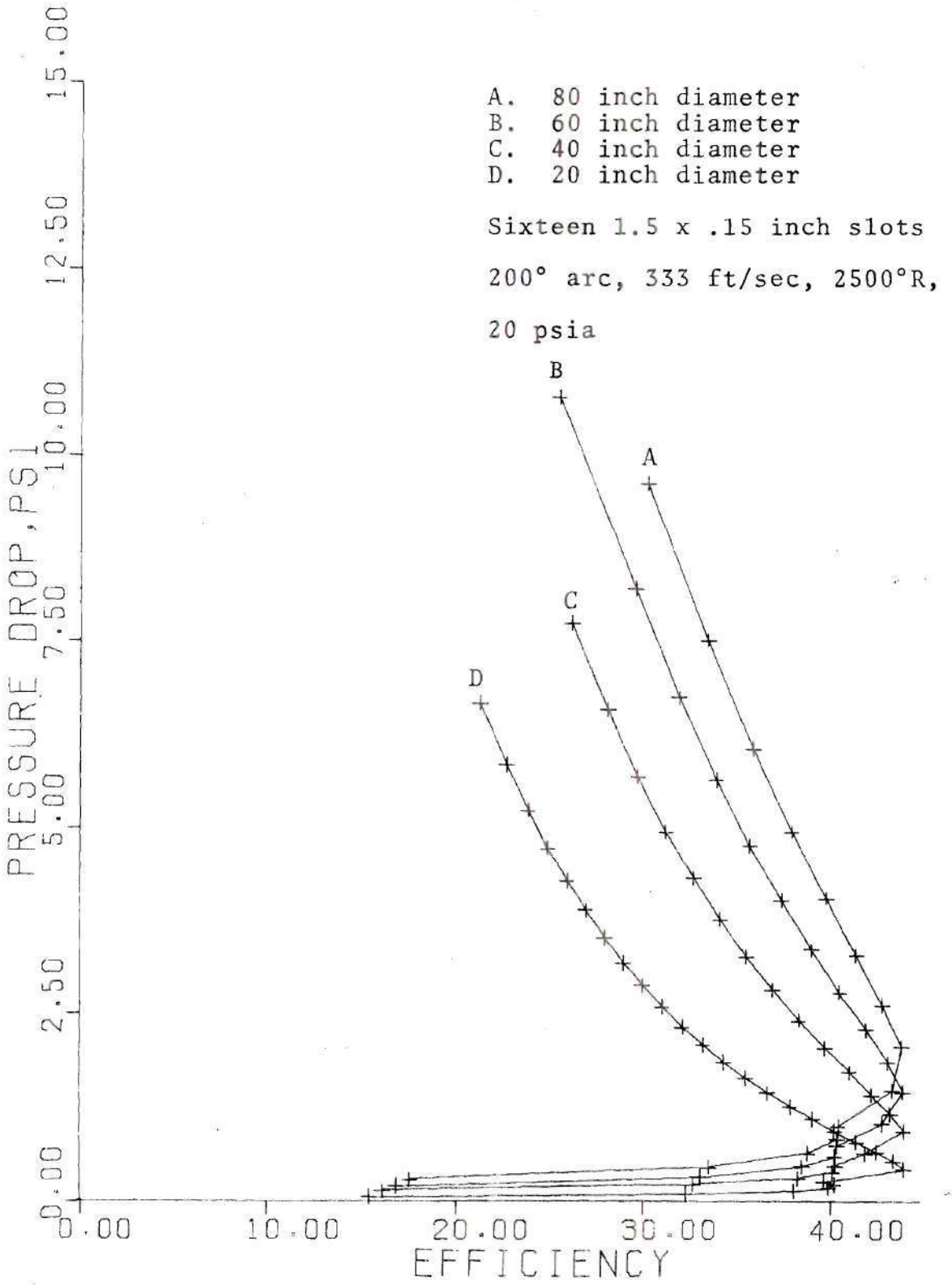

Figure 4-18. Turbine Performance

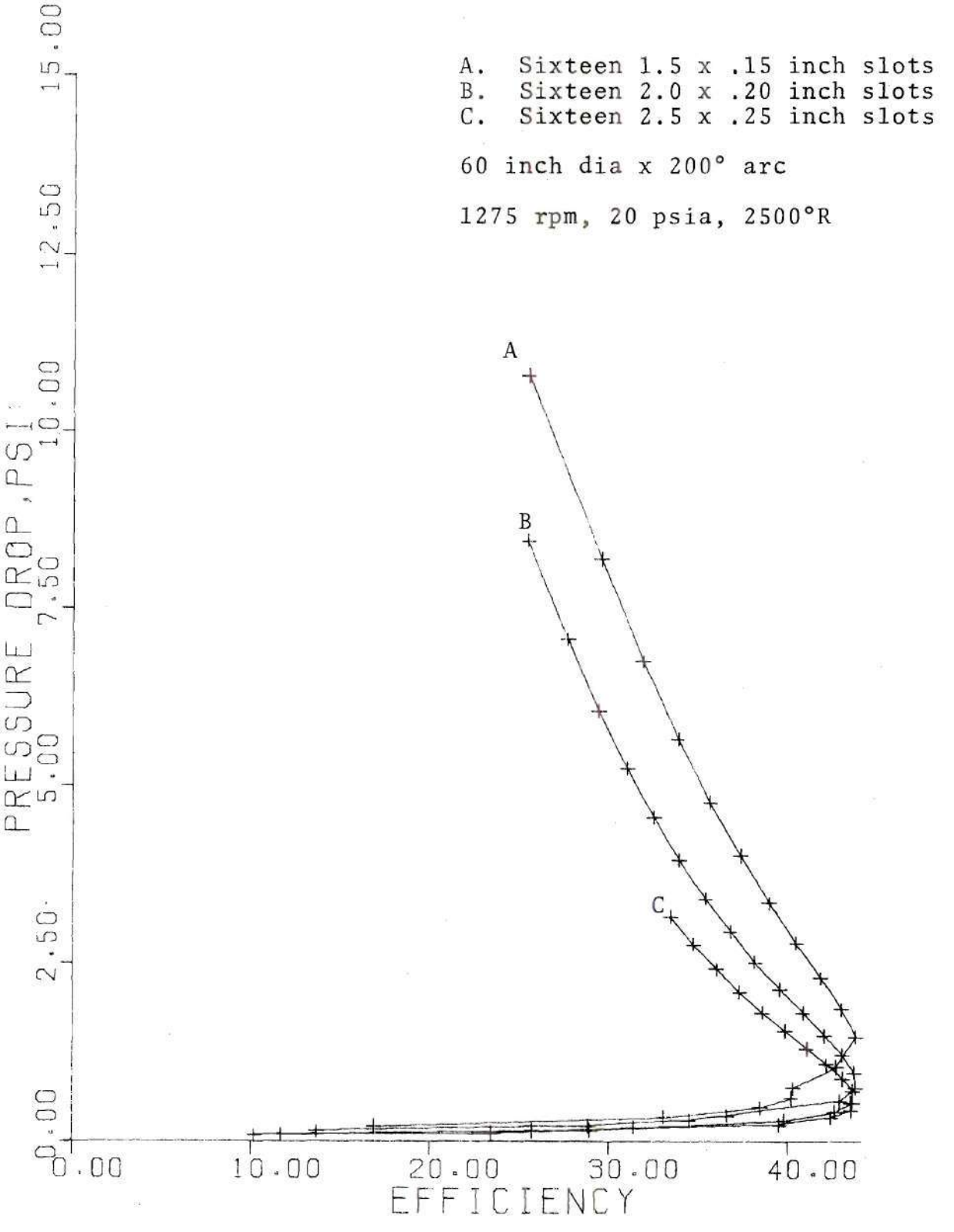

Figure 4-19. Turbine Performance

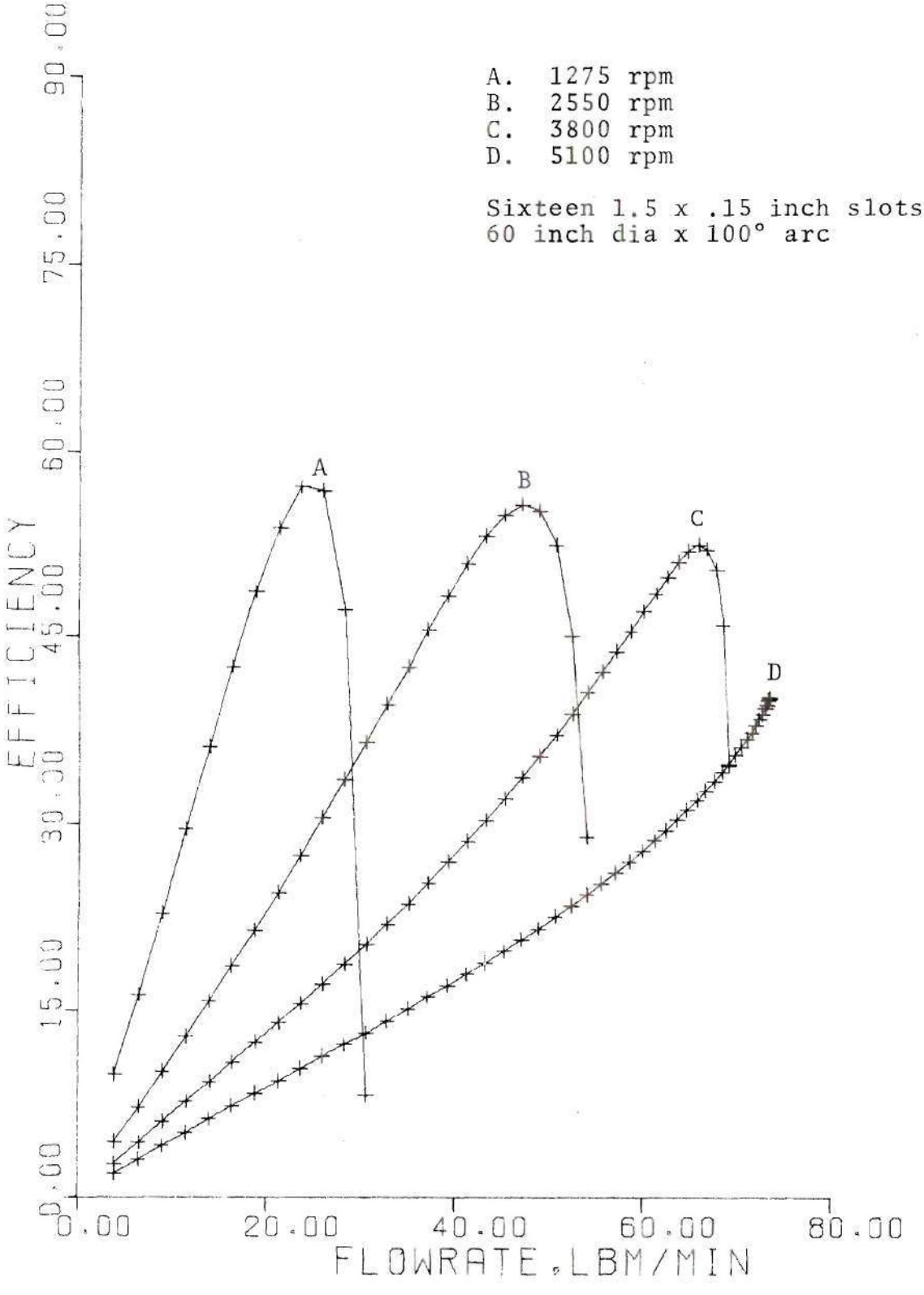

Figure 4-20. Compressor Performance

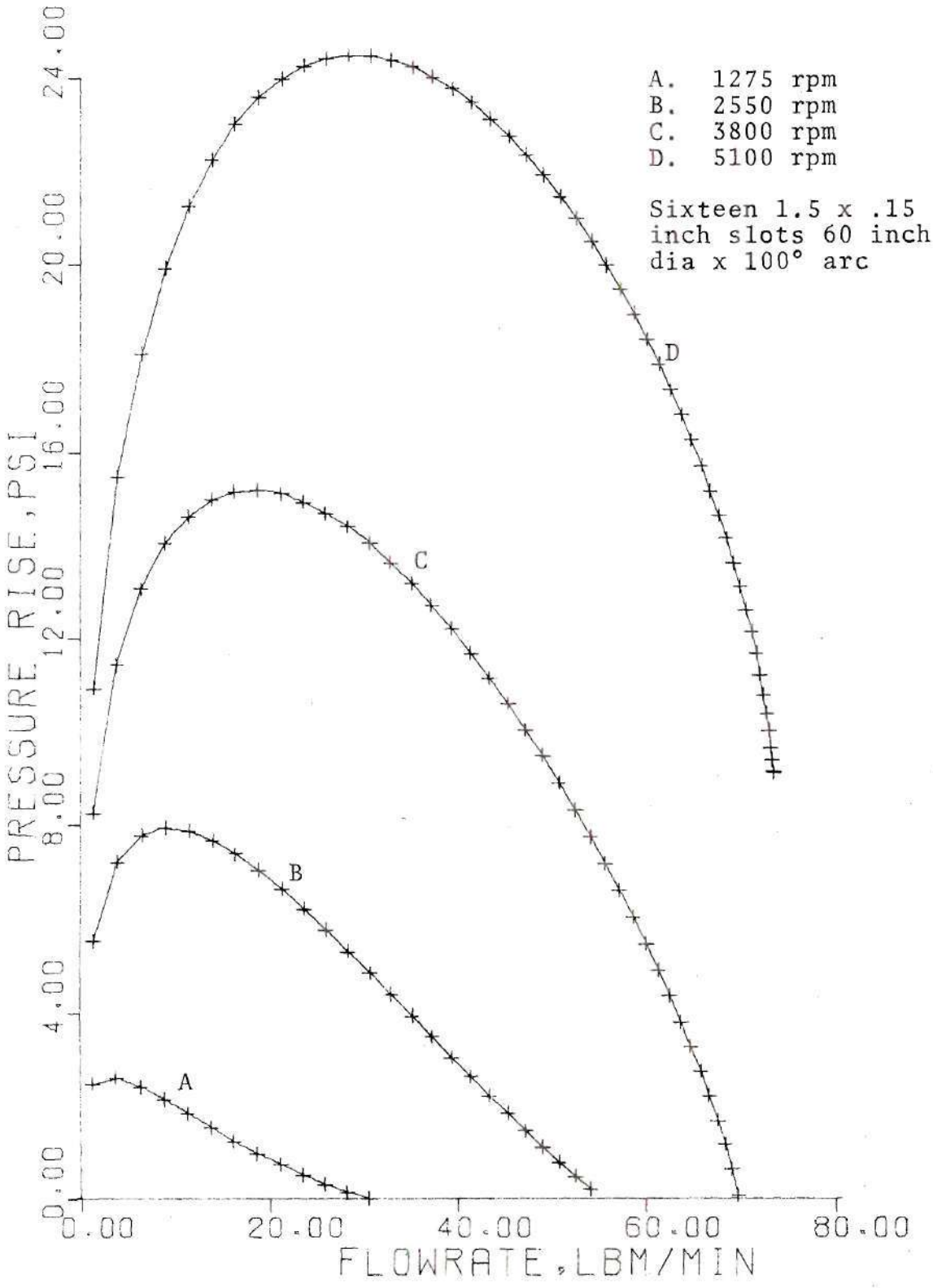

Figure 4-21. Compressor Performance

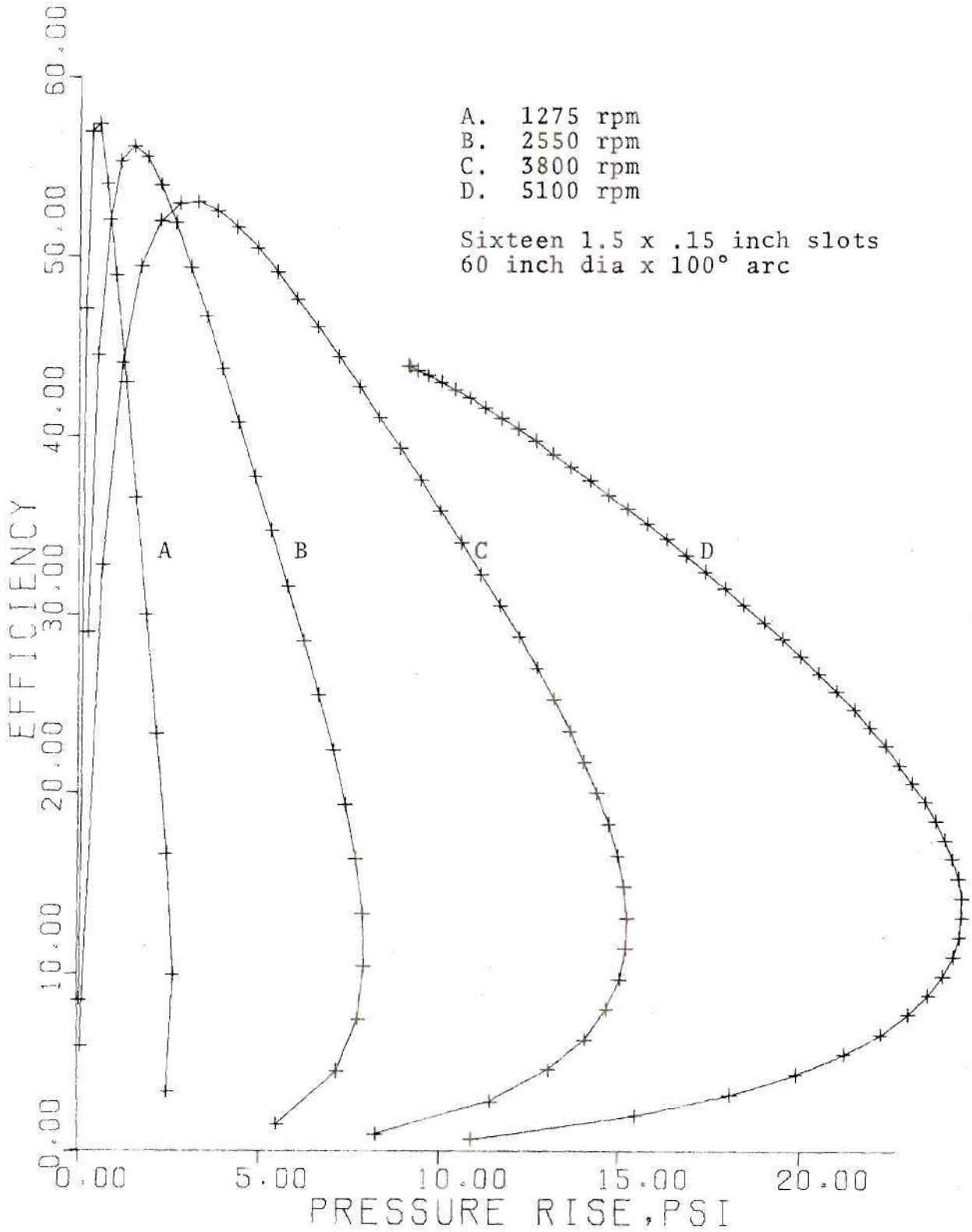

Figure 4-22. Compressor Performance

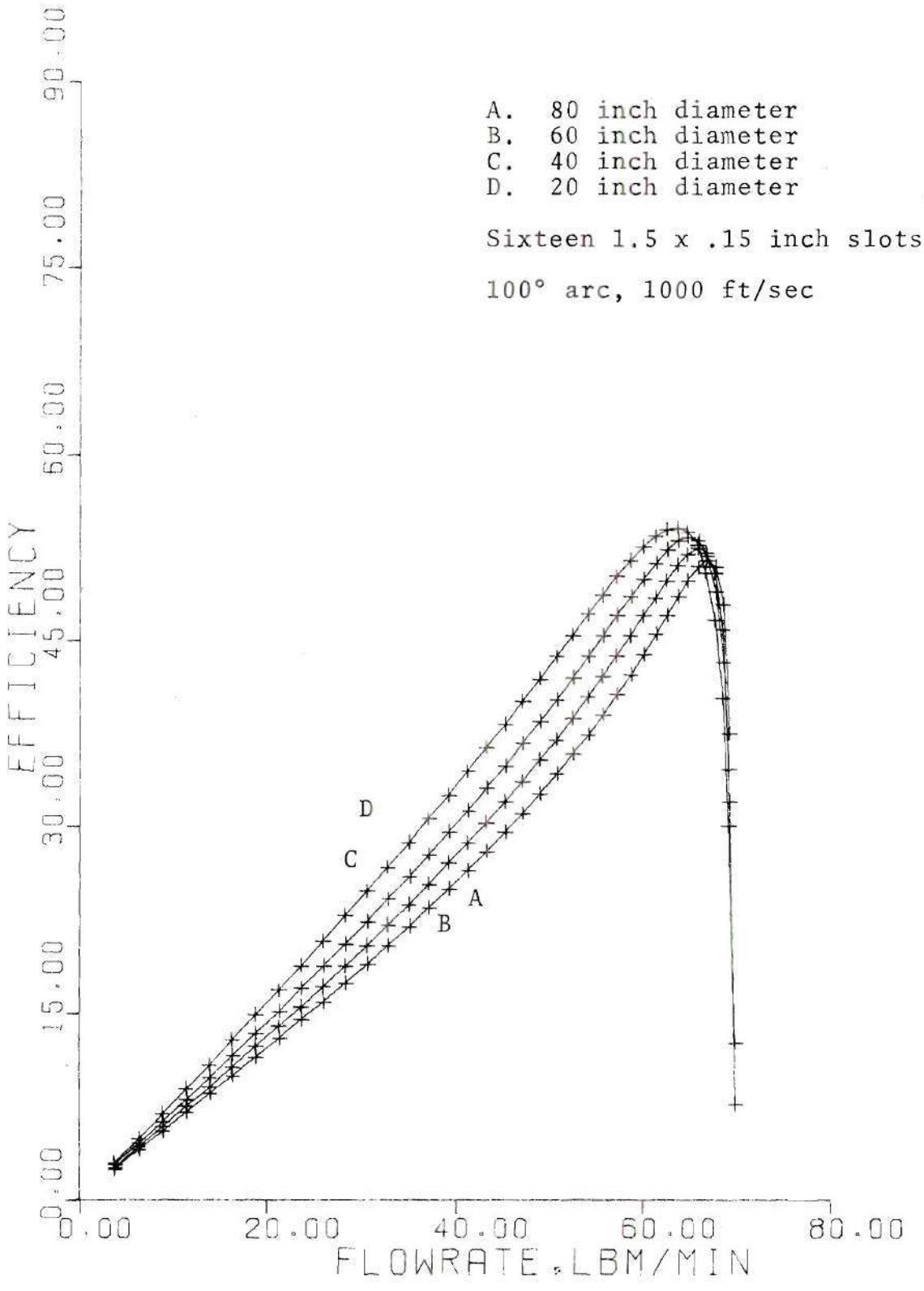

Figure 4-23. Compressor Performance

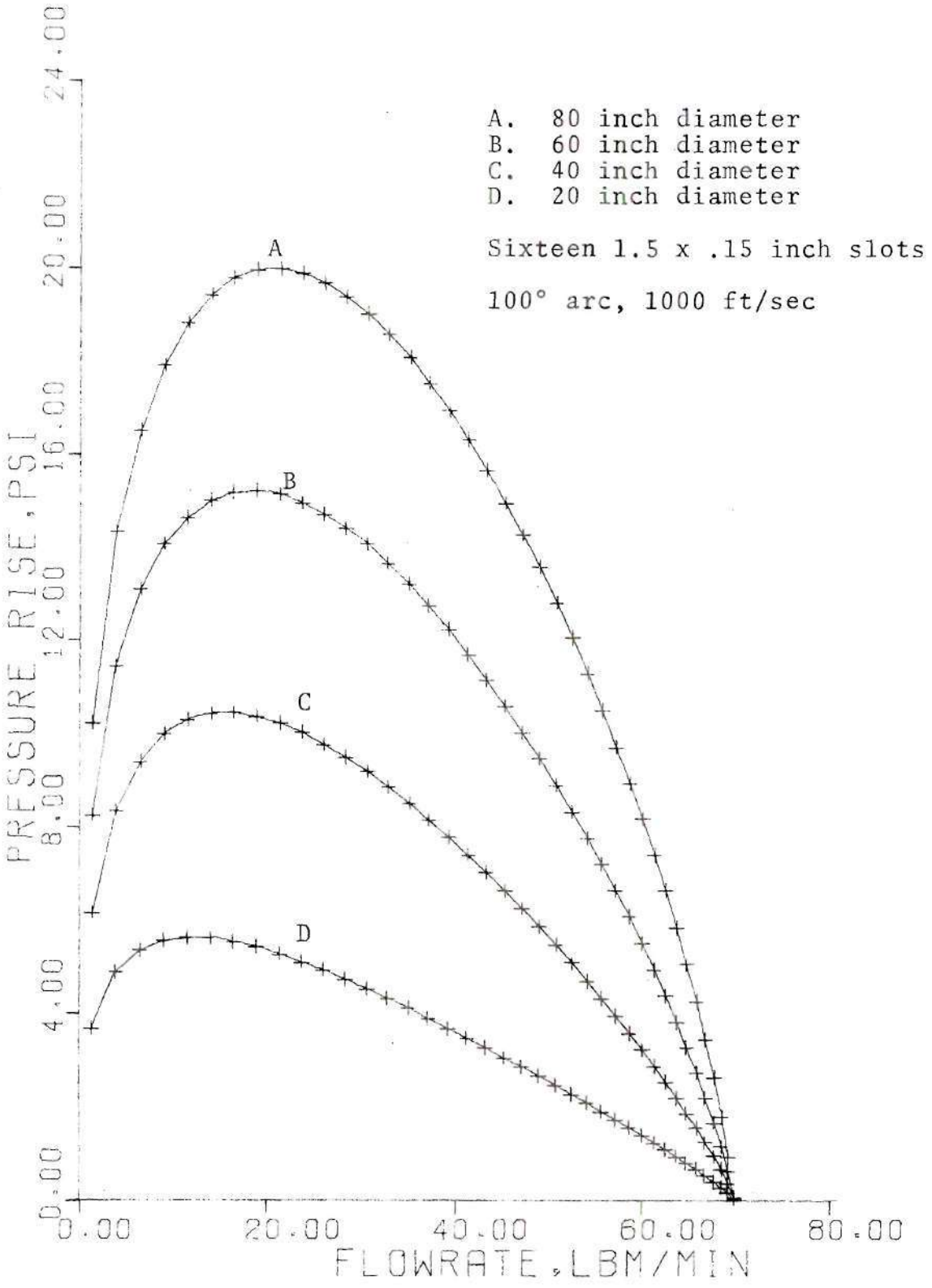

Figure 4-24. Compressor Performance

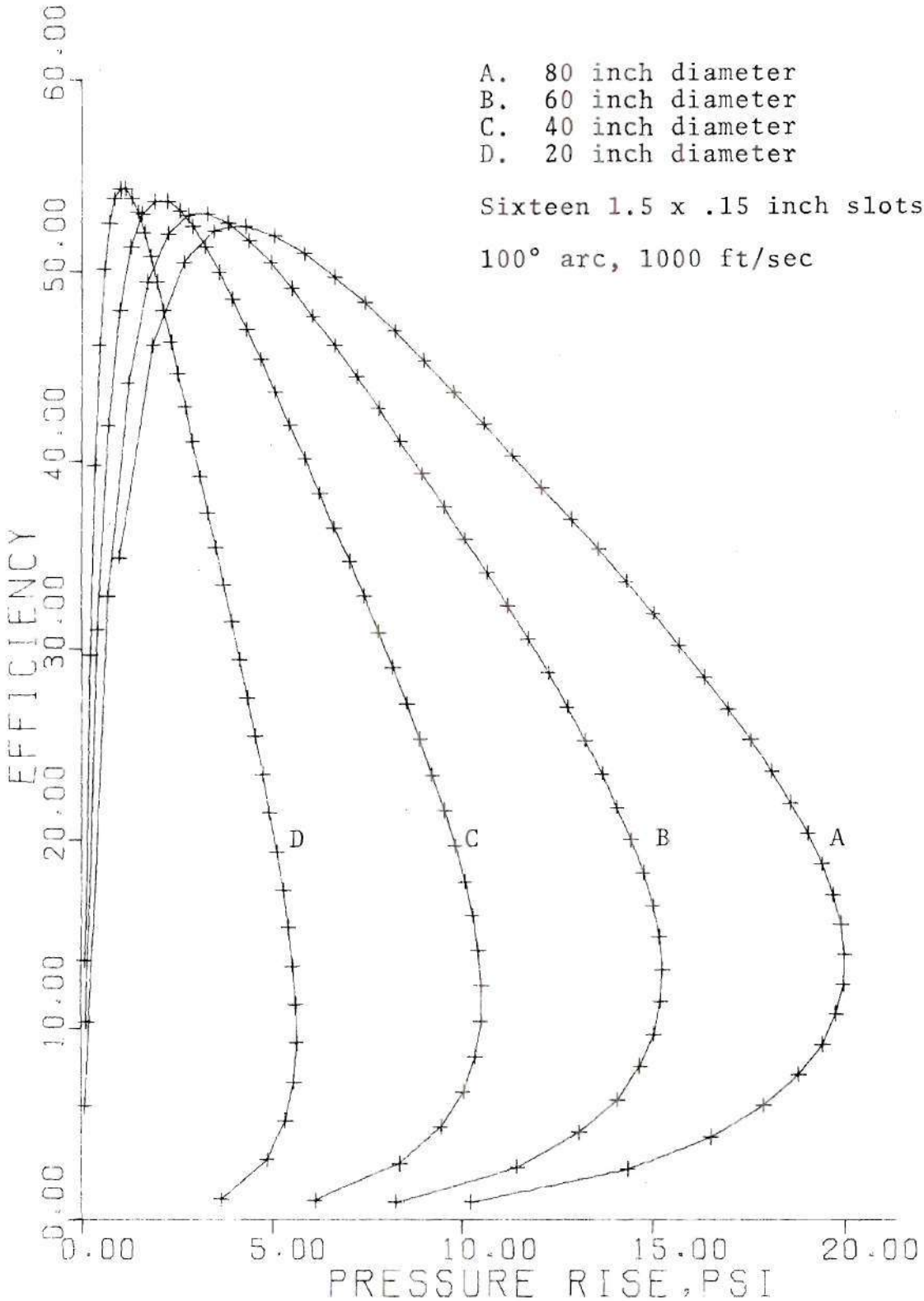

Figure 4-25. Compressor Performance

rotor. Figure 4-26 shows a 60 inch diameter turbine with 1.5 x .15 inch slots operated with and without the comb. The variable area greatly increases pressure ratio, with however a loss of efficiency as indicated in Figure 4-27. The efficiency decrease is largely due to reduction of the effective height to width ratio of the slots. Because the comb takes up a portion of the slot height.

Further construction of the entrance area results in even greater pressure ratios (Figures 4-28). Virtually any pressure ratio desired is attainable, however, with a corresponding decrease in turbine efficiency (Figure 4-29). Of even greater importance, the restricted entrance drastically reduces flowrate which is proportional to unit horsepower output for a given pressure ratio.

4-5. Single Stage Unit Efficiencies

Taking the turbine in conjunction with a compressor and heat source forms a Brayton cycle engine as discussed in Section 2-5. Such an engine utilizing a viscous compressor and turbine (see Figure 4-30) was evaluated. Due to combined low turbine and compressor efficiencies and difficulty in matching performance parameters, unit efficiencies were very low. The maximum discovered was .51 percent at .53 horsepower. Attempts to increase output resulted in negative efficiency. The program is included in Appendix C.

More promising is the possibility of connecting the

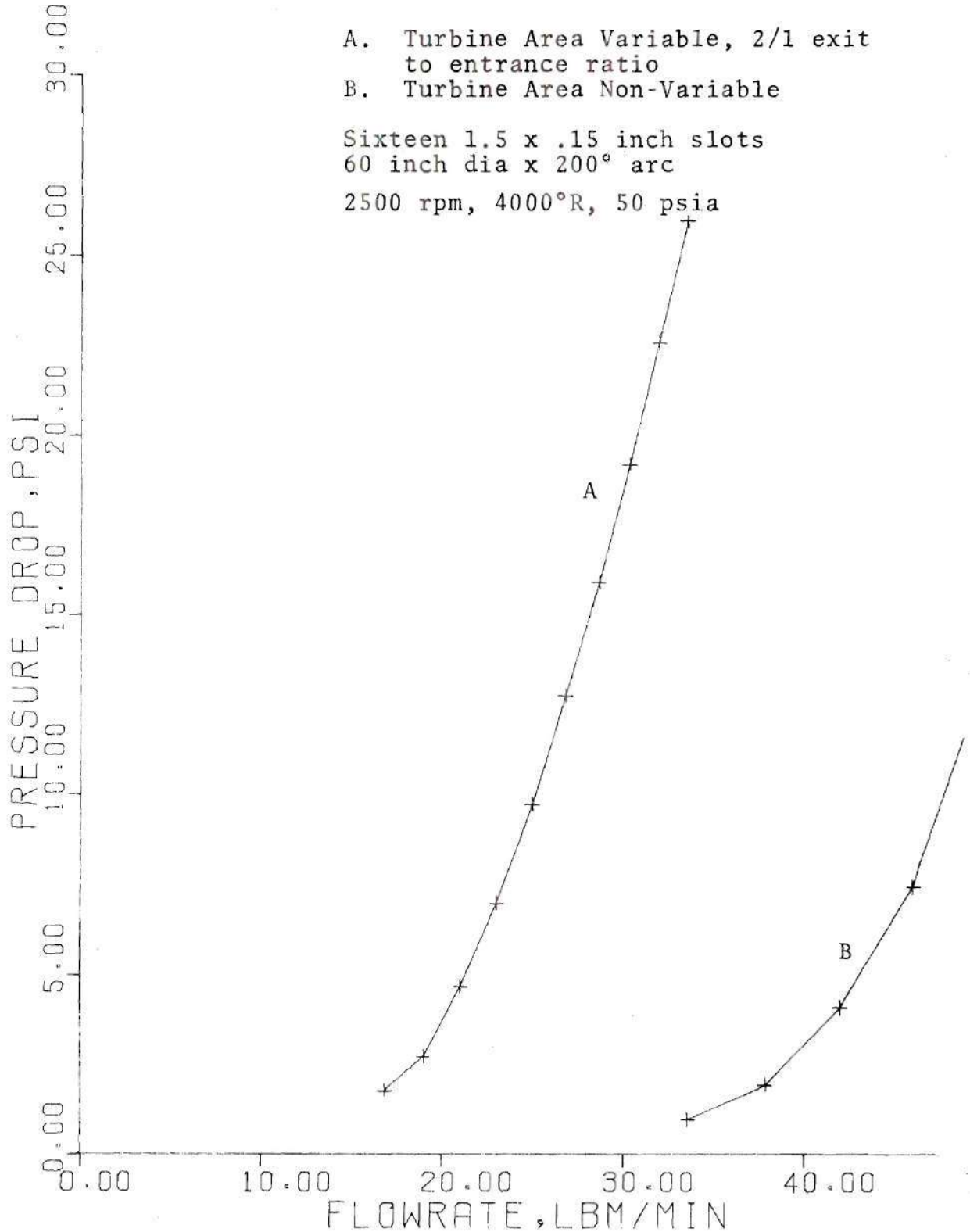

Figure 4-26. Comparison of Variable Area and Regular Turbines

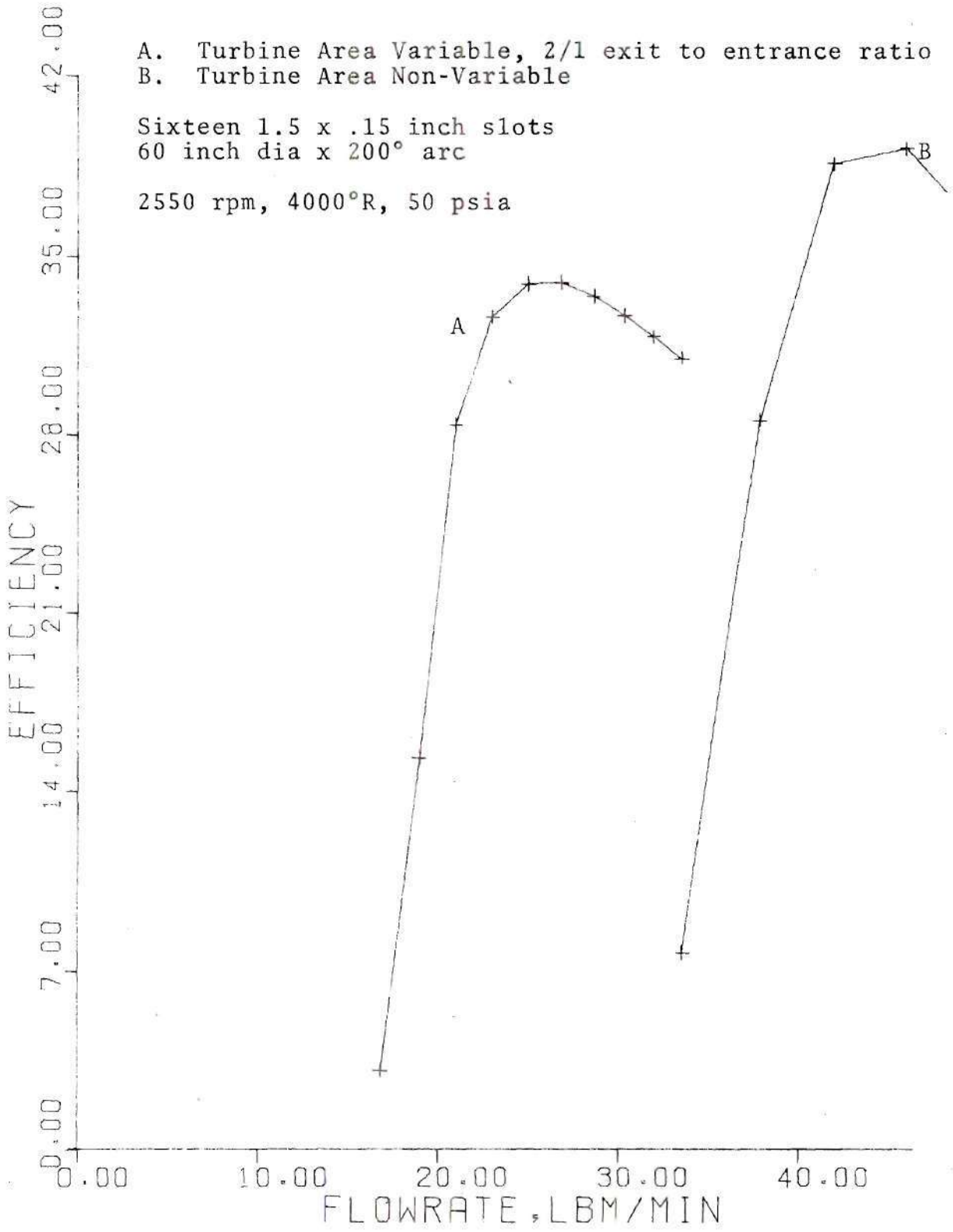

Figure 4-27. Comparison of Variable Area and Regular Turbines

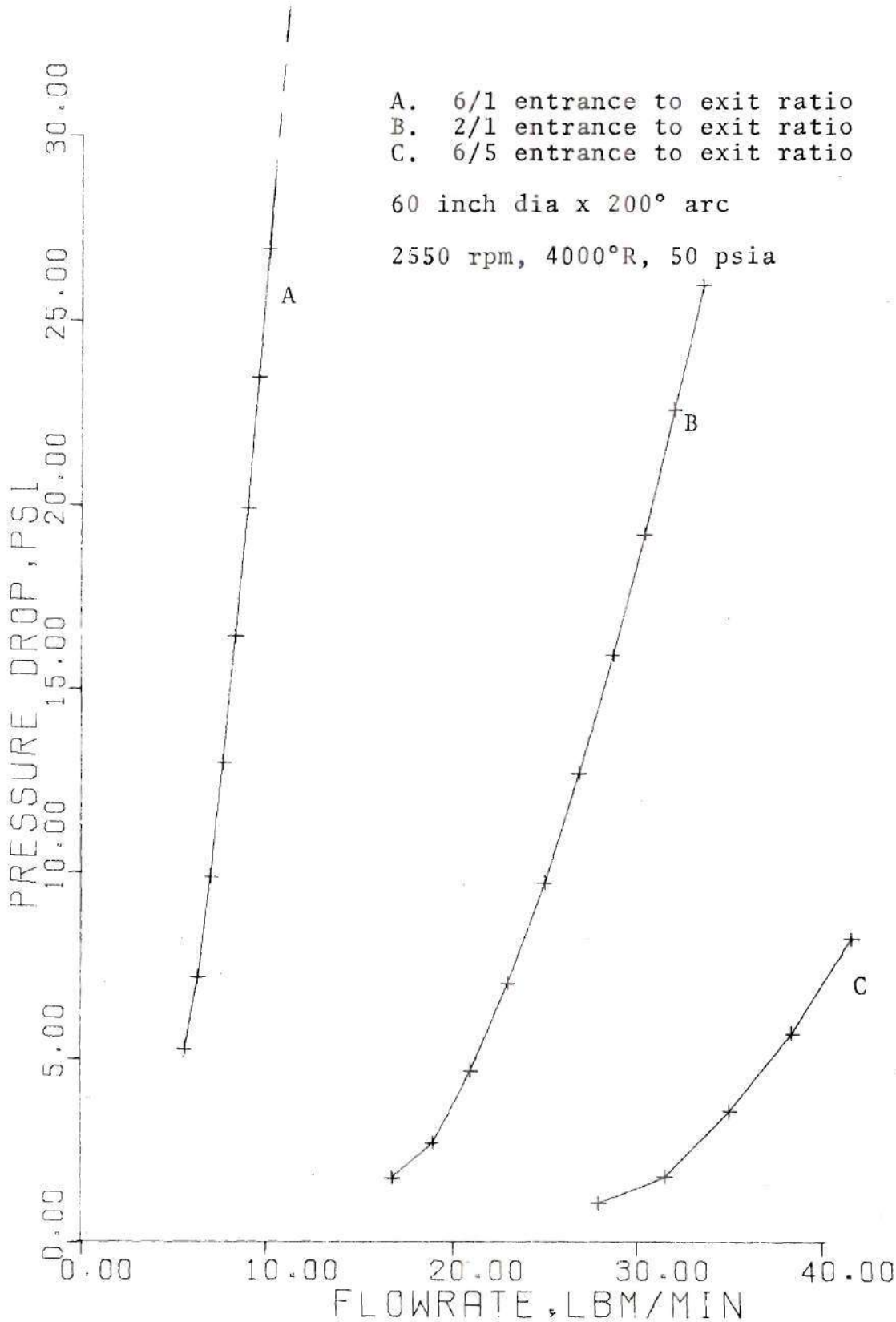

Figure 4-28. Variable Area Turbine Performance

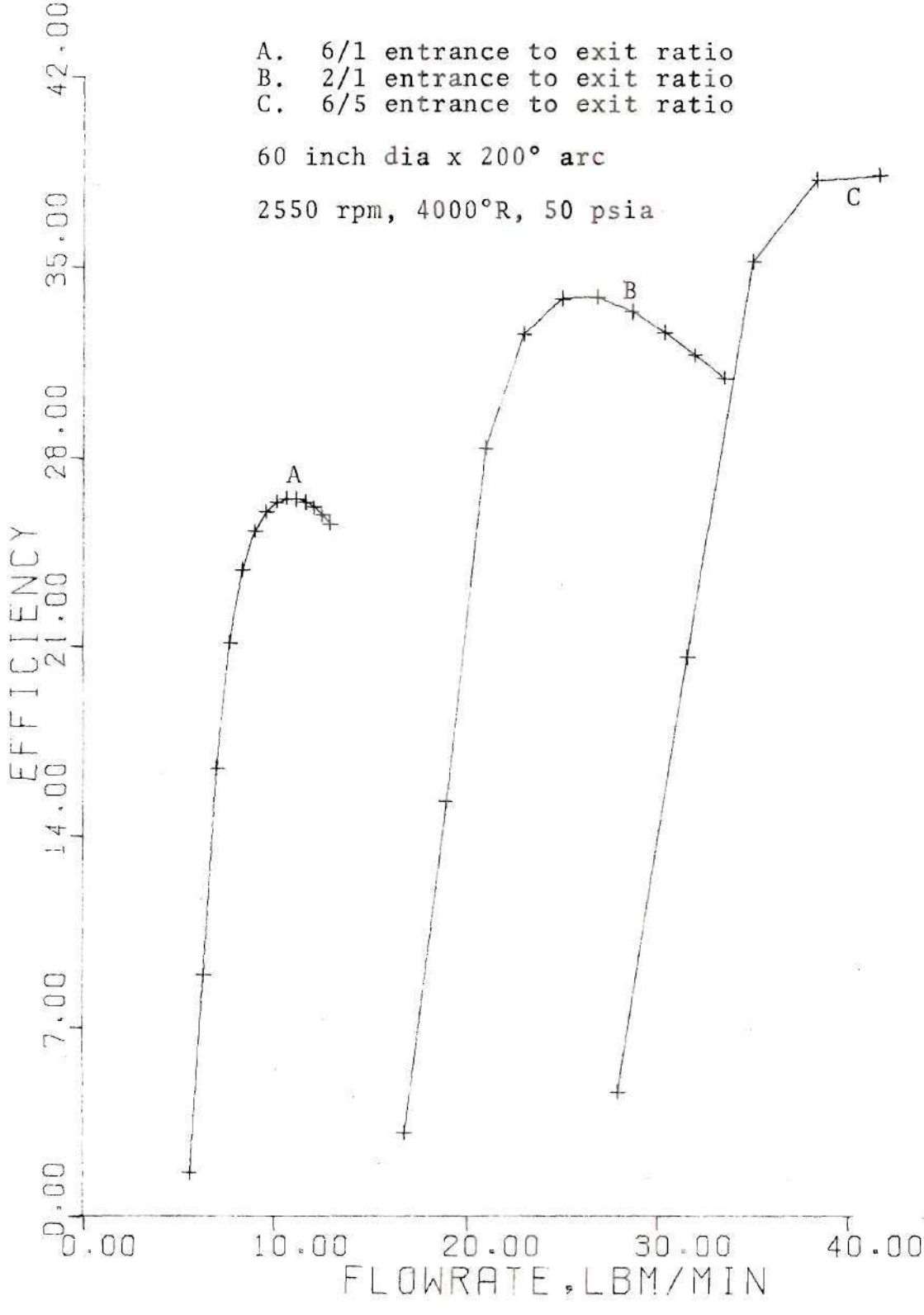

Figure 4-29. Variable Area Turbine Performance

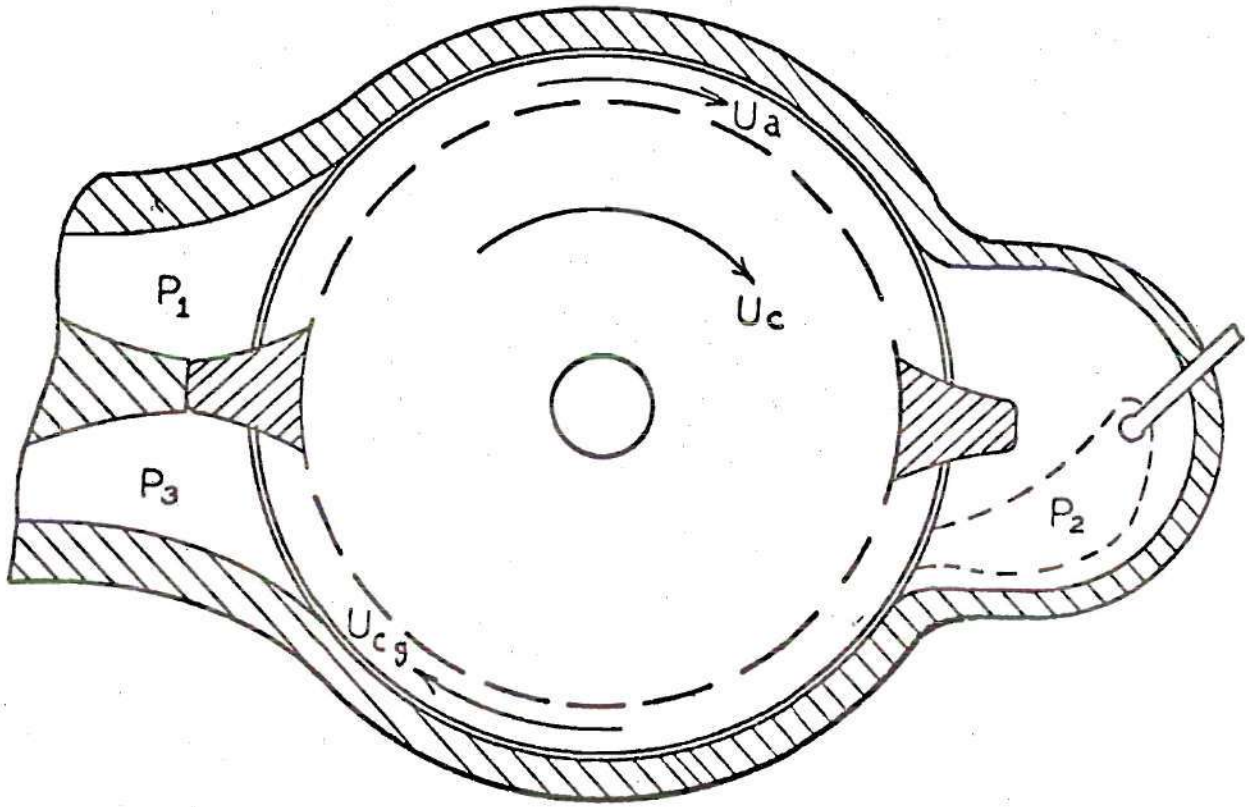

Figure 4-30. Viscous Engine

viscous turbine with a conventional axial flow compressor. Eighty percent was assumed for the efficiency of the conventional compressor. Figure 4-31 shows the effect of turbine efficiency on unit efficiency at various pressure ratios at an entrance temperature of 4000°R. Unfortunately, as previously discussed, pressure ratio is inversely related to turbine efficiency.

Single stage unit efficiencies are calculated with compressor work based on the turbine pressure ratio. For example, a turbine from 90 psia to 60 psia requires a compressor operating on a 1.5 compression ratio. Compressor inlet temperature is taken to be 530°R. Single turbine unit efficiencies with an 80 percent axial compressor are shown in Figures 4-32 and 4-33. These curves turn back on themselves as turbine efficiency decreases. Eventually compressor work exceeds turbine output resulting in negative net horsepower and efficiency.

Increasing maximum temperature to 4000°R and attempting various rotational speeds yields greater overall efficiency and output. Figures 4-34 and 4-35 indicate a potential of 14 hp at 3.2 percent unit efficiency and 56 hp at 2.6 percent unit efficiency.

Greater pressure ratios, therefore, larger unit efficiencies are possible using the variable area turbine discussed in Section 4-4. Comparison of single unit efficiencies with variable and non-variable turbines is given in

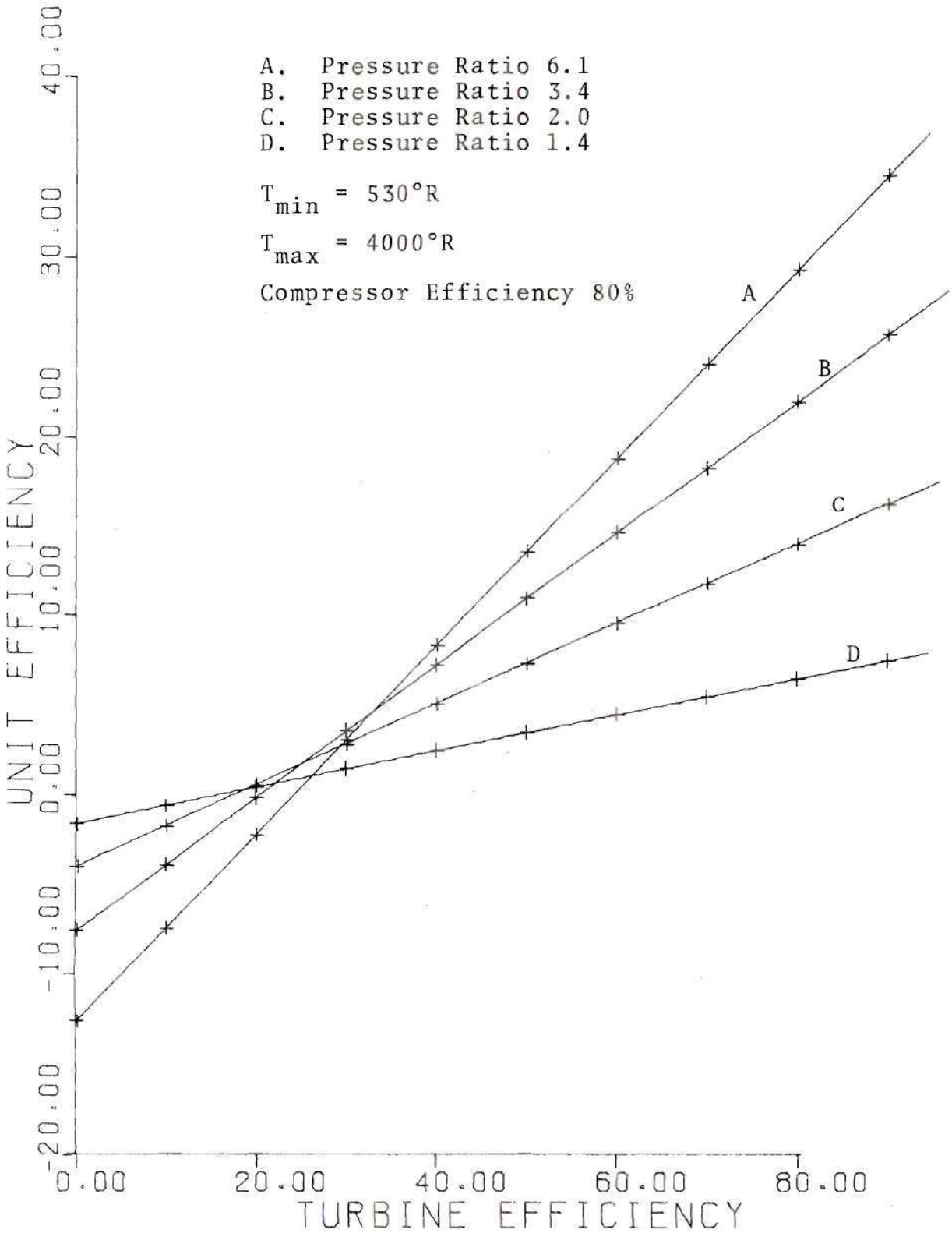

Figure 4-31. Brayton Cycle Efficiencies

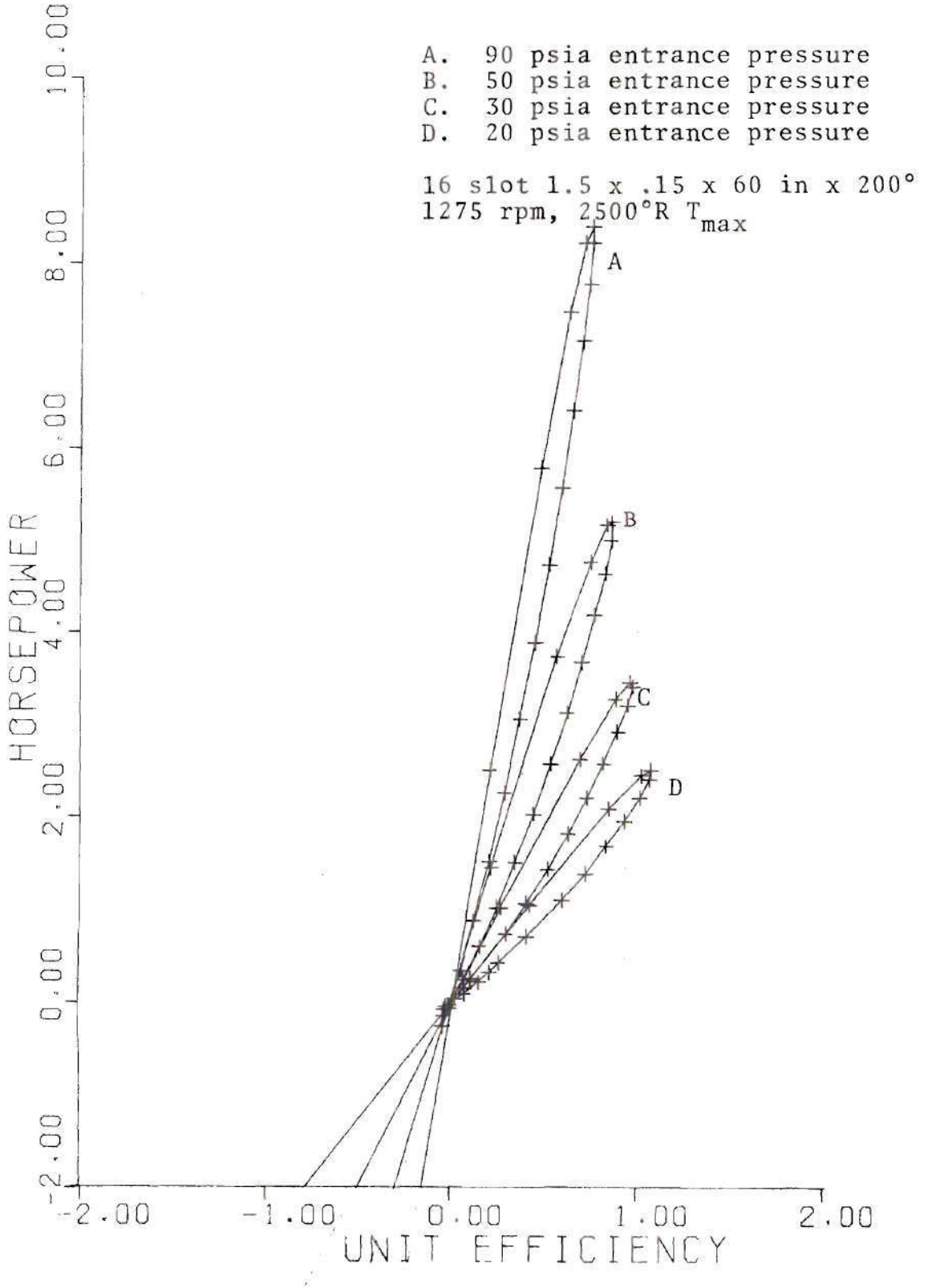

Figure 4-32. Single Stage Unit Efficiency

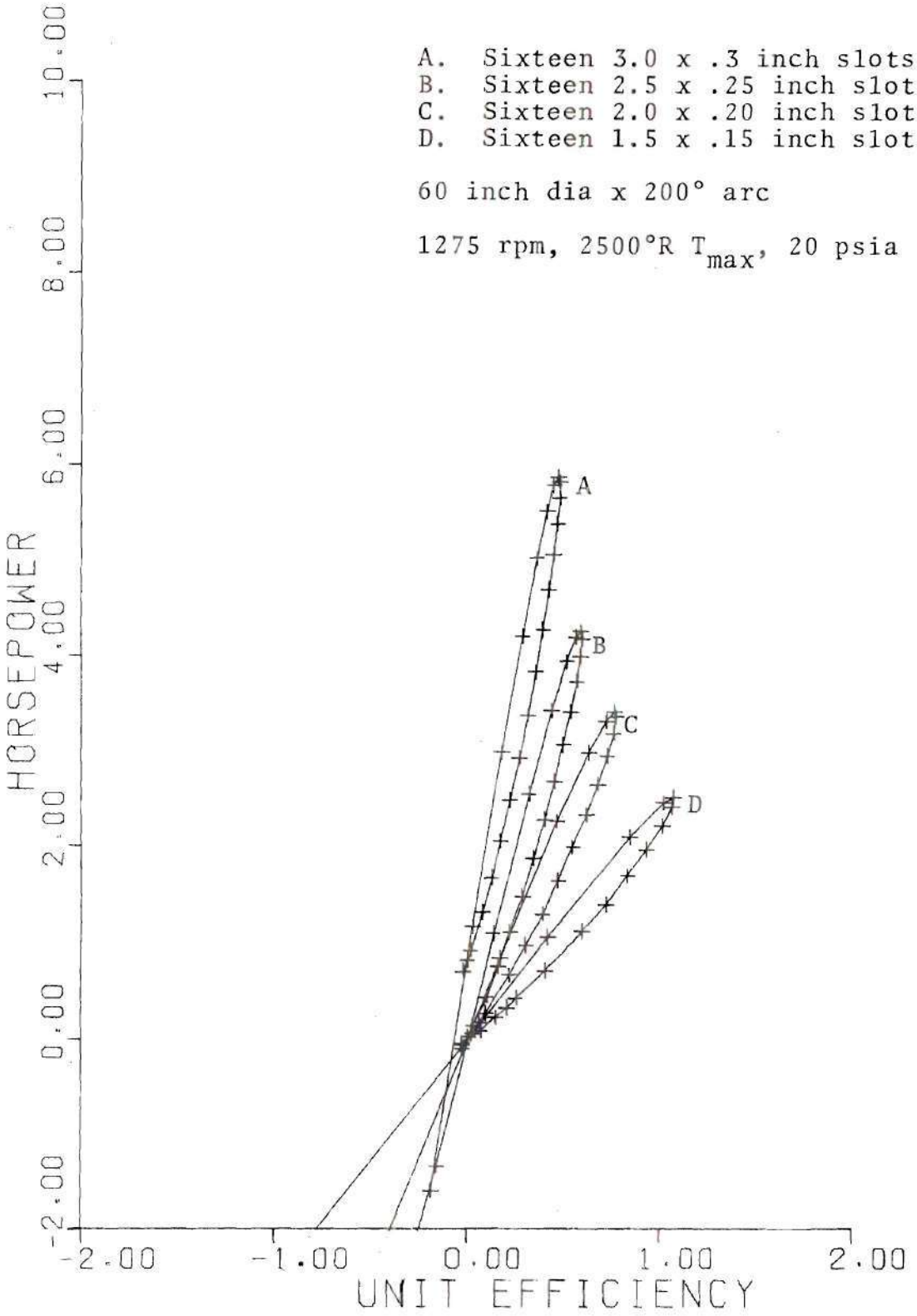

Figure 4-33. Single Stage Unit Efficiency

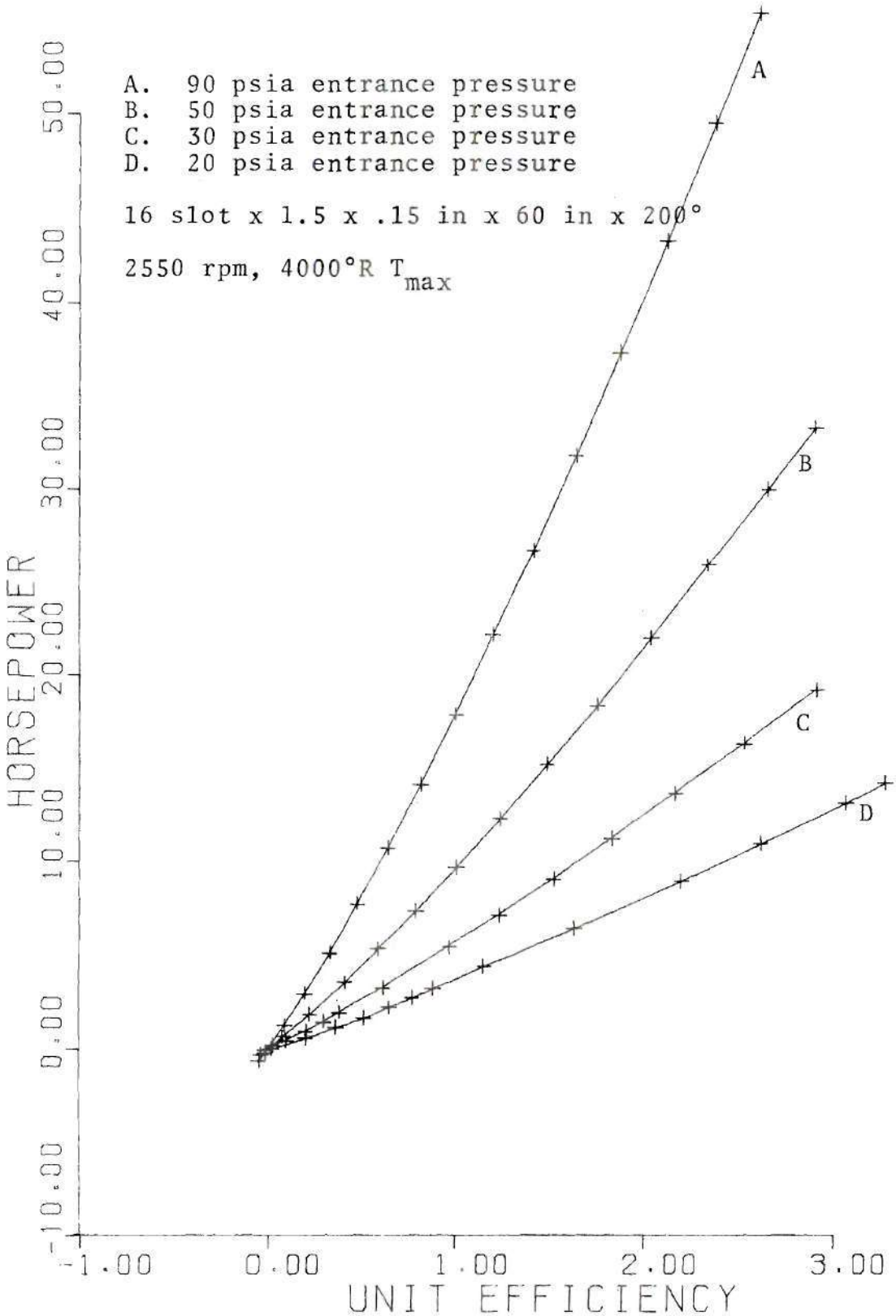

Figure 4-34. Single Stage Unit Efficiency

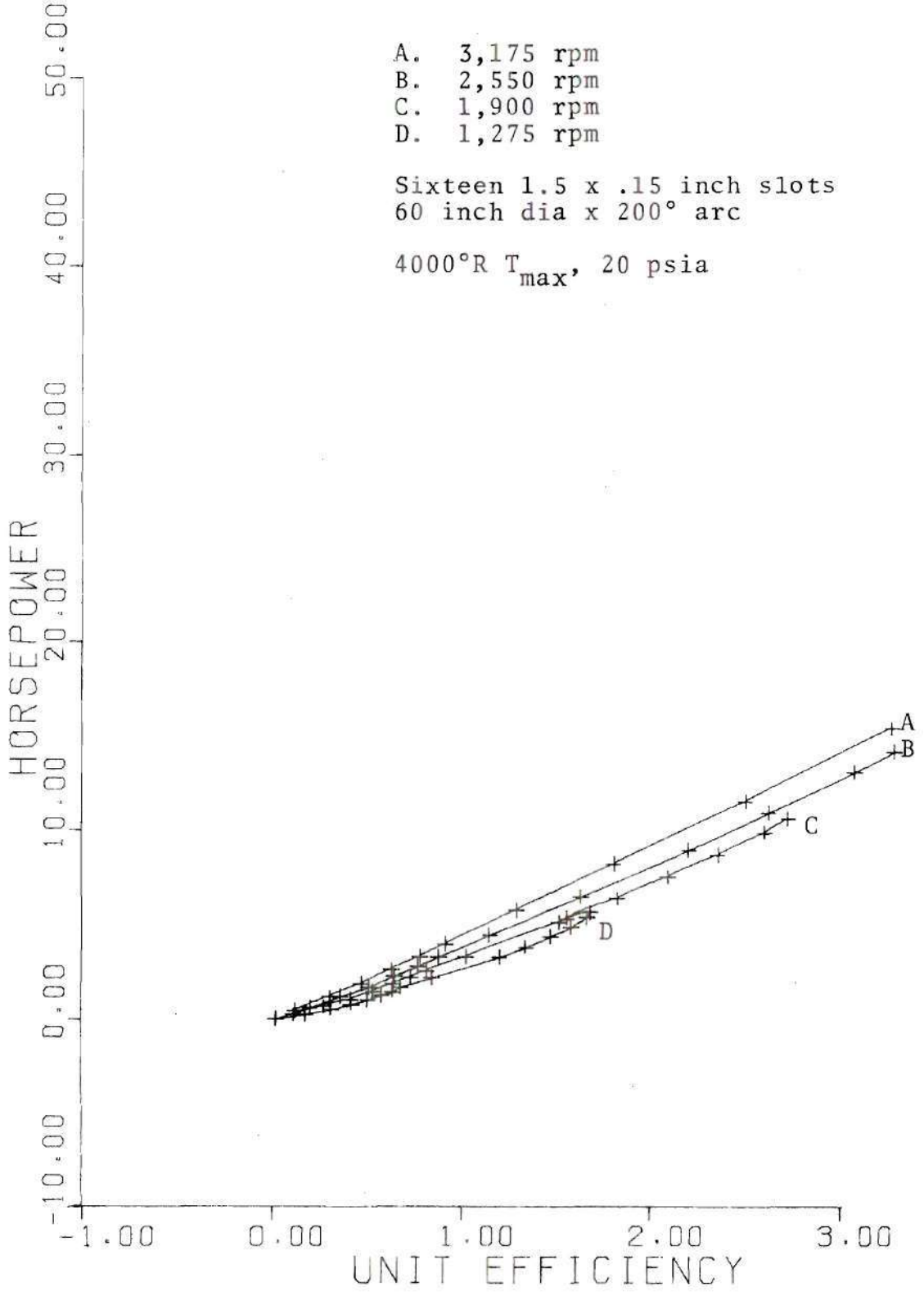

Figure 4-35. Single Stage Unit Efficiency

Figure 4-36. The variable area turbine sacrifices horsepower due to decrease in flowrate for greater unit efficiency. Figure 4-37 shows other degrees of area variation in the turbine. Maximum attainable efficiency for the variable area single stage turbine is 4.5 percent thermal efficiency with 22.2 net horsepower output.

4-6. Multiple Stage Turbine Arrangement

In order to achieve greater unit efficiencies by operating at greater pressure ratios, a concept of operating the viscous turbine in a series has been developed. Figure 4-38 shows a possible arrangement including heat exchangers for cooling the turbine disks.

Five adiabatic multiple stage units have been evaluated for overall performance. In each case, succeeding turbines must have ever increasing numbers of slots to pass the expanding gas and operate at optimum conditions. Variable area turbines have the potential to reduce the equipment requirements (number of turbines) for a given overall pressure ratio. However, they cannot increase either efficiency or horsepower of the multiple stage unit due to decrease in efficiency and flowrate of the individual turbines.

The following cases represent the calculations performed:

Case 1. Eight 1.5 x .15 x 60 x 200° turbines entrance

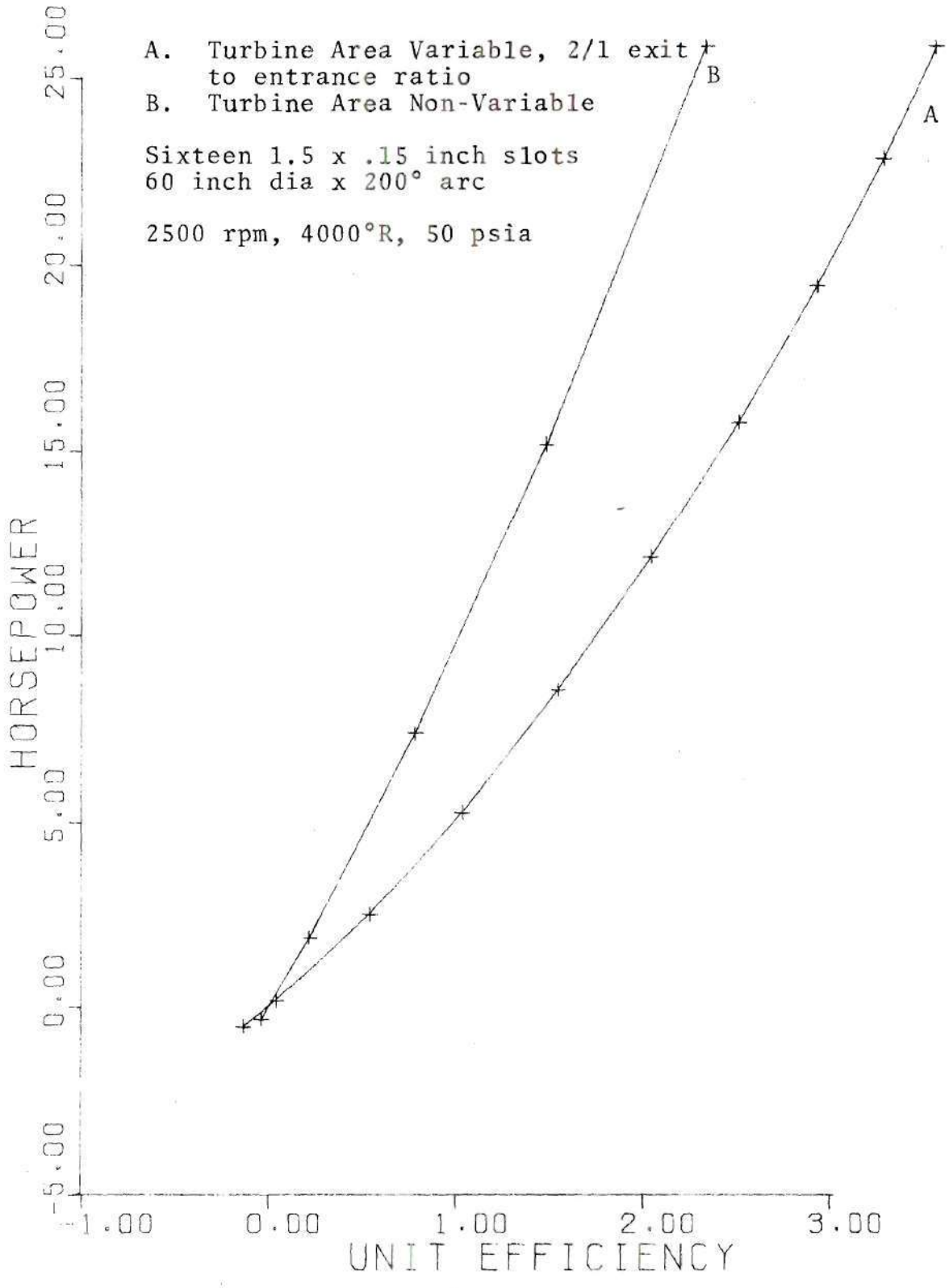

Figure 4-36. Comparison of Variable Area and Regular Turbines for Single Unit Efficiencies

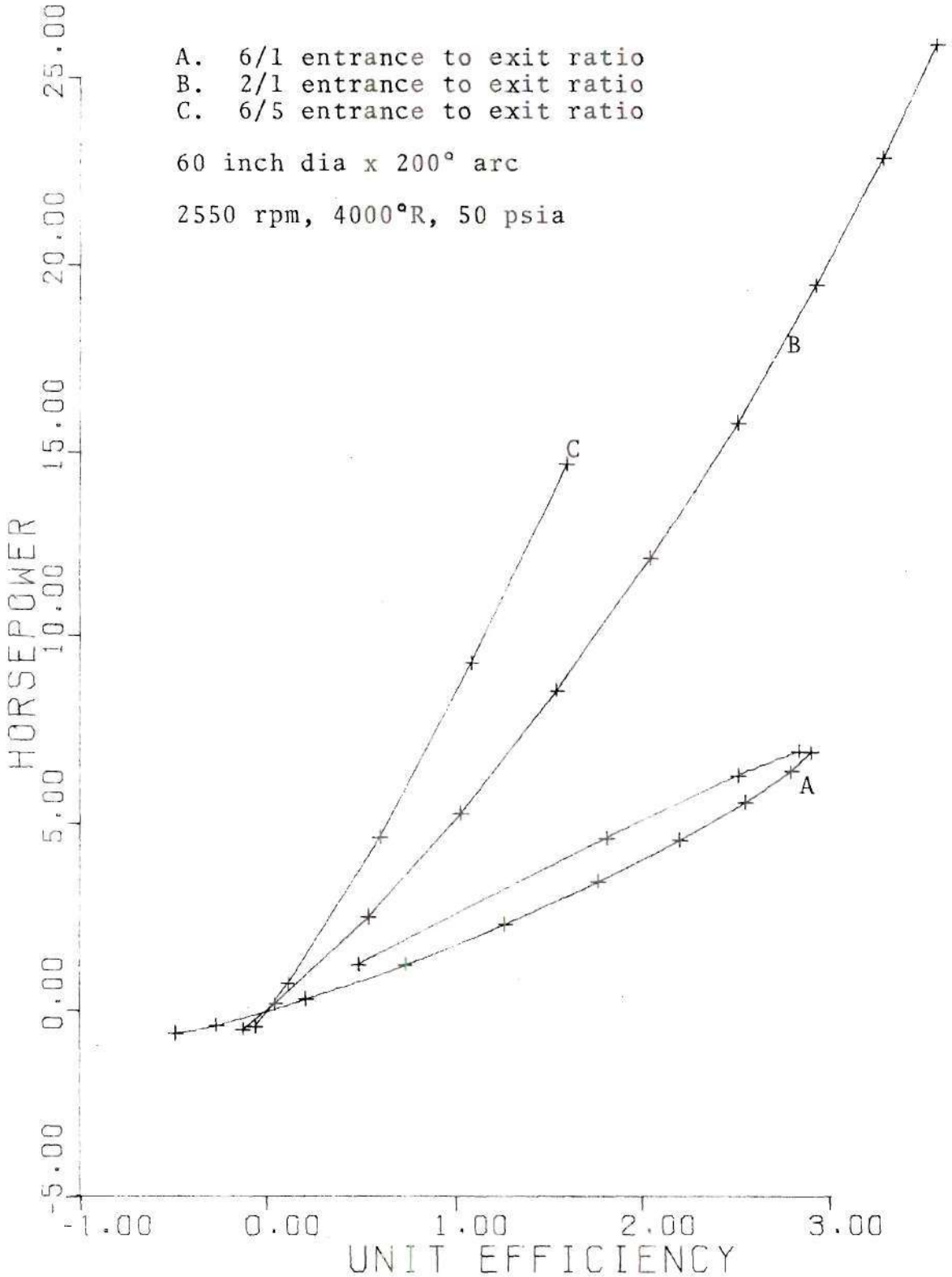

Figure 4-37. Single Unit Efficiency with Variable Area Turbine

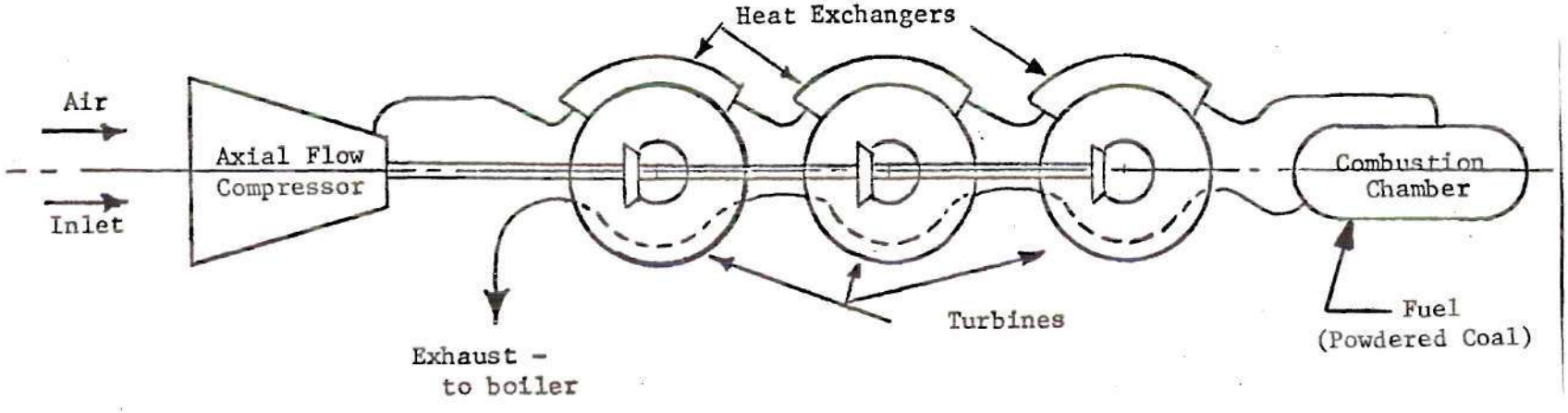

Figure 4-38. Axial Flow Compressor and Viscous Turbines in Series Schematic of Possible Topping Cycle

conditions, 4000°F at 147 psia 80 percent axial compressor at 168.1 lb_m/min 399 total slots, 8.3 ft approximate total length. Unit efficiency 13.9 percent at 440 hp.

Case 2. Eight 1.5 x .15 x 60 x 200° turbines with reheat to max temperature. Entrance conditions, 4000°F at 147 psia, 80 percent axial compressor at 168.1 lb_m/min, 462 total slots, 9.6 ft approximate total length. Unit efficiency 13.3 percent at 557 hp.

Case 3. Eight 1.5 x .15 x 60 x 200° turbines. Entrance conditions, 2500°F at 147 psia, 80 percent axial compressor at 225.3 lb_m/min, 411 total slots, 8.6 ft approximate total length. Unit efficiency 1.3 percent at 25.6 hp.

Case 4. Eight 3.0 x .30 x 60 x 200° turbines entrance conditions, 4000°F at 147 psia, 80 percent axial compressor at 798.0 lb_m/min, 429 total slots, 14.3 ft approximate total length. Unit efficiency 9.3 percent at 1392 hp.

Case 5. Eleven 1.5 x .15 x 60 x 200° turbines entrance conditions, 4000°R at 367.5 psia, 80 percent axial compressor at 420.0 lb_m/min, 1111 total slots, 23.1 approximate total length. Unit efficiency 14.1 percent at 935 hp.

Performance data for each of the eight turbines comprising Cases 1 and 2 are included in Section 4-9, Figures 4-51 through 4-58.

Case 4 of those considered is the most interesting

since it deals with a slot width of .3 inch, which is quite practical. It also combines a relatively high horsepower output with a fair efficiency.

4-7. Heat Transfer Effects

Heat transfer in the turbine or compressor analysis is easily included by defining the average wheel temperature, T_w. Assigning an arbitrary temperature T_w of 2500°R, Case 1 of Section 4-6 was reevaluated to obtain an overall thermal efficiency of 5.7 percent with an output of 219.5 hp.

The decrease in efficiency was caused by high heat losses into the disk due to high forced convection factors. This reduced the gas temperature after the first turbine to 2827°R compared to 3889°R without heat transfer. In subsequent turbines, the gas temperature approaches the wheel temperature reducing the Brayton cycle efficiency greatly. In the last four turbines, the constant wheel temperature actually serves as a source of regeneration by maintaining gas temperature at 2500°F.

Now, in Case 1, with and without heat transfer, two extremes are represented. The first assumes zero heat transfer. The second neglects internal resistance of the disk fins and assumes an average wheel surface temperature. Neither assumption may be valid. Probable operation of the multiple stage unit falls between the 13.9 percent at 440 hp without heat transfer and the 5.7 percent at 219.5 hp with

constant surface temperature.

The possibility of operating at lower gas temperatures to negate heat transfer was investigated in Case 3 of Section 4-6. The lower gas velocities produced by lower temperatures resulted in very low thermal efficiency and output.

4-8. Supersonic Turbine

The mathematical model derived in Chapter II in no way precluded the possibility of supersonic flow in the viscous turbine. By placing a converging-diverging nozzle prior to the turbine entrance supersonic velocities could be introduced into the turbine. Data have been generated and displayed per Figures 4-39 through 4-44. Subsonic data were generated for the same general conditions for comparison and is given per Figures 4-45 through 4-50.

Generally, supersonic turbines have lower peak efficiencies due to greater losses at the static wall. Output in the supersonic turbine is greater with the higher relative velocity between the gas and rotor. However the supersonic turbines have an advantage in respect that much smaller diameters produce equivalent efficiency and output. (See Table 1.) Both supersonic and subsonic turbines are limited by choking.

4-9. General Turbine Performance Data

Performance data for each of the Case 1 and Case 2

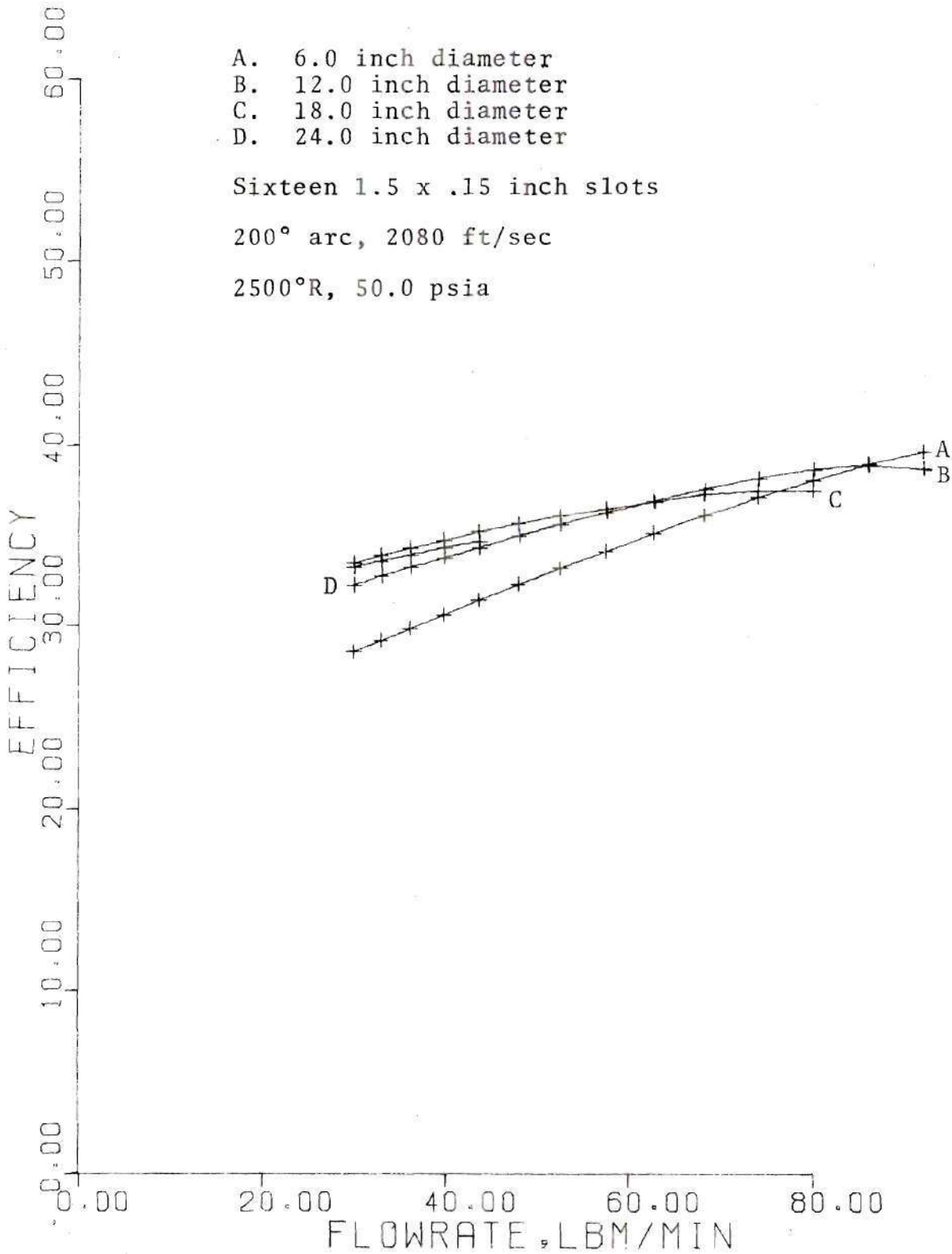

Figure 4-39. Supersonic Turbine Performance

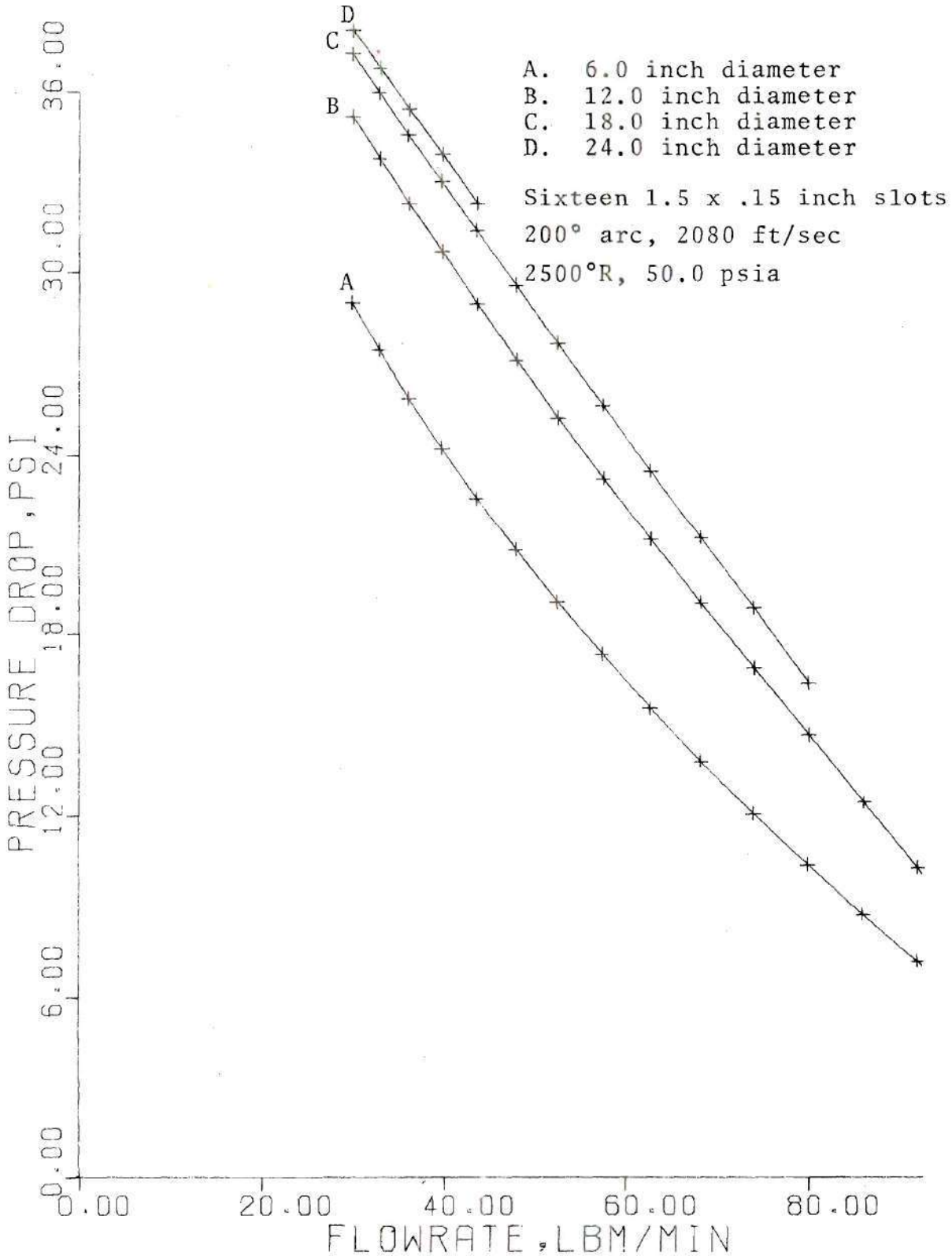

Figure 4-40. Supersonic Turbine Performance

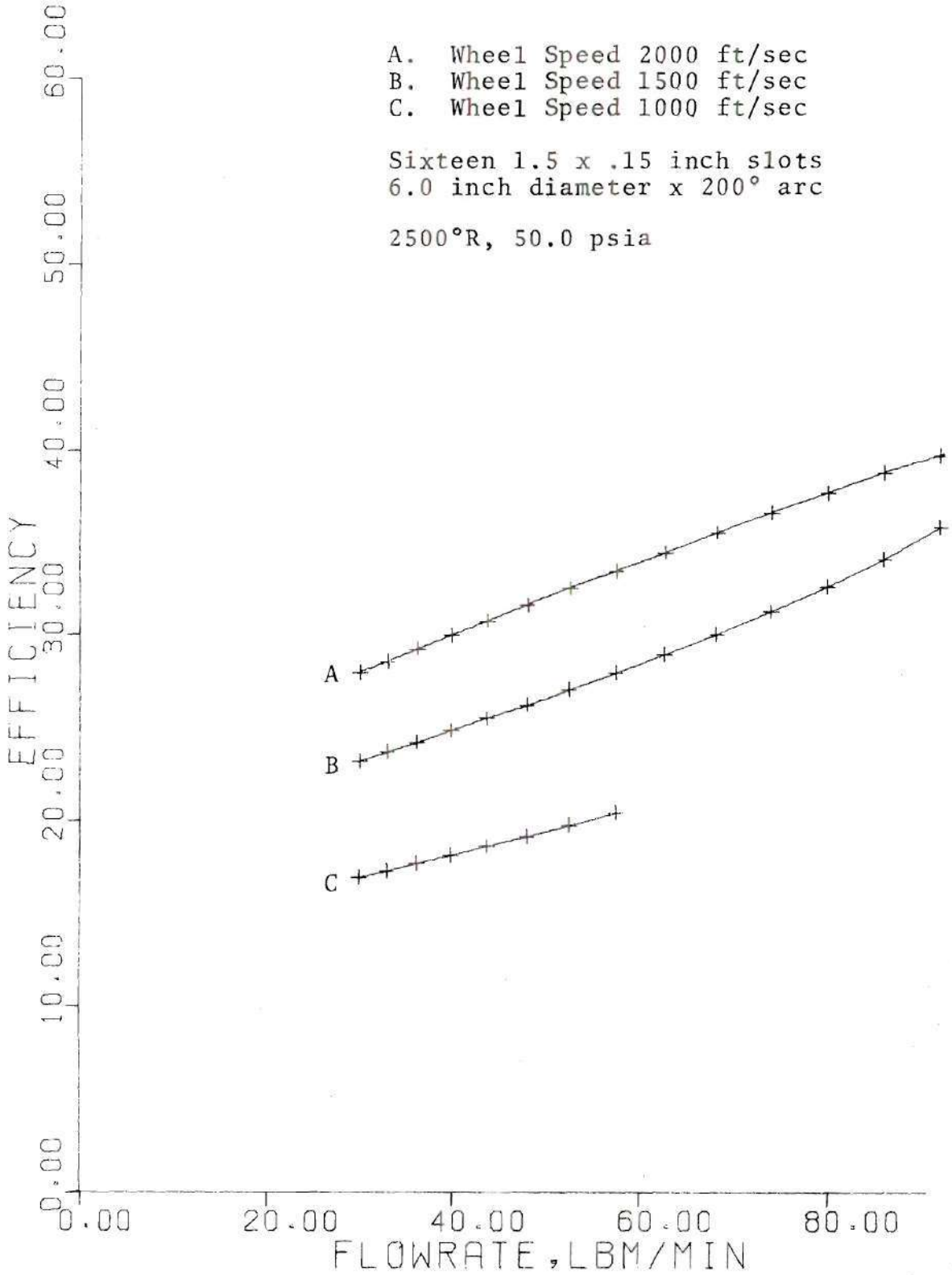

Figure 4-41. Supersonic Turbine Performance

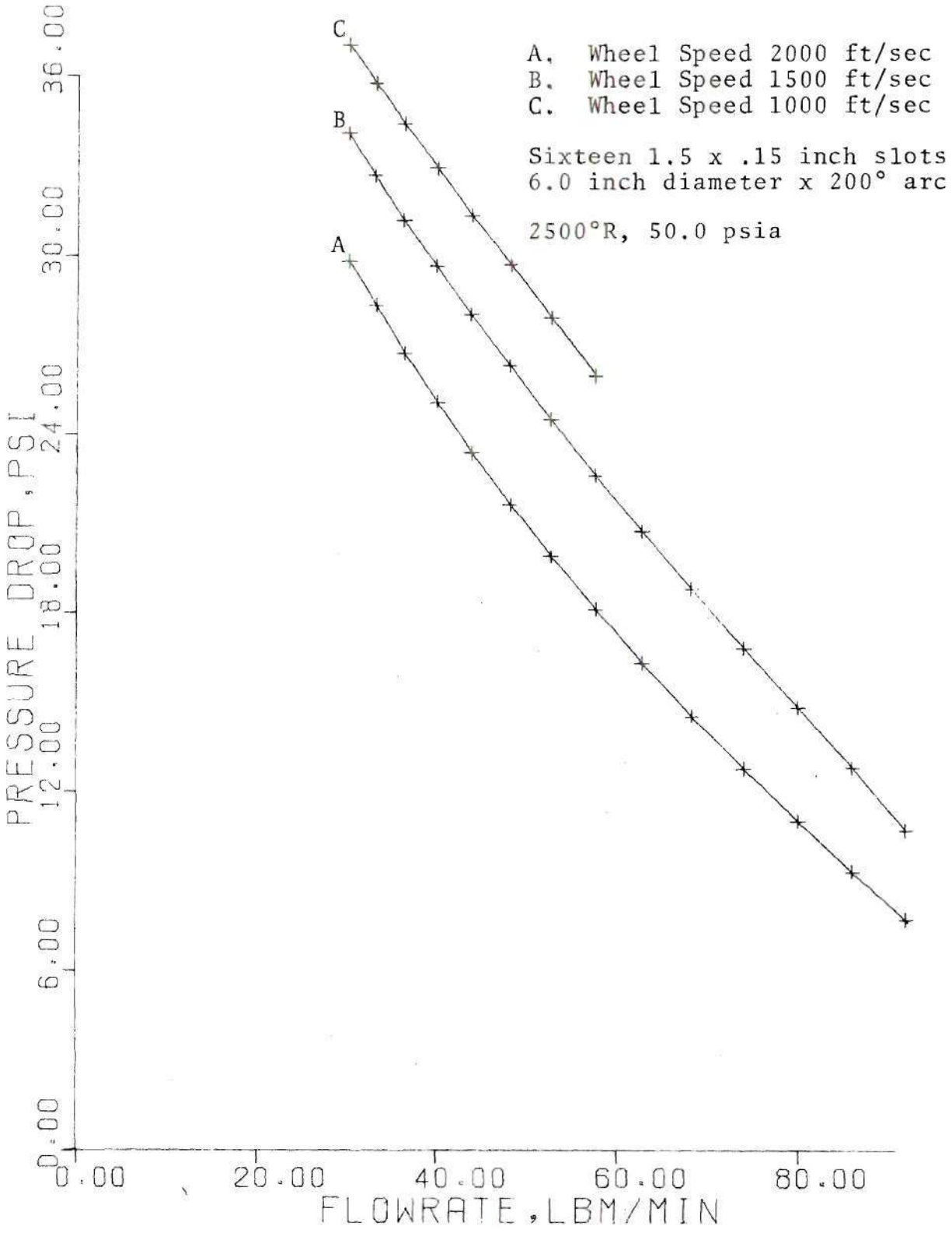

Figure 4-42. Supersonic Turbine Performance

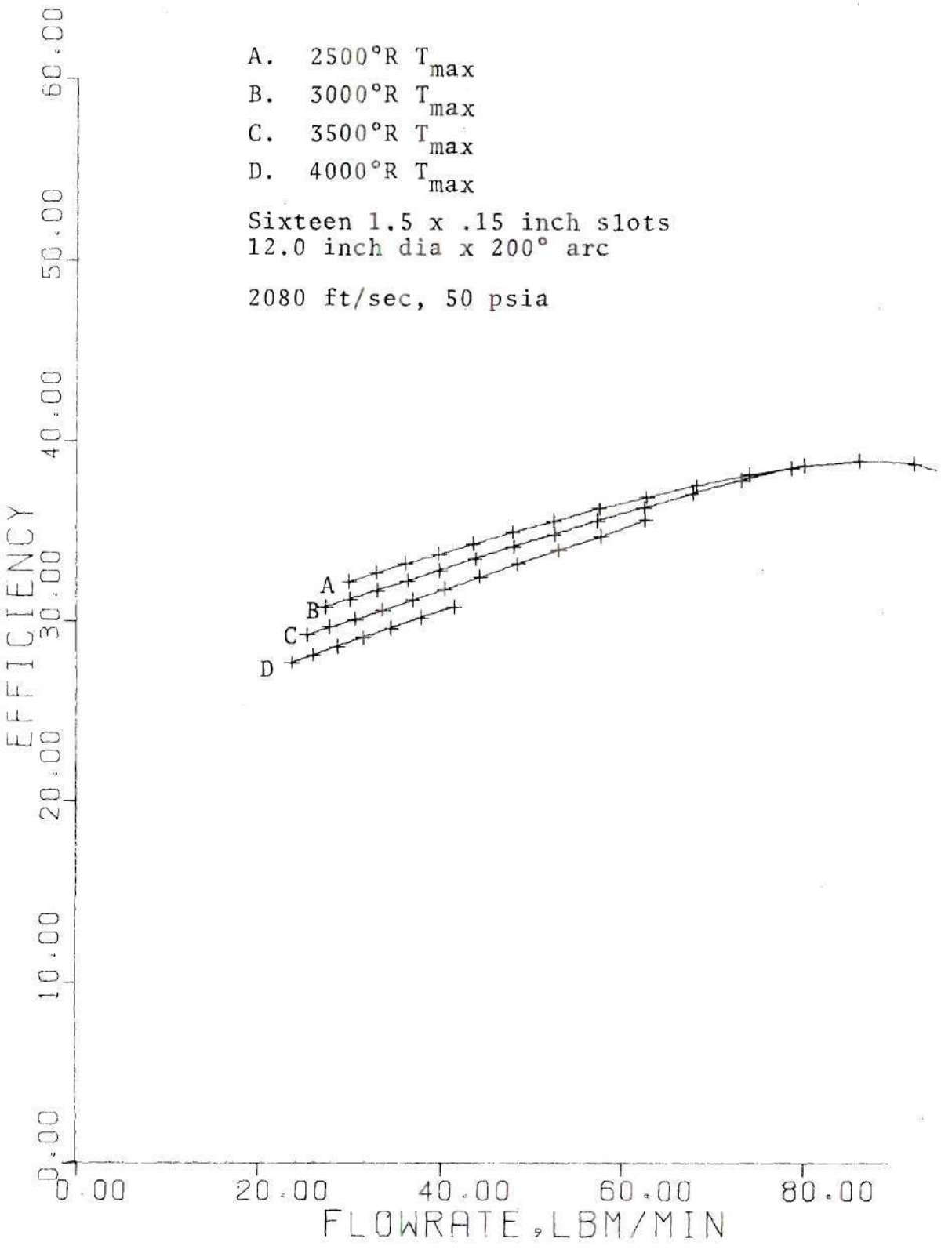

Figure 4-43. Supersonic Turbine Performance

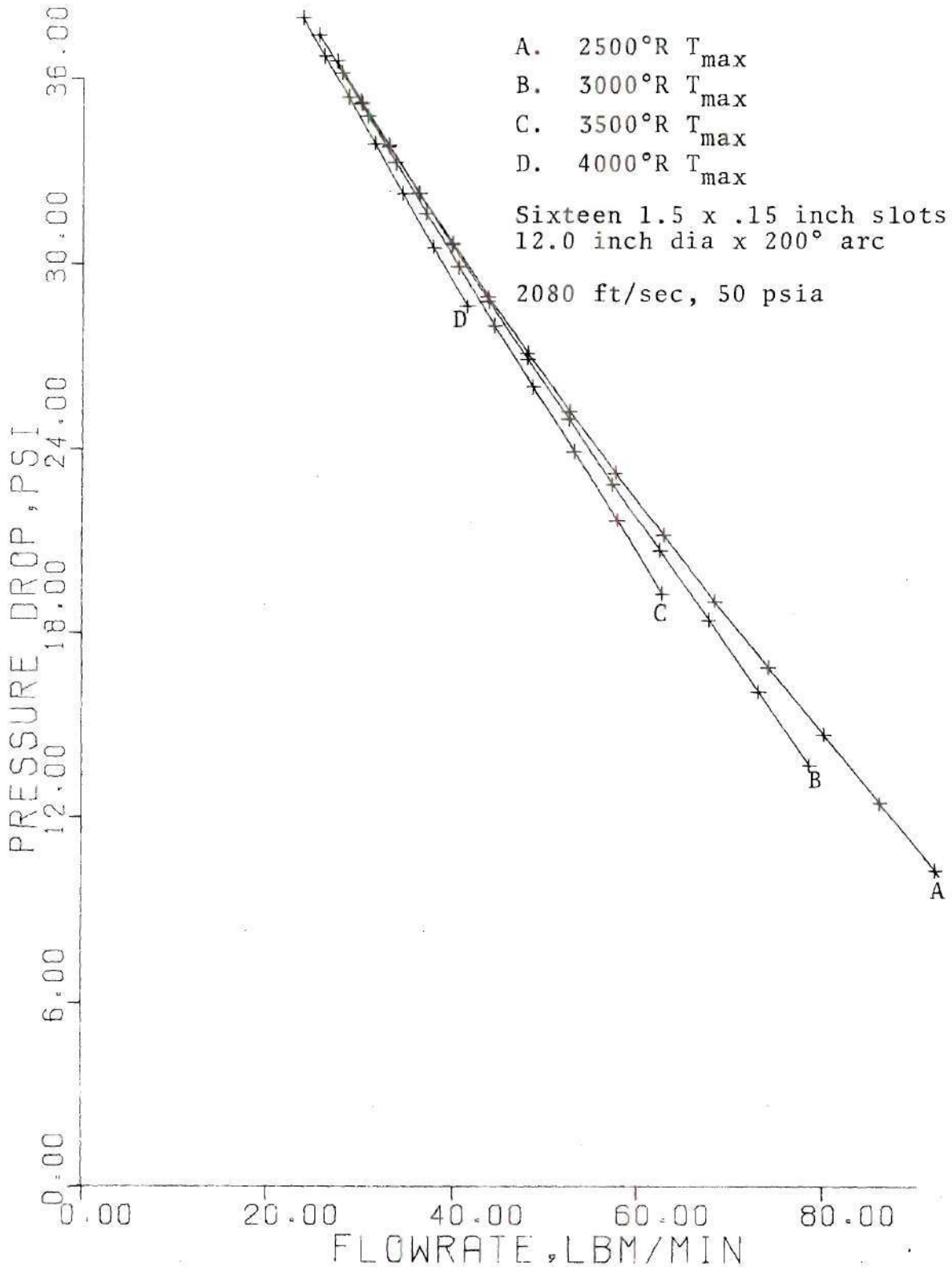

Figure 4-44. Supersonic Turbine Performance

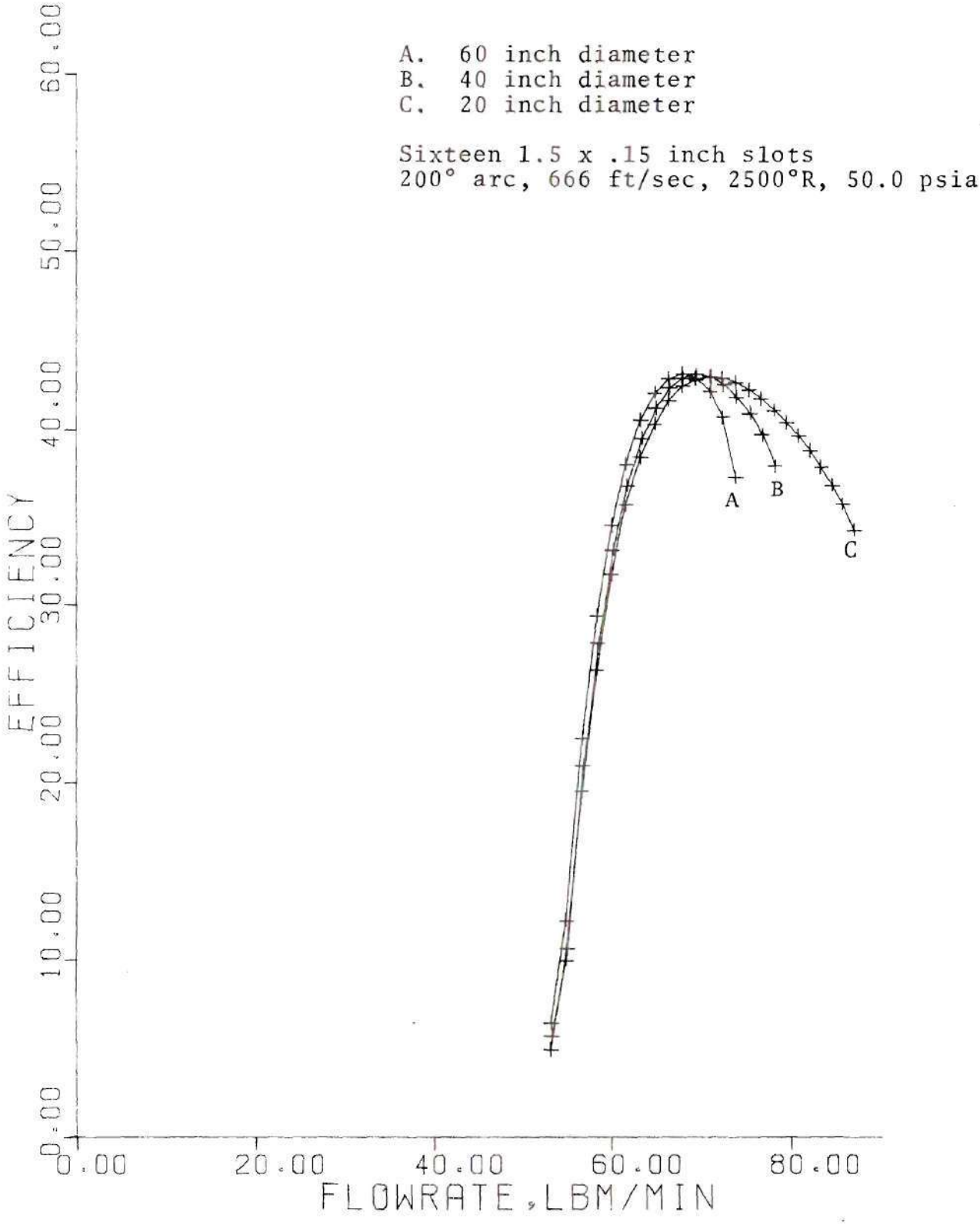

Figure 4-45. Turbine Performance

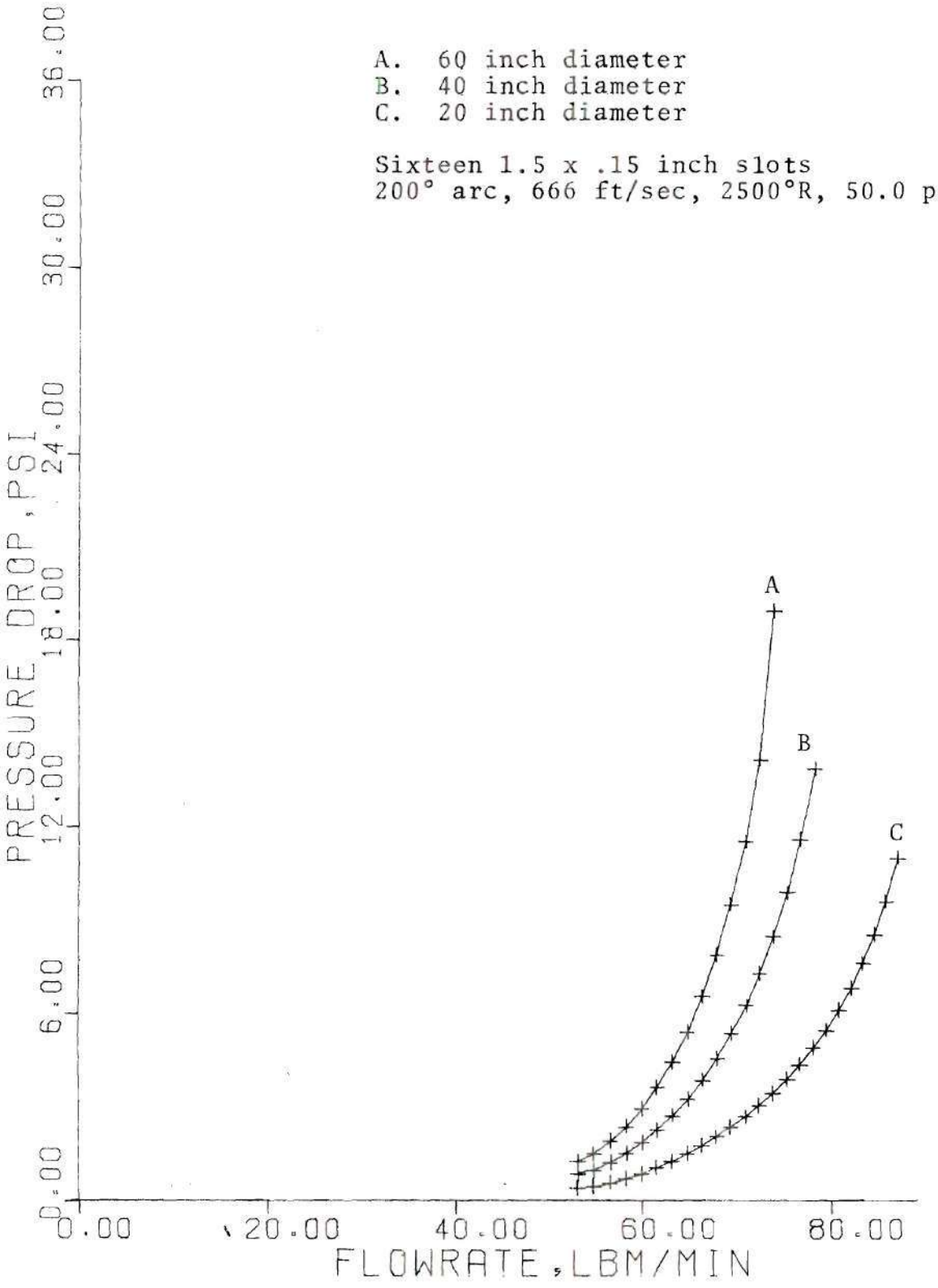

Figure 4-46. Turbine Performance

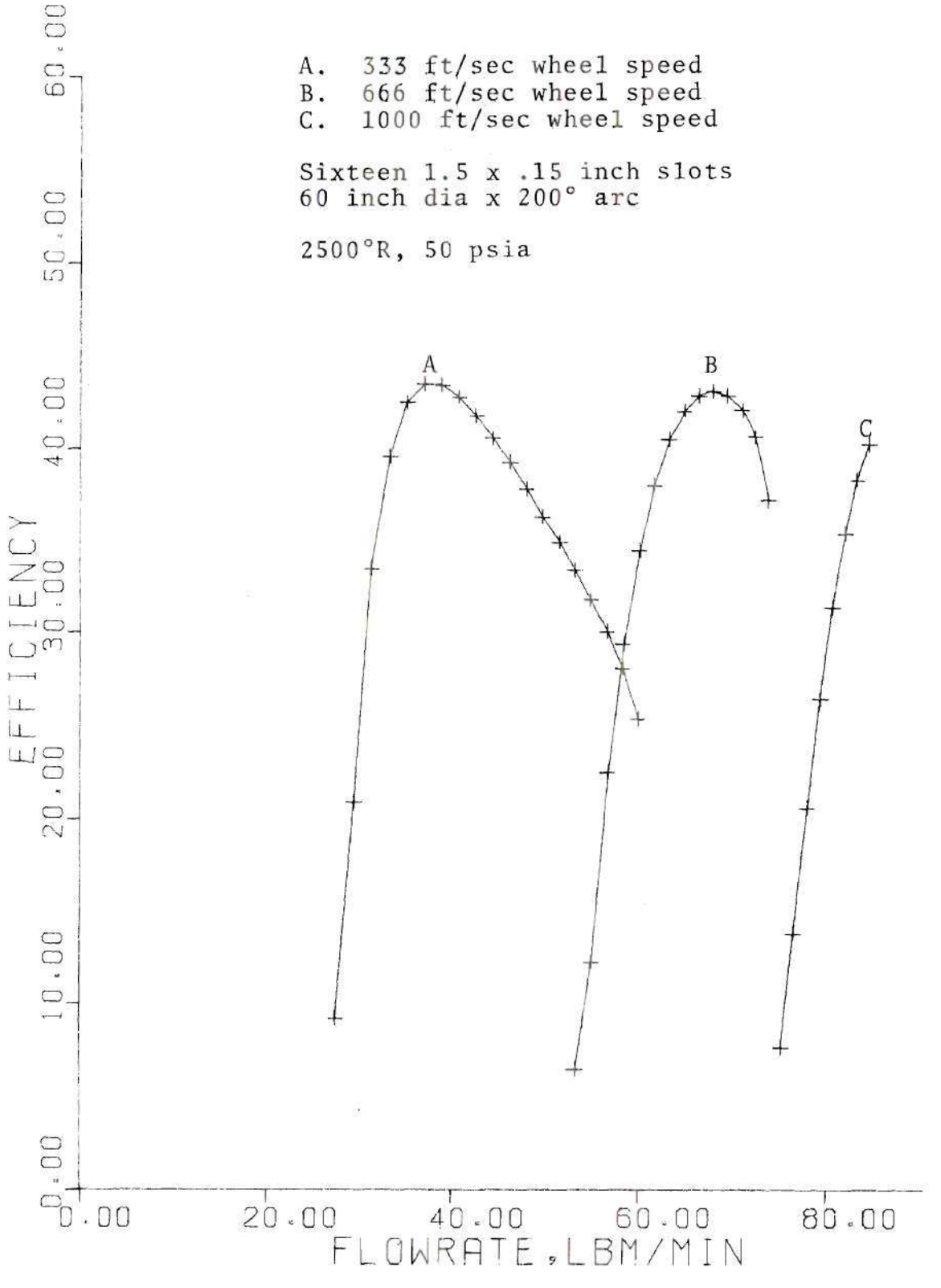

Figure 4-47. Turbine Performance

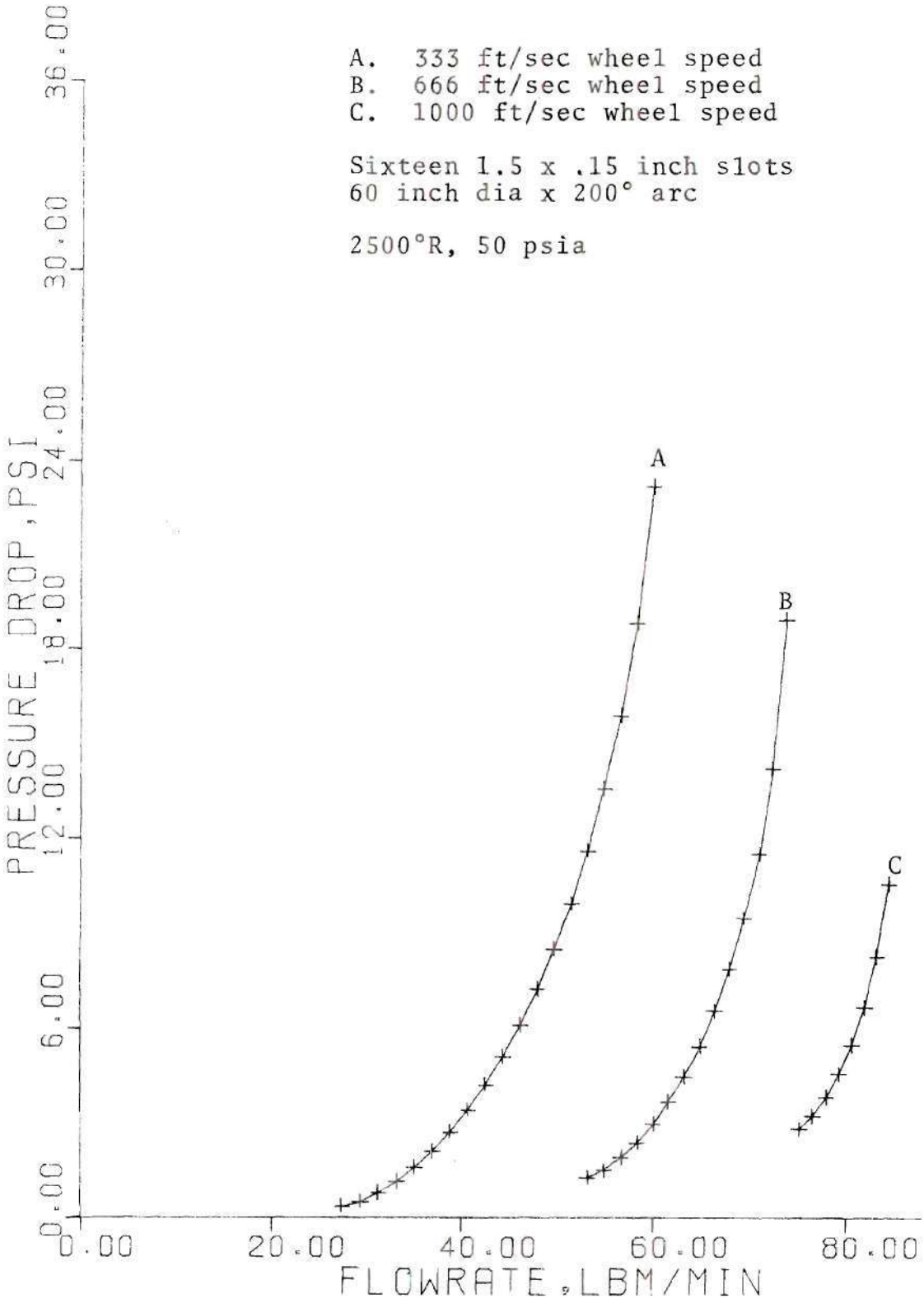

Figure 4-48. Turbine Performance

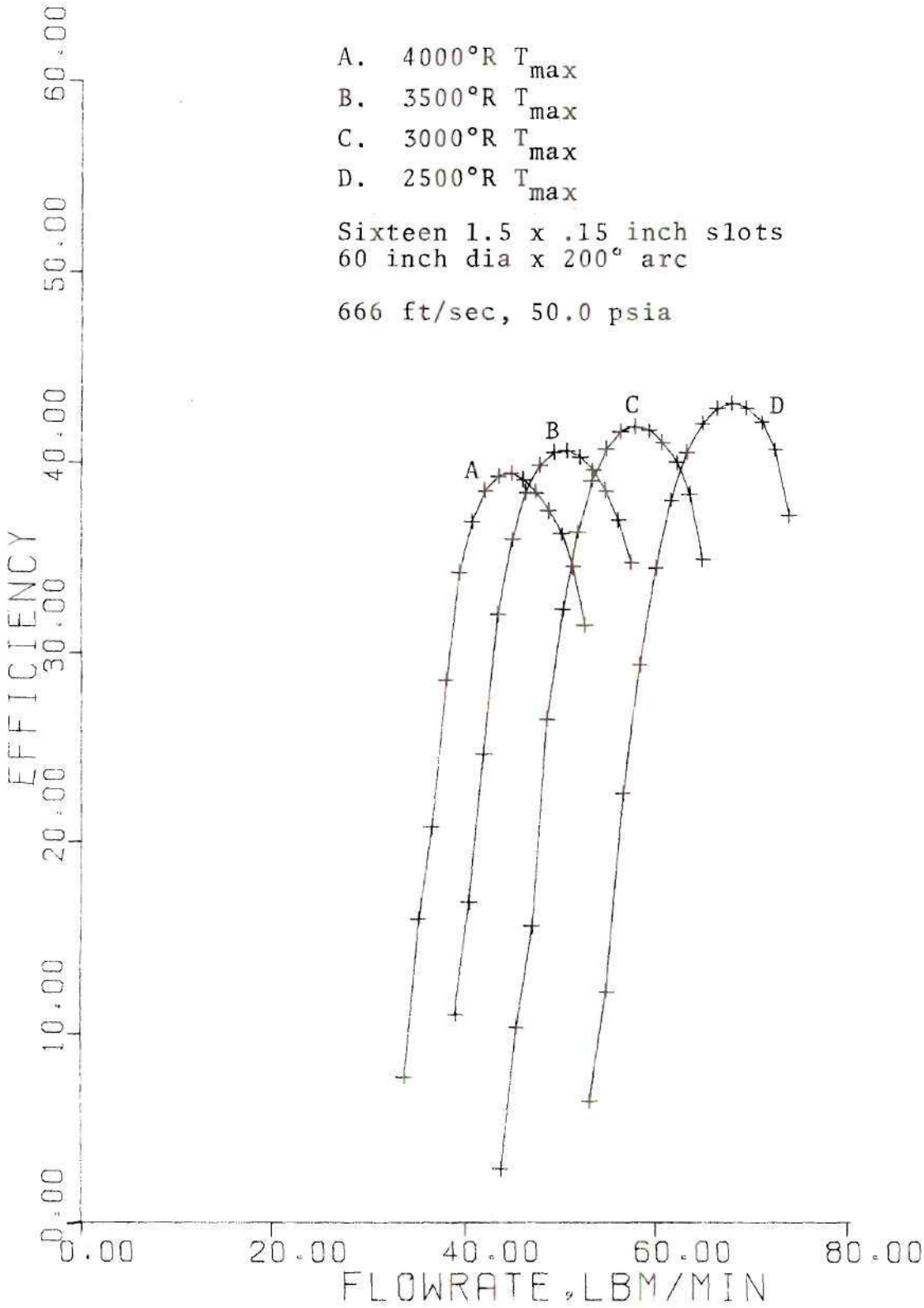

Figure 4-49. Turbine Performance

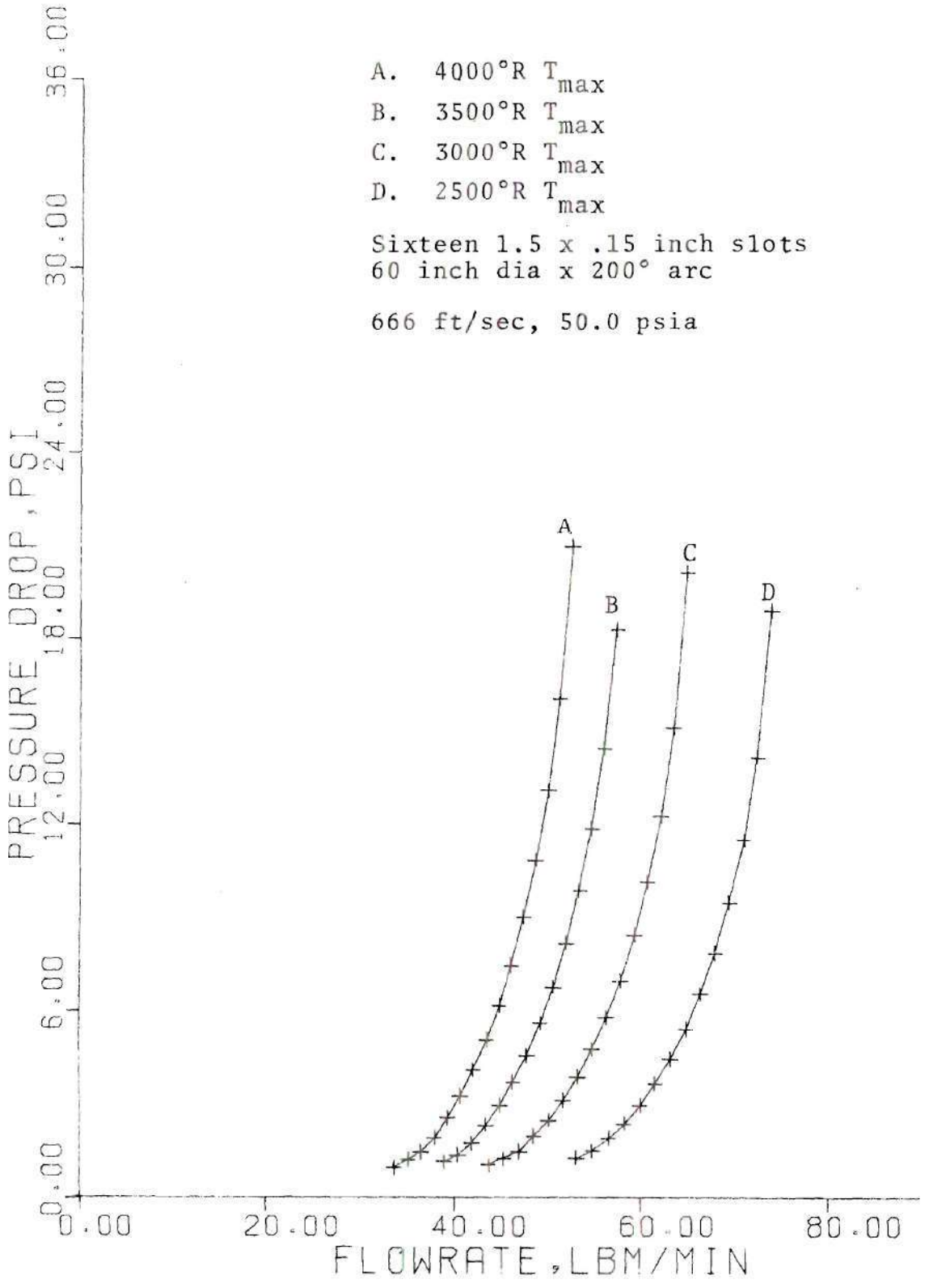

Figure 4-50. Turbine Performance

Table 1. Optimum Cases

Supersonic	Subsonic
18 inch diameter	60 inch diameter
26,500 rpm	3,800 rpm
2500°F	2500°F
Efficiency--37.3%	Efficiency--37.3%
58.2 hp	55.8 hp

turbines of Section 4-6 are given in Figures 4-51 through 4-58. This data, though generated for multiple staged Cases 1 and 2, is generally applicable for 1.5 x .15 x 60 x 200° turbines when the entrance conditions are identical. Interpolation for other cases is recommended. The following ledger (Table 2) defines the entrance conditions for each of the turbines evaluated in Figures 4-51 through 4-58.

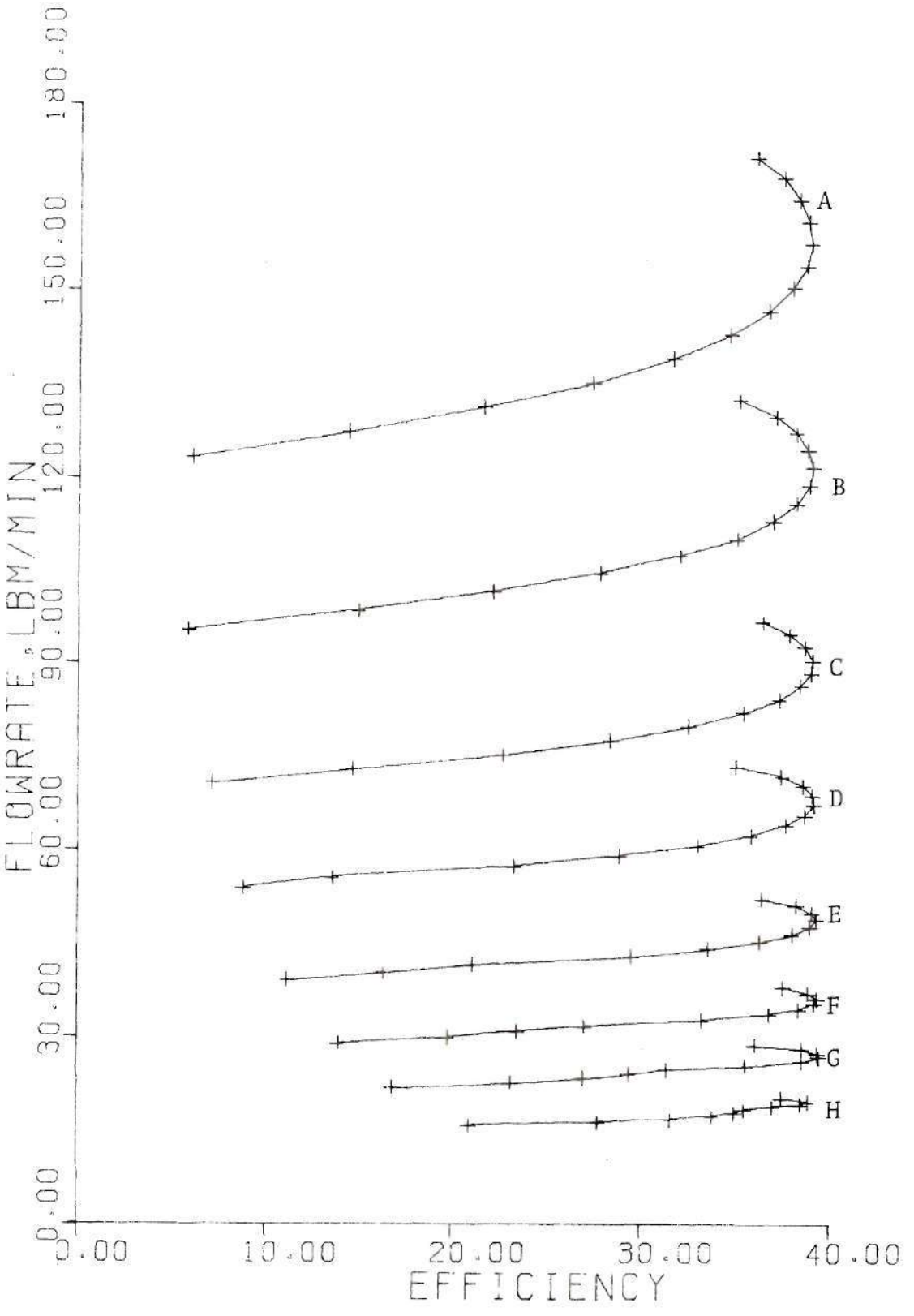

Figure 4-51. Case 1 Turbine Performance

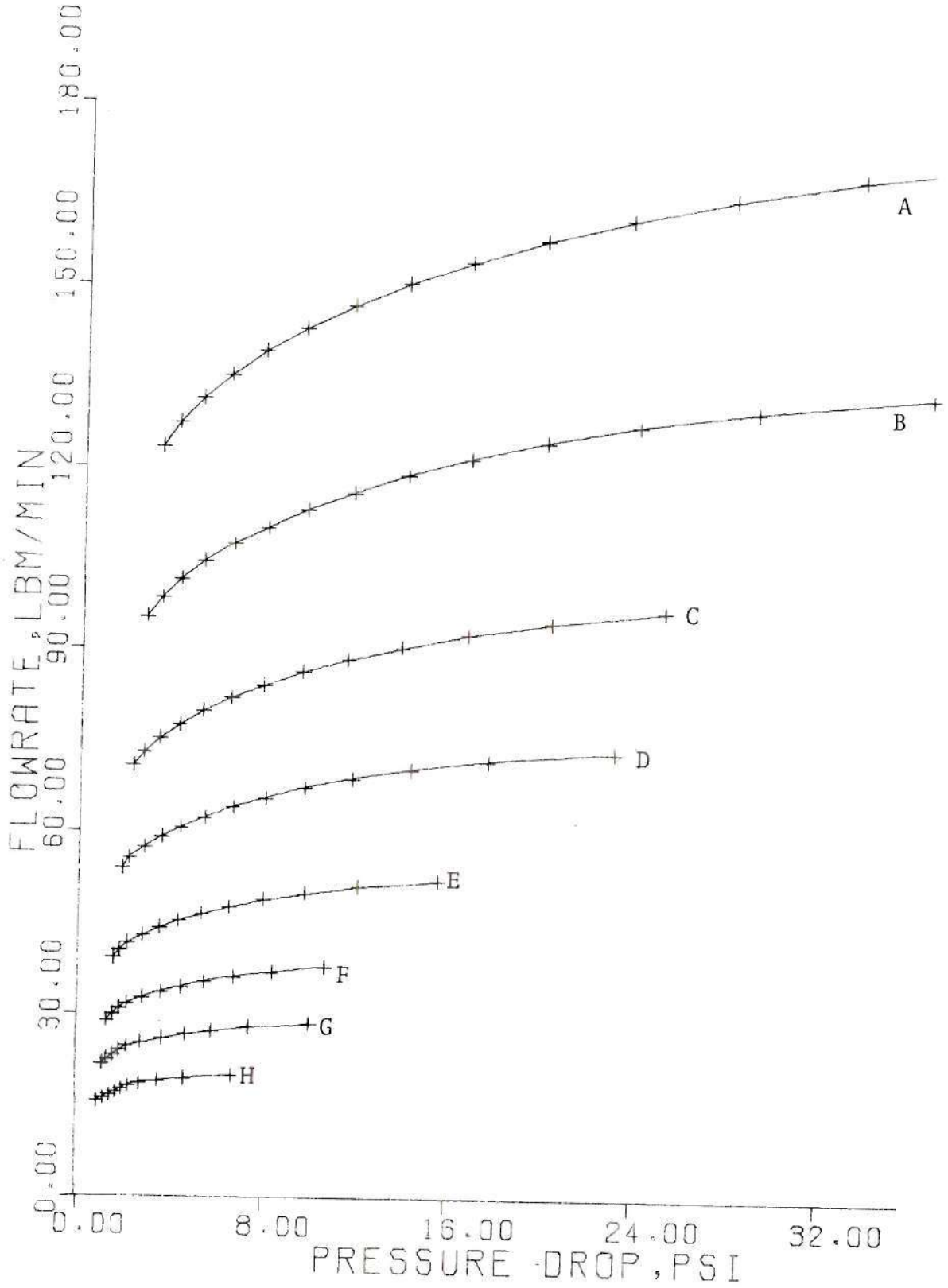

Figure 4-52. Case I Turbine Performance

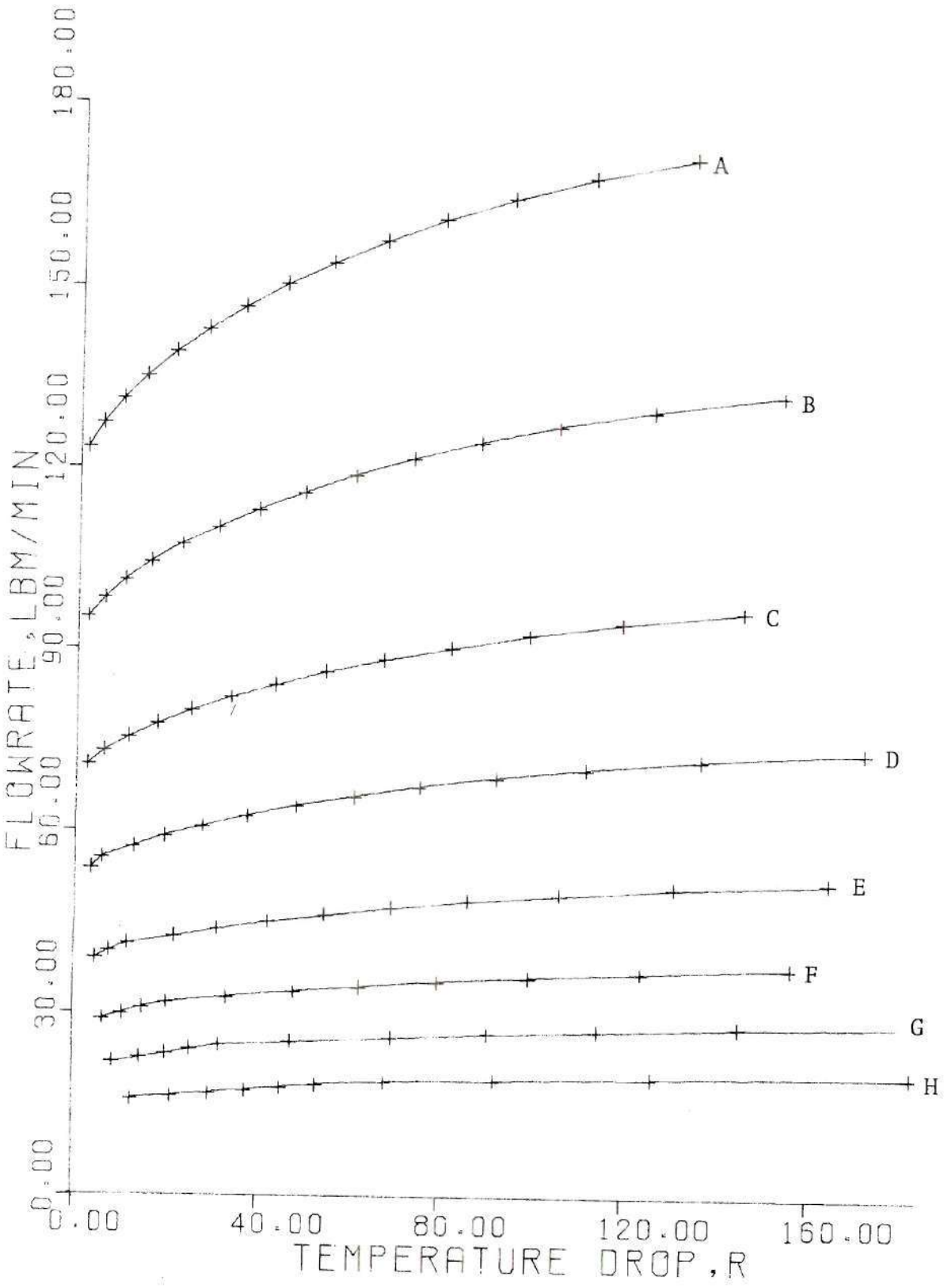

Figure 4-53. Case 1 Turbine Performance

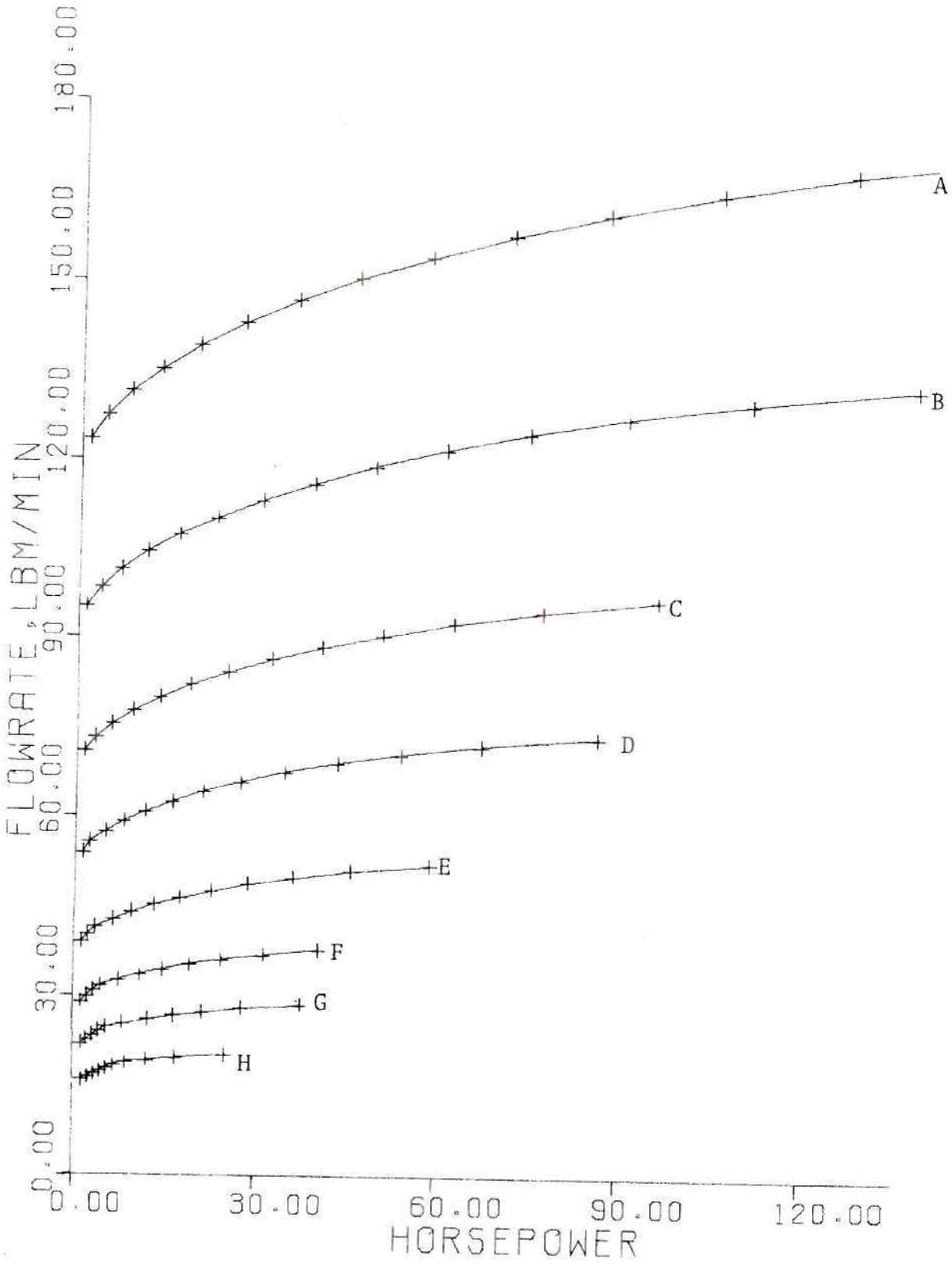

Figure 4-54. Case 1 Turbine Performance

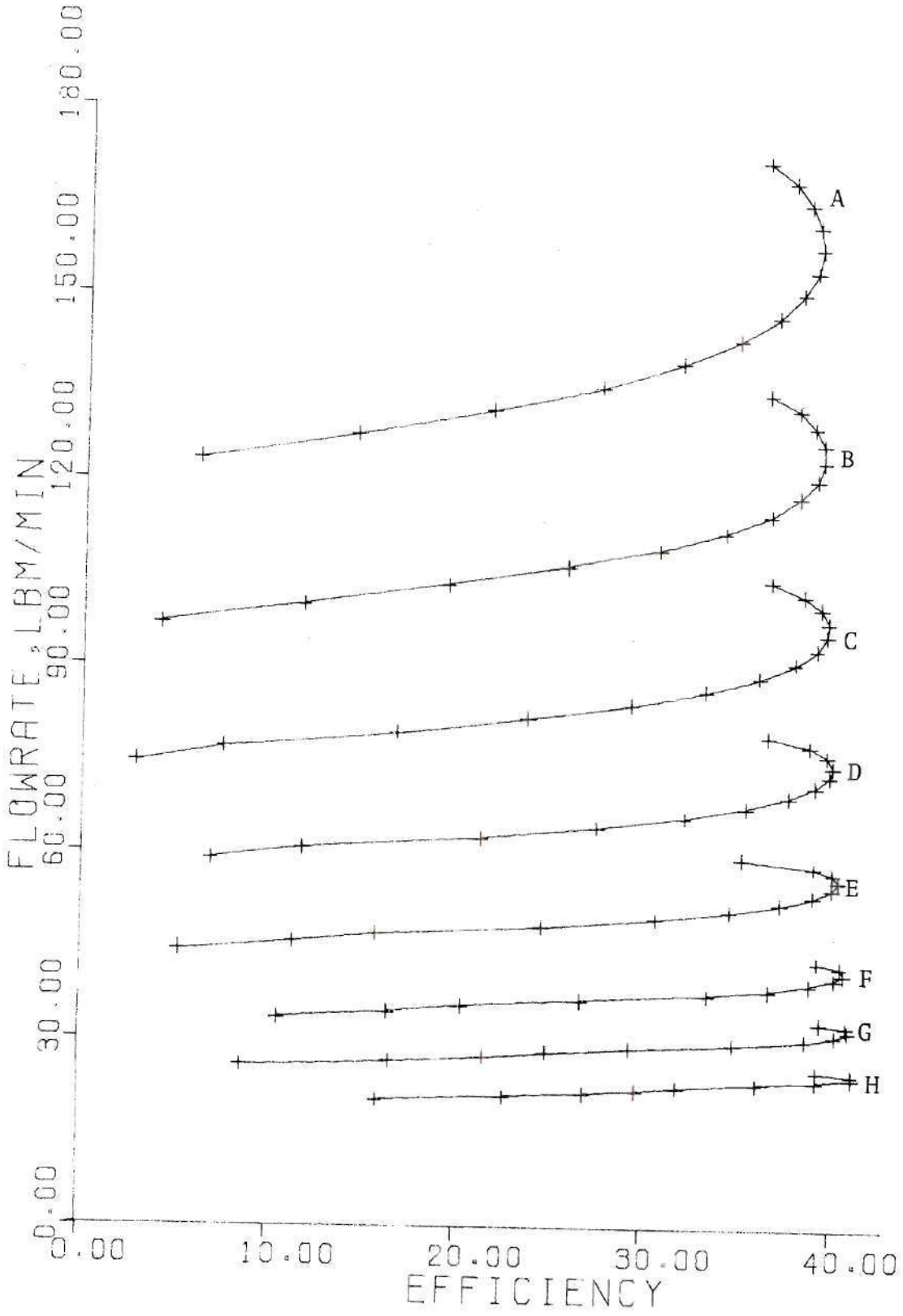

Figure 4-55. Case 2 Turbine Performance

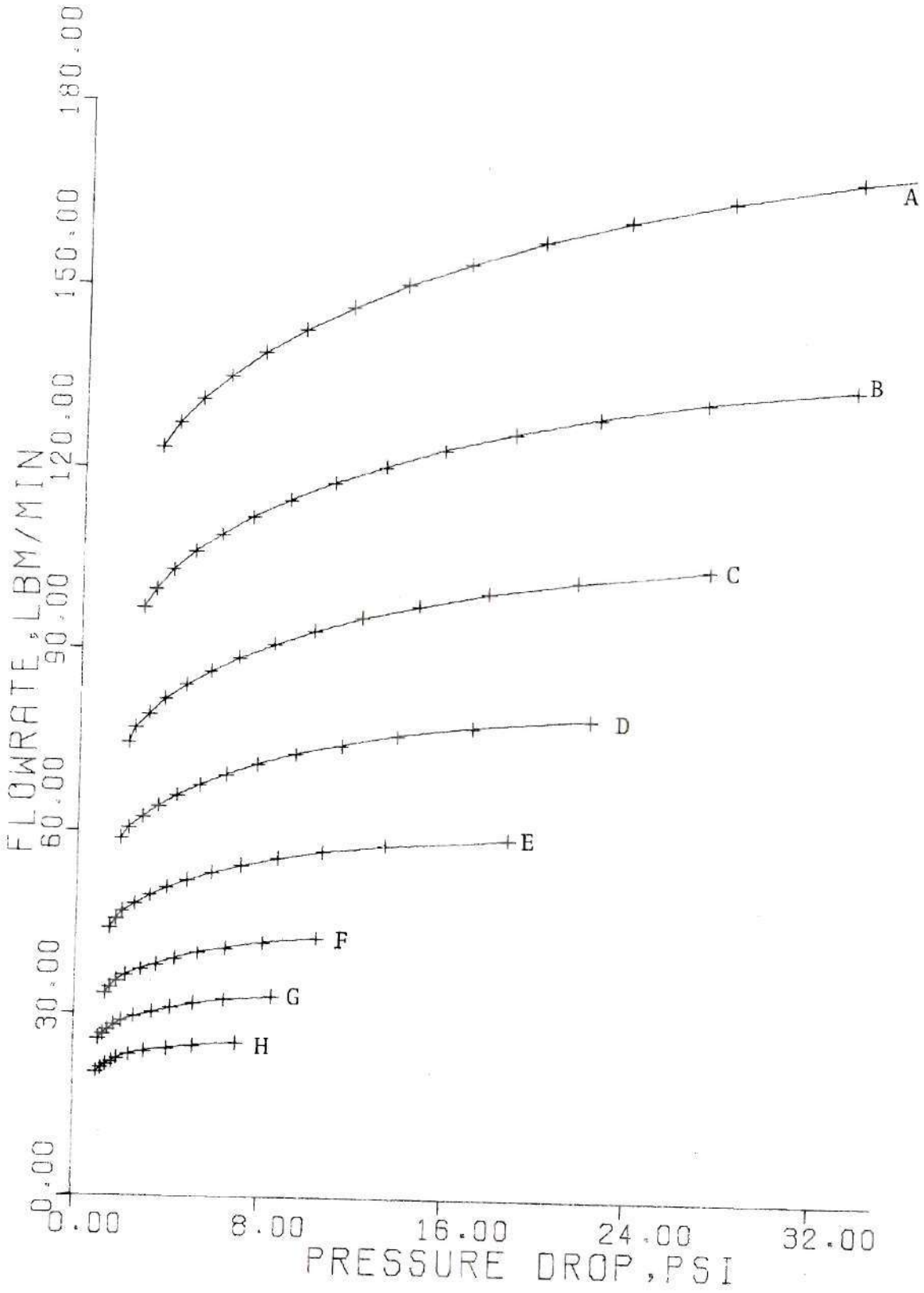

Figure 4-56. Case 2 Turbine Performance

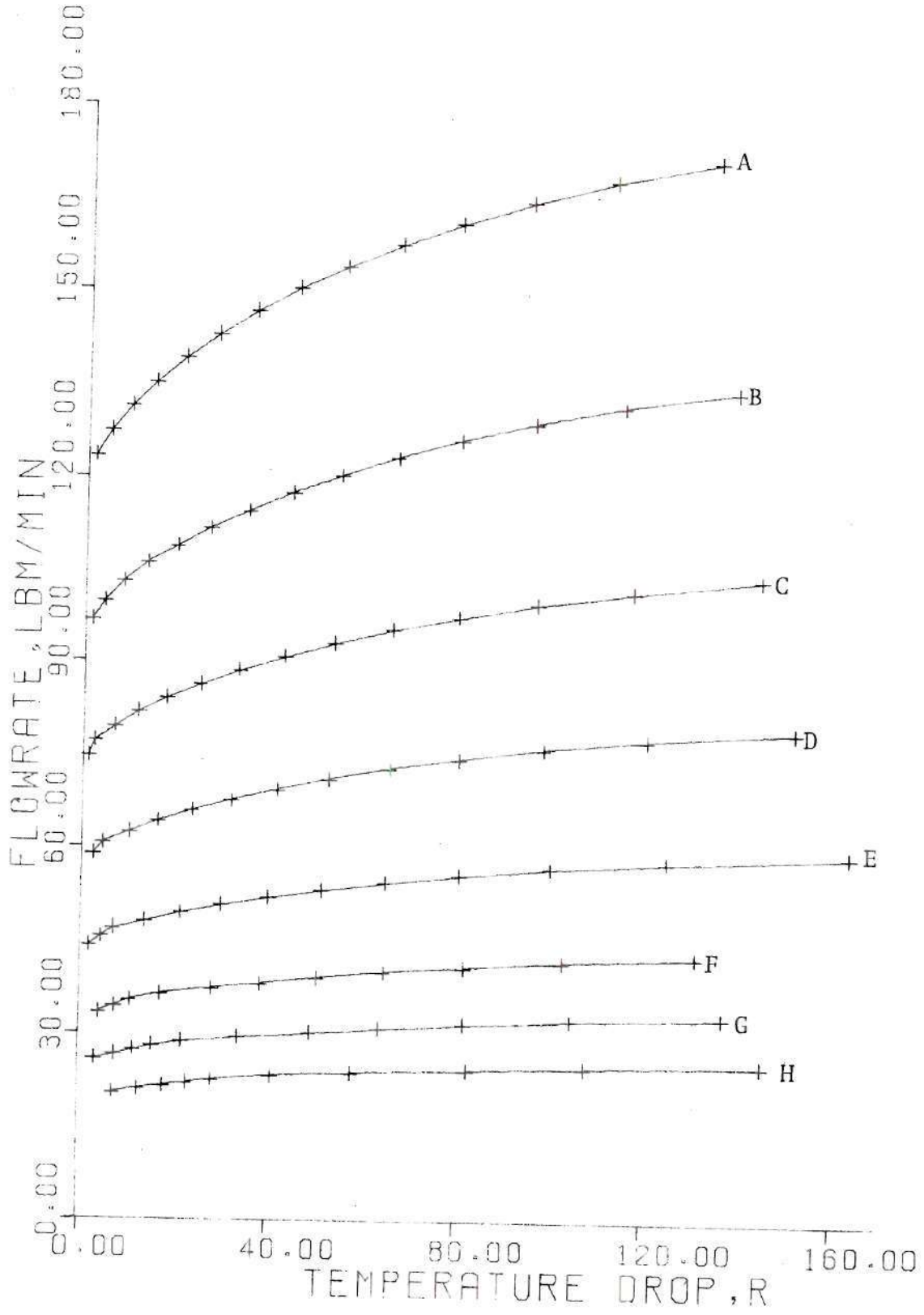

Figure 4-57. Case 2 Turbine Performance

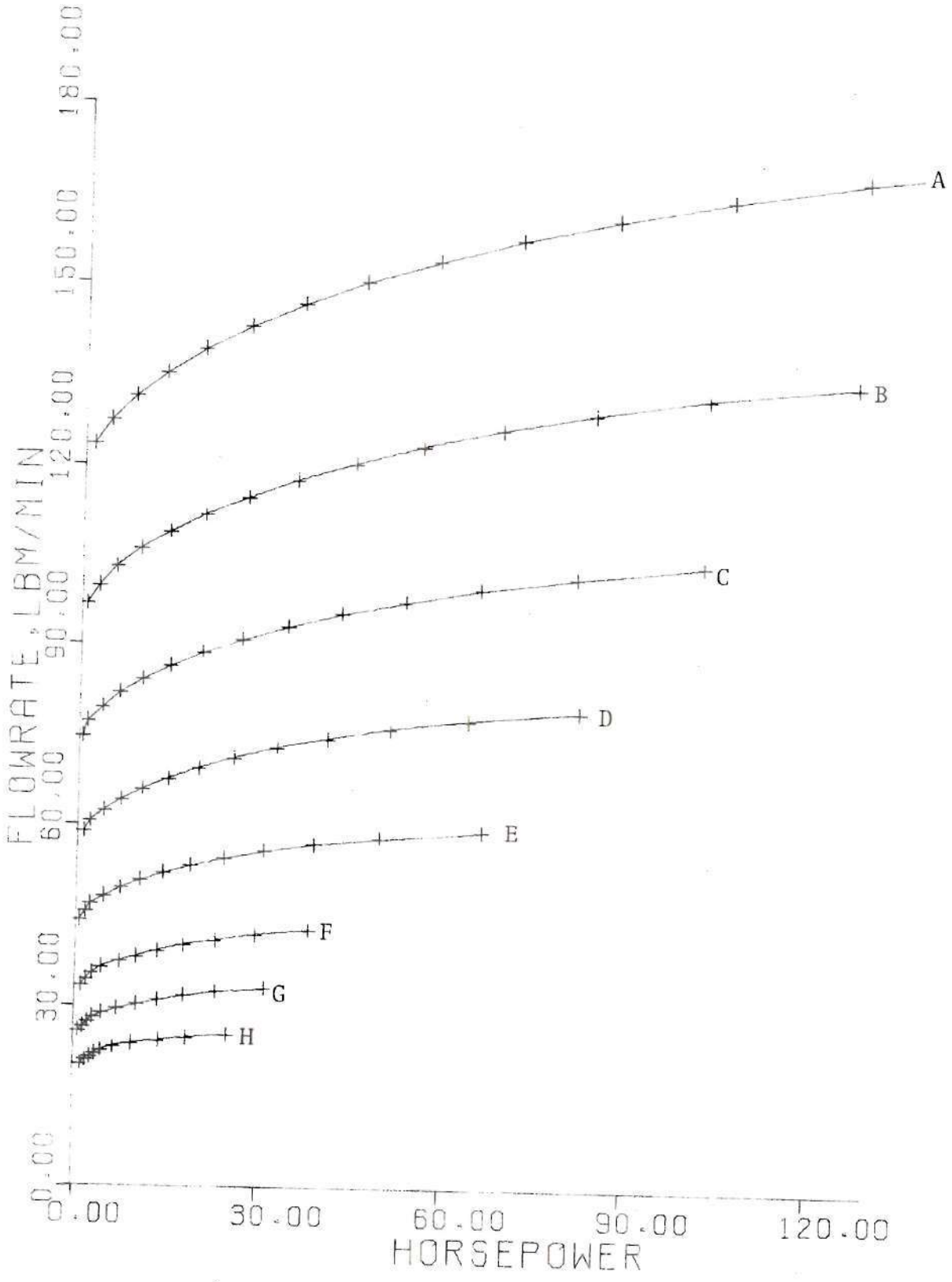

Figure 4-58. Case 2 Turbine Performance

Table 2. Turbine Entrance Conditions

	Case 1	Case 2
A	147 psia, 4000°R	147 psia, 4000°R
B	113.4 psia, 3889°R	113.4 psia, 4000°R
C	86.4 psia, 3775°R	84.4 psia, 4000°R
D	64.9 psia, 3658°R	64.2 psia, 4000°R
E	47.9 psia, 3538°R	46.6 psia, 4000°R
F	34.5 psia, 3413°R	34.5 psia, 4000°R
G	26.4 psia, 3310°R	26.2 psia, 4000°R
H	19.9 psia, 3205°R	18.8 psia, 4000°R

CHAPTER V

CONCLUSIONS AND RECOMMENDATIONS

This study has evaluated and optimized turbine performance on a theoretical basis. The results were shown to be valid by comparison with empirical data and limiting cases. Using the turbine performance characteristics, application as a topping turbine to a coal burning power plant was investigated.

Results indicate that single disk units such as shown in Figure 4-30 have low thermal efficiency and very low output. These are not considered practical for further study. However, using an axial compressor and a series of viscous turbines (Figure 4-38) very attractive efficiency and significant output was attained. Though the size of these units could be prohibitive, variable area geometry and supersonic turbines may offer alternatives to reduce equipment requirements at equivalent outputs.

In this manner, the viscous turbine may present a viable prospect to augment electrical power generation. Further study is recommended in the following areas:

1. Application to existing plants. A survey should be made of operating powerplants to determine the extent of applicability of a viscous topping turbine system. Effect

of the turbine on the steam cycle should also be evaluated. For example, will the boiler effectiveness be reduced when combustion occurs externally? What will refitting the existing plants to accommodate the turbine entail? Persons working in the power industry should be consulted in this portion of the study for suggestions and evaluation.

2. Heat transfer analysis. As discussed in Section 4-7 the heat transfer evaluations in this thesis represent two extremes: zero heat transfer or infinite resistance in the disk, and constant surface temperature or zero heat resistance in the disk. The difference was significant in regard to unit performance. Transient heat conduction analysis into the fins in conjunction with turbine operation needs to be performed in order to correctly ascertain the unit's potential. Possible surface coating of the disk with a high temperature insulative material may also be investigated.

3. Unit optimization. Analysis has indicated that unit efficiency, horsepower, and physical size are mutual tradeoffs. No attempt has been made to optimize the operation with regard to these quantities, because no valid basis for comparison was available. For example, which is the most practical, a 14 percent efficient 500 hp unit or a 9 percent efficient 1000 hp unit? Which is more practical, eight straight area series turbines at 14 percent or four variable area series turbines at 10 percent thermal efficiency.

Thorough optimization will be possible when these criteria are defined.

These recommendations are given in order of importance. Should the results of each study be found favorable, the next phase would be to build a prototype and test operational modes.

APPENDICES

APPENDIX A

VISCOUS TURBINE COMPUTER MODEL

```
      PROGRAM TURBINE(INPUT,OUTPUT,TAPE5=INPUT,TAPE6=OUTPUT)
      DIMENSION  VC(11),PC(11),TC(11),RHOC(11),FC(10),DDC(10)
      DIMENSION TO(99,10),C(99)
      DIMENSION HH(99,10),G(99)
      DIMENSION XX(99,10),YY(99,10),KA(10),KB(10),KD(10)
      DIMENSION X(99),Y(99),IBUF(512)
      DIMENSION PP(99,10),Z(99),BS(99,10),P(99)
      DIMENSION UE(99,10),U(99),HP(99,10),D(99)
      REAL N,MDOT,MA,MD,M,MM,MB
      CALL PLOTS(IBUF,512,9,00)
      CALL PLOT(2.0,1.5,-3)
      CALL FACTOR(1.2)
      PI=3.1416
    4 CONTINUE
C
C     KC AND KK ARE USED FOR PLOTTER INSTRUCTIONS
C     KC REPRESENTS THE NUMBER OF PLOTS,KK THE NUMBER OF CURVES
C
      KC=0
C
C     INPUT DATA
C
    1 READ(5,2) H,W,N,DIA,A3,S,T3,PRST
    2 FORMAT(8F10.0)
      IF(H.EQ.0.0) GO TO 99
      KC=KC+1
      H1=H
      RPM=S*60./PI/DIA
      WRITE(6,3)H,W,N,DIA,A3,S,T3,PRST
    3 FORMAT(8F15.7,/)
      DX=PI*DIA/180.
      KK=0
C
C     FLOWRATE IS CONTROLED BY MACH NUMBER
C
      DO 11 I=1,100,3
      D2=I
      MA=D2*.01
      C3=0.0
      DA=0.0
      H=H1
      QC=0.0
      AA=H1*W*N
C
C     ISENTROPIC ENTRANCE SECTION
C
      T=T3/(1.0+.2*(MA**2.0))
      P=PRST*((T/T3)**3.5)
      MDOT=P*AA*MA*.92/(T**.5)
      RHO=P/(T*639.6)
      V=MDOT/(RHO*AA)
      IF(S.GT.V) GO TO 11
      QC=0.0
```

```
      DRAG=0.0
      VC(1)=V
      PC(1)=P
      TC(1)=T
      RHOC(1)=RHO
C
C     MD IS FLOW THROUGH EACH SLOT
C
      MD=MDOT/N
      TW=2500.
      WRITE(6,44)V,RHO,P,T,MA,TW,MDOT
   44 FORMAT(7F15.5,/)
C
C     BEGIN ITERATION OF CONTROL VOLUMN ANALYSIS
C
      DO 21 J=1,10
      DA=J
      DO 19 IJ=1,10
      H=H*(1.+DA)
      IF(H/W.GT.10.0) GO TO 12
      AA=H*W*N
      D=2.0*H*W/(H+W)
C
C     CALCULATION OF FLUID PROPERTIES
C
      VIS=1.285*((TC(J)/560.0)**1.35)*(1000./(TC(J)+440.))*1.E-5
      CP=(((TC(J)/1000.)-1.0)*.02)+.2486
C
C     CALCULATION OF STRESSES AND CONVECTION FACTOR
C
      REW=(ABS(VC(J)-S))*D*RHOC(J)*12.0/VIS
      CALL FF (REW,FW)
      HW=RHOC(J)*CP*FW*(ABS(S-VC(J)))/8.0
      TAUW=FW*RHOC(J)*(ABS(S-VC(J)))*(S-VC(J))/3091.2
      REC=VC(J)*D*RHOC(J)*12.0/VIS
      CALL FF (REC,FX)
      TAUC=FX*RHOC(J)*(VC(J)**2.0)/3091.2
C
C     CALCULATION OF WORK,FORCE,AND HEAT TRANSFER
C
      DQC(J)=(TW-TC(J))*HW*((2.0*H)+W)*DX/MD
      FC(J)=TAUW*((2.0*H)+W)*DX
      DW=FC(J)*S/(MD*9336.3)
      C1=FC(J)/(H*W)-TAUC*DX/H
      C2=(DQC(J)+DW)/CP
      C6=MD/(H*W*TC(J)*53.3*32.2*144.0)
      C7=MD/(H*W*TC(J)*CP*32.2*778.*144.)
      BB=C3
      C3=C6-C7-(RHOC(J)/VC(J))
      IF(BB/C3.LT.0.0) GO TO 12
      C4=((C1/(53.3*TC(J)*12.0))-(C2*RHOC(J)/TC(J)))
C
C     COMBINATION OF FUNCAMENTAL EQUATIONS
```

```
C
      DV=C4/C3
C
C     CONTINUITY EQUATION
C
      DRHO=-RHOC(J)*DV/VC(J)
C
C     MOMENTUM EQUATION
C
      DP=-(M0*DV/(H*W*32.2*12.0))+C1
C
C     ENERGY EQUATION
C
      DT=C2-(VC(J)*DV/(CP*32.2*144.0*778.))
C
      IF(IJ.NE.1) GO TO 18
      WRITE(6,45)VC(J),TC(J),PC(J),DRAG,CT,C2,DV,DW,DQC(J),D8
      WRITE(6,46)DV,C1,C2,C6,C7,C3,C4,TAUW,TAUC,FW,H
   18 CONTINUE
      QC=QC+DQC(J)
      DRAG=DRAG+FC(J)*N
      VC(J)=VC(J)+DV
      M=VC(J)/12./(SQRT(2402.8*TC(J)))
      IF(M.GT.1.0) GO TO 12
      PC(J)=PC(J)+DP
      TC(J)=TC(J)+DT
      RHOC(J)=MDOT/(VC(J)*AA)
   19 CONTINUE
      VC(J+1)=VC(J)
      PC(J+1)=PC(J)
      TC(J+1)=TC(J)
      RHOC(J+1)=RHOC(J)
   21 CONTINUE
C
C     FINISH CONTROL VOLUMN ITERATION
C
      D8=11.0
      J=11
      WRITE(6,45)VC(J),TC(J),PC(J),DRAG,CT,C2,DV,DW,DQC(J),D8
      WRITE(6,46)DV,C1,C2,C6,C7,C3,HH,TAUW,TAUC,TC(J),M
   45 FORMAT(10F10.3)
   46 FORMAT(11E12.5,/)
      V=VC(11)
      T=TC(11)
      RHO=RHOC(11)
      P=PC(11)
      IF(P.LT.0.0) GO TO 12
C
C     ISENTROPIC EXIT SECTION
C
      MB=(V/12.0)/(SQRT(2402.8*T))
      PT=P*((1.0+.2*(MB**2.0))**3.5)
      DELP=PT-PRST
```

```
C
C       CALCULATION OF TURBINE EFFICIENCY,HORSEPOWER,AND SINGLE STAGE
C       UNIT EFFICIENCY
C
        WT=MDOT*CP*T3*(((PT/PRST)**.286)-1.)
        WA=DRAG*S/(778.*12.)
        EFF=WA/WT
        T2=530.*(((PRST/PT)**.286))
        WC=MDOT*.243*(T2-530.)/.8
        TA=(T2+T3)/2.
        CP=(((TA/1000.)-1.)*.02)+.2486
        QIN=MDOT*CP*(T2-T3)
        TEFF=(WA+WC)/QIN
        WRITE(6,47)DELP,MDOT,EFF,WA,TEFF
   47   FORMAT(8F15.4,/,/,/)
C
C       DATA PREPARED FOR PLOTTER
C
        KK=KK+1
        HP(KK,KC)=(WA+WC)/(-.707)
        PP(KK,KC)=DELP*(-1.)
        TO(KK,KC)=(WA*(-1.0))/(.29*MDOT)+(QC*(-1.0))/.29
        BS(KK,KC)=WA*(-1.0)
        XX(KK,KC)=MDOT*60.
        YY(KK,KC)=EFF*100.
        UE(KK,KC)=TEFF*100.
        HH(KK,KC)=H/H1
        KA(KC)=KK+1
        KB(KC)=KK+2
        KD(KC)=KK
   11   CONTINUE
   12   CONTINUE
        GO TO 1
   99   CONTINUE
C
C       PLOTTER INSTRUCTIONS
C
        CALL AXIS(0.0,0.0,"FLOWRATE,LBM/MIN",-16,5.0,0.0,0.0,10.)
        CALL AXIS(0.0,0.0,"PRESSURE DROP,PSI",17,5.0,90.0,0.0,5.0)
        KF=KC
        DO 97 KC=1,KF
        KE=KA(KC)
        O(KE)=-5.0
        C(KE)=0.0
        U(KE)=-1.0
        Y(KE)=0.0
        Z(KE)=0.00
        X(KE)=0.0
        KE=KB(KC)
        O(KE)=5.0
        C(KE)=40.0
        X(KE)=10.
        Z(KE)=5.0
```

```
      U(KE)=1.0
      Y(KE)=7.0
      KE=KC(KC)
      DO 96 L=1,KE
      U(L)=UE(L,KC)
      Z(L)=PP(L,KC)
      X(L)=XX(L,KC)
      Y(L)=YY(L,KC)
      C(L)=TC(L,KC)
      O(L)=HP(L,KC)
      G(L)=HH(L,KC)
      B(L)=BS(L,KC)
C
C     PRINT OUT PLOT DATA
C
      WRITE(6,47) X(L),Y(L),Z(L),U(L),O(L),B(L),C(L),G(L)
   96 CONTINUE
      CALL LINE(X(1),Z(1),KE,1,1,3)
   97 CONTINUE
      CALL PLOT(9.0,0.0,-3)
C
C     RETURN TO READ ADDITIONAL SETS OF DATA
C
      IF(A3.EQ.0.0) GO TO 4
      CALL PLOT(0.0,0.0,999)
      STOP
      END
```

APPENDIX B

SUBROUTINES

```
C      FRICTION FACTOR SUBROUTINE
C
       SUBROUTINE FF (RE,F)
       IF(RE.GT.2000.) GO TO 23
C
C      LAMINAR
C
       F=71.0/RE
       GO TO 26
C
C      TURBULENT
C
   23  F=.05
       D1=-.05
       DO 25 JJ=1,10
       D2=JJ
       F=F+D1*(2.0**(-D2))
       D3=1.0/(SQRT(F))
       D4=2.0*(ALOG10(RE*(SQRT(F))))-.8
       IF(D3.GT.D4) GO TO 24
       D1=-.05
       GO TO 25
   24  D1=.05
   25  CONTINUE
   26  CONTINUE
       RETURN
       END
```

```
      SUBROUTINE ISO (A1,A2,V,RHO,P,T,MDOT,MB)
      REAL MDOT,MB
      A=A1
      MB=(V/12.0)/(SQRT(2402.8*T))
      PT=P*((1.0+.2*(MB**2.0))**3.5)
      WRITE(6,34)A,V,P,T
   34 FORMAT(4E15.4)
      DO 30 K=1,100
      DO 33 KM=1,100
      MB=(V/12.0)/(SQRT(2402.8*T))
      X=((A2/A1)**.001)
      DA=((A*X)-A)*(ABS(1.0-MB))
      C8=-MDOT/(A*P*32.2*12.0)
      CP=(((T/1000.)-1.0)*.02)+.2486
      C9=V/(CP*T*32.2*144.0*778.)
      C10=(1.0/V)+C8+C9
      DV=-DA/(A*C10)
      DP=-(MDOT*DV)/(A*32.2*12.0)
      DT=-(V*DV)/(CP*32.2*144.0*778.0)
      A=A+DA
      V=V+DV
      T=T+DT
      P=PT/((1.0+.2*(MB**2.0))**3.5)
      IF(DA.LT.0.0.AND.A.LT.A2)GO TO 32
      IF(DA.GT.0.0.AND.A.GT.A2)GO TO 32
   33 CONTINUE
      WRITE(6,31)A,V,P,T,C8,C9,C10,MB
   31 FORMAT(8E15.4)
   30 CONTINUE
   32 WRITE(6,31)A,V,P,T,C8,C9,C10,MB
      RETURN
      END
```

APPENDIX C

VISCOUS COMPRESSOR AND TURBINE UNIT COMPUTER PROGRAM

```
      PROGRAM ENGINE1(INPUT,OUTPUT,TAPE5=INPUT,TAPE6=OUTPUT)
      REAL N,MDOT,MA,MD,M,MM,MB
      DIMENSION  VC(11),PC(11),TC(11),RHOC(11),FC(10),DQC(10)
      DIMENSION  VT(11),PT(11),TT(11),RHOT(11),FT(10),DQT(10)
      PI=3.1416
    1 READ(5,2) H,W,N,DIA,A3,RPM,T3,A4
    2 FORMAT(8F10.0)
      IF(H.EQ.0.0) GO TO 99
      WRITE(6,3) H,W,N,DIA,A3,A4,RPM,T3
    3 FORMAT(8F15.7,/)
      S=RPM*PI*DIA/60.0
      AA=H*W*N
      D=2.0*H*W/(H+W)
      DX=(PI*DIA/3.0)/10.
      DX=DX/10.
      MA=.5
      TW=2000.0
      D1=0.0
      QC=0.0
      QT=0.0
      QT=0.0
C
C     CONVERGENCE OF MDOT,TW
C
      DO 11 I=1,10
      D2=I
      MA=MA+D1*(2.0**(-D2))
      MA=D2*.1
      IF(QT+QC)15,16,17
   15 TW=TW+100.0
      GO TO 16
   17 TW=TW-100.0
   16 CONTINUE
C
C     ISENTROPIC 1 TO A
C
      T=530.0/(1.0+.2*(MA**2.0))
      P=14.7*((T/530.0)**3.5)
      MDOT=P*AA*MA*.92/(T**.5)
      RHO=P/(T*639.6)
      V=MDOT/(RHO*AA)
C
C     FLOW THROUGH COMPRESSOR
C
      QC=0.0
      DRAG=0.0
      MD=MDOT/N
      VC(1)=V
      PC(1)=P
      TC(1)=T
      RHOC(1)=RHO
      WRITE(6,44)V,RHO,P,T,MA,TW,MDOT
   44 FORMAT(7F15.5,/)
      DO 20 J=1,10
      J8=J
C
C     IF MACH RELATIVE TO WHEEL EXCEEDS ONE REDUCE RELATIVE VELOCITY
```

```
C
      M=(ABS(VC(J)-S))/12.0/(SQRT(2402.8*TC(J)))
      IF(M-1.0)21,21,22
   22 CONTINUE
      IF(S.GT.VC(J))D1=1.0
      IF(S.LT.VC(J))D1=-1.0
      GO TO 10
   21 CONTINUE
      DO 19 IJ=1,10
      VIS=1.485*((TC(J)/560.0)**1.35)*(1000./(TC(J)+440.))*1.E-5
      CP=(((TC(J)/1000.)-1.0)*.02)+.2486
      REW=(ABS(VC(J)-S))*D*RHOC(J)*12.0/VIS
C
C     CALCULATE FW,FC,TAU,HW   COMPRESSOR
C
      CALL FF (REW,FW)
      HW=RHOC(J)*CP*FW*(ABS(S-VC(J)))/8.0
      TAUW=FW*RHOC(J)*(ABS(S-VC(J)))*(S-VC(J))/3091.2
      REC=VC(J)*D*RHOC(J)*12.0/VIS
      CALL FF (REC,FX)
      TAUC=FX*RHOC(J)*(VC(J)**2.0)/3091.2
      DQC(J)=(TW-TC(J))*HW*((2.0*H)+W)*DX/MD
      DQC(J)=0.0
      FC(J)=TAUW*((2.0*H)+W)*DX
C
C     CALCULATE VELOCITY INCREMENT   COMPRESSOR
C
      DW=FC(J)*S/(MD*9336.0)
      C1=FC(J)/(H*W)-TAUC*DX/H
      C2=(DQC(J)+DW)/CP
      C6=MD/(H*W*TC(J)*53.3*32.2*144.0)
      C7=RHOC(J)*VC(J)/(TC(J)*CP*32.2*778.*144.)
      C3=C6-C7-(RHOC(J)/VC(J))
      C4=((C1/(53.3*TC(J)*12.0))-(C2*RHOC(J)/TC(J)))
      DV=C4/C3
C
C     CONTINUITY EQUATION
C
      DRHO=-RHOC(J)*DV/VC(J)
C
C     MOMENTUM EQUATION
C
      DP=-(MD*DV/(H*W*32.2*12.0))+C1
C
C     ENERGY EQUATION
C
      DT=C2-(VC(J)*DV/(CP*32.2*144.0*778.))
C
      IF(IJ.NE.1) GO TO 18
      WRITE(6,45)VC(J),TC(J),PC(J),DRAG,DT,C2,DV,DW,DQC(J),D8
      WRITE(6,46)DV,C1,C2,C6,C7,C3,HW,TAUW,TAUC,C4,RHOC(J)
   46 FORMAT(11E12.5,/)
   45 FORMAT(10F10.3)
   18 CONTINUE
      QC=QC+DQC(J)*N
      DRAG=DRAG+FC(J)*N
      VC(J)=VC(J)+DV
```

```
      PC(J)=PC(J)+DP
      TC(J)=TC(J)+DT
      RHOC(J)=MDOT/(VC(J)*AA)
   19 CONTINUE
      VC(J+1)=VC(J)
      PC(J+1)=PC(J)
      TC(J+1)=TC(J)
      RHOC(J+1)=MDOT/(VC(J+1)*AA)
   20 CONTINUE
      D8=11.0
      J=11
      WRITE(6,45)VC(J),TC(J),PC(J),DRAG,DT,C2,DV,DW,DQC(J),D8
      WRITE(6,46)DV,C1,C2,C6,C7,C3,HW,TAUW,TAUC,TC(J),VC(J)
      V=VC(11)
      RHO=RHOC(11)
      P=PC(11)
      T=TC(11)
C
C     ISENTROPIC 8 TO 2
C
      CALL ISO (AA,A3,V,RHO,P,T,MDOT,M8)
      V2=V
      P2=P
      T2=T
      RHO2=RHO
C
C     COMBUSTION 2 TO 3
C
      CP=((((T3+T2)/2000.)-1.0)*.32)+.2486
      FUEL=MDOT*CP*(T3-T2)
      T=T3
      RHO=P/(53.3*T*12.0)
      RHO3=RHO
      V=MDOT/(RHO*A3)
      V3=V
C
C     ISENTROPIC 3 TO C
C
      CALL ISO (A3,AA,V,RHO,P,T,MDOT,M8)
      IF(T.LT.0.0) GO TO 10
      IF(M8.LT.1.0) GO TO 6
      D1=-1.0
      GO TO 10
    6 CONTINUE
C
C     FLOW THROUGH TURBINE
C
      QT=0.0
      PUSH=0.0
      VT(1)=V
      PT(1)=P
      TT(1)=T
      RHOT(1)=RHO
      DO 50 L=1,10
      D8=L
C
C     IF MACH RELATIVE TO WHEEL EXCEEDS ONE REDUCE RELATIVE VELOCITY
```

```
C
      M=(ABS(VT(L)-S))/12.0/(SQRT(2402.8*TT(L)))
      IF(M-1.0)51,51,52
   52 CONTINUE
      IF(S.GT.VT(L))D1=1.0
      IF(S.LT.VT(L))D1=-1.0
      GO TO 10
   51 CONTINUE
      DO 57 LI=1,10
      VIS=1.285*((TT(L)/560.0)**1.35)*(1000./(TT(L)+440.))*1.E-5
      CP=(((TT(L)/1000.)-1.0)*.02)+.2486
      REW=(ABS(VT(L)-S))*D*RHOT(L)*12.0/VIS
C
C     CALCULATE FW,FC,TAU,HW   TURBINE
C
      CALL FF (REW,FW)
      HW=RHOT(L)*CP*FW*(ABS(S-VT(L)))/3.0
      TAUW=FW*RHOT(L)*(ABS(VT(L)-S))*(VT(L)-S)/3091.2
      REC=VT(L)*D*RHOT(L)*12.0/VIS
      CALL FF (REC,FX)
      TAUC=FX*RHOT(L)*(VT(L)**2.0)/3091.2
      DQT(L)=(TW-TT(L))*HW*((2.0*H)+W)*DX/MD
      DQT(L)=0.0
      FT(L)=TAUW*((2.0*H)+W)*DX
C
C     CALCULATE VELOCITY INCREMENT   TURBINE
C
      DW=FT(L)*(-1.0*S)/(MD*9336.0)
      C1=-FT(L)/(H*W)-TAUC*DX/H
      C2=(DQT(L)+DW)/CP
      C6=MD/(H*W*TT(L)*53.3*32.2*144.0)
      C7=RHOT(L)*VT(L)/(TT(L)*CP*32.2*778.*144.)
      C3=C6-C7-(RHOT(L)/VT(L))
      C4=((C1/(53.3*TT(L)*12.0))-(C2*RHOT(L)/TT(L)))
      DV=C4/C3
C
C     CONTINUITY EQUATION
C
      DRHO=-RHOT(L)*DV/VT(L)
C
C     MOMENTUM EQUATION
C
      DP=-(MD*DV/(H*W*32.2*12.0))+C1
C
C     ENERGY EQUATION
C
      DT=C2-(VT(L)*DV/(CP*32.2*144.0*778.))
C
      IF(LI.NE.1) GO TO 58
      WRITE(6,45)VT(L),TT(L),PT(L),PUSH,DT,C2,DV,DW,DQT(L),D8
      WRITE(6,46)DV,C1,C2,C6,C7,C3,HW,TAUW,TAUC,C4,RHOT(L)
   58 CONTINUE
      QT=QT+DQT(L)*N
      PUSH=PUSH+FT(L)*N
      VT(L)=VT(L)+DV
      PT(L)=PT(L)+DP
      TT(L)=TT(L)+DT
```

```
      RHOT(L)=MDOT/(VT(L)*AA)
   57 CONTINUE
      VT(L+1)=VT(L)
      PT(L+1)=PT(L)
      TT(L+1)=TT(L)
      RHOT(L+1)=MDOT/(VT(L+1)*AA)
   50 CONTINUE
      D8=11.0
      L=11
      WRITE(6,45)VT(L),TT(L),PT(L),PUSH,DT,C2,DV,DW,DQT(L),D8
      WRITE(6,46)DV,C1,C2,C6,C7,C3,HW,TAUW,TAUC,TT(L),VT(L)
      V=VT(11)
      RHO=RHOT(11)
      P=PT(11)
      T=TT(11)
C
C     CHECK MACH LEAVING TURBINE
C
      M=(V/12.0)/(SQRT(2402.8*T))
      IF(M-1.0)95,95,96
   96 CONTINUE
C
C     SHOCK AT EXIT NEGLECTING DIFFUSER
C
      D5=(M**2.)*(1.+.2*(M**2.))/((1.+(1.4*(M**2.)))**2.)
      MM=1.0
      D1=-1.0
      DO 70 II=1,10
      D2=II
      MM=M1+D1*(2.**(-D2))
      D6=(MM**2.)*(1.+.2*(MM**2.))/((1.+(1.4*(MM**2.)))**2.)
      IF(D5.GT.D6) GO TO 71
      D1=-1.0
      GO TO 70
   71 D1=1.0
   70 CONTINUE
      P=P*(1.0+(1.4*(M**2.)))/(1.0+(1.4*(MM**2.)))
      GO TO 97
C
C     ISENTROPIC EXPANSION THROUGH DIFFUSER
C
   95 CALL ISO (AA,A4,V,RHO,P,T,MDOT,M3)
C
C     IF P IS LESS THAN ATMOSPHERIC  REDUCE FLOWRATE
C
   97 IF(I.LT.10) GO TO 98
      WRITE(6,94) P
   94 FORMAT(F10.5)
   98 IF(P-14.7)75,12,76
   75 D1=-1.0
      WRITE(6,49) P,T,V,I
   49 FORMAT(4F15.5/,/,/)
      GO TO 10
C
C     IF P IS GREATER THAN ATMOSPHERIC  INCREASE FLOWRATE
C
   76 D1=1.0
```

```
      WRITE(6,49) P,T,V,M
      GO TO 10
   10 CONTINUE
C
C     CALCULATE OVERALL OUTPUT
C
   12 TORQUE=(PUSH-DRAG)*DIA/24.0
      POWER=TORQUE*6.2832*RPM/(778.*60.)
      EFF=POWER/FUEL
      WRITE(6,4)TORQUE,POWER,EFF,VC(1),MDOT,P2,T2,VT(11),M,V,P,T,TW
    4 FORMAT(7F15.7,/,6F15.7,/,/)
   11 CONTINUE
      GO TO 1
   99 STOP
      END
```

REFERENCES

1. Dusadeenoad, S., "Characteristics of a Viscous Flow Compressor," M.S. Thesis, Georgia Institute of Technology, September, 1970.

2. Caldwell, J. S., "Efficiency of a Viscous Flow Compressor," M.S. Thesis, Georgia Institute of Technology, June, 1973.

3. Colwell, G. T. and Jackson, T. W., Turbine-Compressor, United States Patent No. 3,751,908, August 14, 1973.

4. Yalcin. A. I., "Theoretical Study of a Viscous Turbine," M.S. Thesis, Georgia Institute of Technology, March, 1975.

5. Tesla, Nikola, Turbine, Official Gazette U. S. Patents No. 1061206 5/1913.

6. John, E. A., Gas Dynamics, First Edition, Allyn and Bacon Company, 1974.

7. Schlichting, H., Boundary-Layer Theory, Sixth Edition, McGraw-Hill Company, 1968.

8. White, F. M., Viscous Fluid Flow, First Edition, McGraw-Hill Company, 1974.

9. Reynolds, W. C., Thermodynamics, Second Edition, McGraw-Hill Company, 1968.

10. Kreith, F., Principles of Heat Transfer, Second Edition, McGraw-Hill Company, 1965.

11. Keenan and Kaye, Gas Tables, First Edition, Wiley Incorporated, 1966.

12. Cooper and Smith, Standard Fortran, First Edition, Houghton Mifflin, 1973.